UNIVERSIDADE ESTADUAL PAULISTA
"JÚLIO DE MESQUITA FILHO"
Campus de São José do Rio Preto

ANDRÉ LUIZ BORGES MACHADO

Isotermas de sorção, cinética de secagem e propriedades termodinâmicas de plantas alimentícias não convencionais

São José do Rio Preto

2024

ANDRÉ LUIZ BORGES MACHADO

ISOTERMAS DE SORÇÃO, CINÉTICA DE SECAGEM E PROPRIEDADES TERMODINÂMICAS DE PLANTAS ALIMENTÍCIAS NÃO CONVENCIONAIS

Tese apresentada como parte dos requisitos para obtenção do título de Doutor em Engenharia e Ciência de Alimentos, junto ao Programa de Pós-Graduação em Alimentos, Nutrição e Engenharia de Alimentos, do Instituto de Biociências, Letras e Ciências Exatas da Universidade Estadual Paulista "Júlio de Mesquita Filho", Câmpus de São José do Rio Preto.

Financiadoras: CAPES (001), CNPq (314459/2021-9) e FAPESP (2022/05272-8)

Orientador: Prof. Dr. Javier Telis Romero

Coorientadora: Profª. Drª. Priscila Alonso dos Santos

Coorientadora: Profª. Drª. Guadalupe Luna Solano

São José do Rio Preto

2024

B732i

Borges-Machado, André Luiz

Isotermas de sorção, cinética de secagem e propriedades termodinâmicas de plantas alimentícias não convencionais / André Luiz Borges-Machado. -- São José do Rio Preto, 2024

189 p.

Tese (doutorado) - Universidade Estadual Paulista (UNESP), Instituto de Biociências Letras e Ciências Exatas, São José do Rio Preto

Orientador: Javier Telis-Romero

Coorientadora: Priscila Alonso dos Santos

1. Ora-pro-nóbis. 2. Taioba. 3. Sementes de pimenta Jalapeño. I. Título.

Sistema de geração automática de fichas catalográficas da Unesp. Biblioteca da Universidade Estadual Paulista (UNESP), Instituto de Biociências Letras e Ciências Exatas, São José do Rio Preto. Dados fornecidos pelo autor(a).

André Luiz Borges Machado

ISOTERMAS DE SORÇÃO, CINÉTICA DE SECAGEM E PROPRIEDADES TERMODINÂMICAS DE PLANTAS ALIMENTÍCIAS NÃO CONVENCIONAIS

Tese apresentada como parte dos requisitos para obtenção do título de Doutor em Engenharia e Ciência de Alimentos, junto ao Programa de Pós-Graduação em Alimentos, Nutrição e Engenharia de Alimentos, do Instituto de Biociências, Letras e Ciências Exatas da Universidade Estadual Paulista "Júlio de Mesquita Filho", Câmpus de São José do Rio Preto.

Financiadoras: CAPES (001), CNPq (314459/2021-9) e FAPESP (2022/05272-8)

Orientador: Prof. Dr. Javier Telis Romero

Coorientadora: Profª. Drª. Priscila Alonso dos Santos

Coorientadora: Profª. Drª. Guadalupe Luna Solano

COMISSÃO EXAMINADORA

Prof. Dr. Javier Telis Romero
(Presidente / Orientador – DETA/IBILCE)

Prof. Dr. Osvaldo Resende
(IF Goiano – Câmpus Rio Verde)

Profª. Drª. Fernanda Ferreira Freitas
(IQ/UFG – Câmpus Samambaia)

Drª. Bianca Guimarães
(DETA/IBILCE)

São José do Rio Preto

23 de maio 2024

DEDICATÓRIA

Dedico este trabalho aos meus pais, Lauro e Divina Márcia e à minha irmã, Laura. Dedico também, a todos aqueles que contribuíram de certa forma para que eu chegasse até aqui.

AGRADECIMENTOS

Primeiramente, a Deus e a Meishu-Sama pela sabedoria, calma e luz recebida para que eu pudesse chegar até aqui.

Aos meus pais, Lauro e Divina Márcia, e minha irmã Laura pela confiança, carinho, por nunca duvidarem do meu potencial e serem o meu combustível para lutar durante toda essa caminhada que chamamos de vida.

Ao meu estimado orientador Prof. Dr. Javier Telis Romero pela confiança, apoio, atenção e por sempre me estimular a pensar além.

À minha amiga e coorientadora Prof. Dra. Priscila Alonso dos Santos pela amizade, por permitir que eu realizasse os experimentos de secagem no laboratório sob sua responsabilidade no IF Goiano, e por quando eu ainda estava na graduação me estimular a fazer mestrado e doutorado.

A todos os professores que tive desde 1997, quando comecei meus estudos.

Aos meus amigos, Dr. Marcio Augusto Ribeiro Sanches e Dra. Maria Júlia Neves Martins, confesso que não encontrei palavras para expressar à minha gratidão a vocês. Vocês me fortaleceram quando pensei em desistir.

À minha amiga, Dra. Kamilla Soares Silva, pela amizade, parceria durante estes 6 anos de pós-graduação e, por me ajudar a sempre enxergar além do que meus olhos conseguem ver.

Aos meus amigos, Lauro Filho, Jesus Galvão, Juliana Parize, Cláudia Catarino, Luciana Parize, Maria Siqueira, Raíssa Matos e Jerônimo Moraes, por acreditarem em mim quando eu nem eu mesmo acreditava.

Aos colegas de doutorado: Caroline Fuzetti, Mari Garcia, Rodrigo Evangelista, Marcello Bertucci e Micael Almeida me fizeram rir perante as dificuldades e gargalhar com as facilidades.

Agradeço a você, que se porventura esqueci-me de mencionar aqui, mas contribuiu para que eu chegasse aqui. Meus sinceros agradecimentos.

O presente trabalho foi realizado com apoio da Coordenação de Aperfeiçoamento de Pessoal de Nível Superior - Brasil (CAPES) - Código de Financiamento 001.

À FAPESP, pelo apoio financeiro, concedido por meio do Processo nº 2022/05272-8, Fundação de Amparo à Pesquisa do Estado de São Paulo (FAPESP).

Ao Conselho Nacional de Desenvolvimento Científico e Tecnológico (CNPq), pela concessão de recursos (processo 314459/2021-9).

E como diria Snoop Dogg: Por último, mas não menos importante, quero agradecer-me por acreditar em mim. Quero agradecer-me por fazer todo esse trabalho duro. Quero agradecer por não ter folga. Eu quero agradecer por nunca desistir. Quero agradecer-me por sempre ser doador e tentar dar mais do que recebo. Quero agradecer por tentar fazer mais certo do que errado. Quero agradecer-me por ser apenas eu em todos os momentos.

EPÍGRAFE

“Sou como a haste fina

Qualquer brisa verga

Nenhuma espada corta”

(Maria Bethânia Viana Teles Veloso)

RESUMO

O problema da insegurança alimentar mundial já não estava indo ao encontro de uma solução até 2030 conforme prevê o programa da FAO para zerar a fome até o citado ano. A pandemia de COVID-19 agravou ainda mais o problema. No Brasil, a insegurança alimentar é realidade para aproximadamente 9 milhões de brasileiros. Neste contexto, muitas plantas consideradas invasoras, pragas ou inços, na verdade, possuem grande potencial alimentício e podem contribuir para a redução da insegurança. A fim de se fornecer informações sobre o comportamento higroscópico em temperaturas de armazenamento (5-40 ºC) e de secagem (40-80 ºC), foram determinadas as isotermas de sorção das folhas de ora-pro-nóbis (*Pereskia aculeata* Miller), folhas, pecíolo e rizoma de taioba (*Xanthosoma taioba* E.C.Gonç.) e de sementes de pimenta Jalapeño (*Capsicum annuum*) via método gravimétrico utilizando soluções saturadas de diferentes sais. Dentre os cincos modelos ajustados aos dados experimentais via regressão não linear, o modelo de GAB foi escolhido para descrever as isotermas das plantas estudadas, bem como apresentaram formato sigmoide sendo classificadas como BET Tipo II. O teor de água de equilíbrio aumentou com o incremento da umidade relativa e redução da temperatura para as plantas analisadas. O calor isostérico líquido de sorção das folhas de ora-pro-nóbis, folhas, pecíolo e rizoma de taioba e das sementes de pimenta Jalapeño diminuiu com o aumento do teor de água de equilíbrio. A teoria da compensação entalpia-entropia foi comprovada nas condições de armazenamento e secagem. Os mecanismos de dessorção de todas as plantas estudadas não são espontâneos. Com relação à cinética de secagem, o modelo de Weibull foi o que melhor descreveu a razão de teor de água em função do tempo para as folhas de ora-pro-nóbis, rizoma de taioba e sementes de pimenta Jalapeño. Já o modelo Logarítmico melhor se ajustou aos dados de folhas e pecíolos de taioba. O coeficiente de difusão aumentou com o incremento da temperatura de secagem para as diferentes partes de planta. A energia de ativação das folhas de ora-pro-nóbis, folhas, pecíolo e rizoma de taioba e das sementes de pimenta Jalapeño foi estimada, em $kJ \cdot mol^{-1}$, em 65,81; 68,47; 34,80; 29,68 e 30,30; respectivamente.

Palavras-chave: Modelo de GAB. Taioba. Pimenta Jalapeño. Ora-pro-nóbis. Modelo de Weibull.

ABSTRACT

The problem of global food insecurity was not on track to be solved by 2030 as envisioned by the FAO program to eradicate hunger by that year. The COVID-19 pandemic further exacerbated the issue. In Brazil, food insecurity is a reality for approximately 9 million Brazilians. In this context, many plants considered invasive, pests, or weeds have great food potential and can contribute to reducing insecurity. To provide information on the hygroscopic behavior at storage temperatures (5-40 ºC) and drying temperatures (40-80 ºC), the sorption isotherms of ora-pro-nóbis leaves (*Pereskia aculeata* Miller), leaves, stems, and tubers of taioba (*Xanthosoma taioba* E.C.Gonç.), and Jalapeño pepper seeds (*Capsicum annuum*) were determined using the gravimetric method with saturated solutions of different salts. Among the five models fitted to the experimental data via nonlinear regression, the GAB model was chosen to describe the isotherms of all the plants studied, which exhibited a sigmoidal shape and were classified as BET Type II. The equilibrium moisture content increased with increasing relative humidity and decreasing temperature for all plants. The net isosteric heat of sorption of ora-pro-nóbis leaves, leaves, stems, and tubers of taioba, and Jalapeño pepper seeds decreased with increasing equilibrium moisture content. The enthalpy-entropy compensation theory was confirmed under storage and drying conditions. The desorption mechanisms of all studied plants are non-spontaneous. Regarding drying kinetics, the Weibull model was the best fit to describe the moisture ratio as a function of time for ora-pro-nóbis leaves, taioba tubers, and Jalapeño pepper seeds. Meanwhile, the Logarithmic model better fit the data for taioba leaves and stems. The diffusion coefficient increased with increasing drying temperature for the different plant parts. The activation energy of ora-pro-nóbis leaves, leaves, stems, and tubers of taioba, and Jalapeño pepper seeds was estimated, in $kJ \cdot mol^{-1}$, at 65.81, 68.47, 34.80, 29.68, and 30.30, respectively.

Keywords: GAB model. Cocoyam. Jalapeño pepper. Ora-pro-nóbis. Weibull model.

LISTA DE FIGURAS

Capítulo 1 – Revisão de literatura

Capítulo 2 – Water desorption isotherms and thermodynamic properties of Ora-pro-nóbis (*Pereskia aculeata* Miller)

Capítulo 3 - Thin layer convective drying kinetics of ora-pro-nóbis (*Pereskia aculeata* Miller) leaves

Capítulo 6 - Drying kinetics and water adsorption properties of jalapeño pepper seeds (*Capsicum annuum* L.): A study aiming at their recovery and integral exploitation

LISTA DE TABELAS

Capítulo 1 – Revisão de literatura

Capítulo 2 – Water desorption isotherms and thermodynamic properties of Ora-pro-nóbis (*Pereskia aculeata* Miller)

Capítulo 3 - Thin layer convective drying kinetics of ora-pro-nóbis (*Pereskia aculeata* Miller) leaves

Capítulo 4 - Desorption properties of taioba (*Xanthosoma taioba* E.G. Gonç.) leaves, stems, and tubers: A non-conventional edible plant

Capítulo 5 - Drying kinetics and thermodynamic approach of taioba (*Xanthosoma taioba* E. C. Gonç.): leaves, stems, and tubers

LISTA DE TABELAS SUPLEMENTARES

SUMÁRIO

INTRODUÇÃO

Antes da pandemia de COVID-19, o problema da insegurança alimentar não estava indo ao encontro de uma solução até 2030. A prevalência de desnutrição que permaneceu constante nos últimos cinco anos, aumentou 1,5% em 2020 e atingiu um nível de 9,9%, tornando este objetivo ainda mais desafiador (FAO *et al.*, 2021). No Brasil, nos últimos dois anos, o número de pessoas vivendo em severa insegurança alimentar saltou de 10,3 para 19,1 milhões. Neste período, a fome se tornou realidade para aproximadamente 9 milhões de brasileiros (PENSSAN, 2021).

A insegurança alimentar existente é justificada pela incapacidade das classes mais pobres de obterem os alimentos necessários para uma alimentação saudável e equilibrada. As projeções de crescimento populacional, da expansão das cidades, do aumento do consumo per capita e das restrições no uso de terra nas próximas décadas fazem mais relevante o debate sobre a incapacidade de atender às necessidades humanas por alimentos (SAATH; FACHINELLO, 2018).

Uma das alternativas para solução da insegurança alimentar é a pesquisa sobre plantas de potencial alimentício, entretanto, pouco consumidas. Muitas plantas são denominadas "daninhas", "invasoras", "inços" e até nocivas, somente devido ao fato de se desenvolverem em meio às culturas tradicionais ou em locais em que as pessoas acham que não podem ou não devem ocorrer. No entanto, muitas destas espécies têm grande importância alimentícia (KINUPP; LORENZI, 2014). Plantas alimentícias não convencionais (PANC) são aquelas presentes em determinadas localidades ou regiões exercendo influência na alimentação de uma população tradicional, entretanto não estão organizadas enquanto cadeia produtiva propriamente dita (BRASIL, 2010).

As PANC geram autonomia para as pessoas que desejam buscar os nutrientes que necessitam e os sabores que mais lhe agradam. Em conjunto, integradas com as comunidades humanas, culturas biodiversas, esta autonomia é também fator de autoafirmação e emancipação, no que se pode chamar de soberania alimentar e ecológica (KELEN *et al.*, 2015). Plantas como a ora-pro-nóbis, taioba e as sementes de pimenta Jalapeño podem ser consideradas PANC.

A ora-pro-nóbis (*Pereskia aculeata* Miller) é uma planta trepadeira, que pertence à família *Cactaceae*, sendo nativo do Sul e América Central e América tropical, que é naturalmente distribuído do Nordeste para o sul do Brasil (SHARIF *et al.*, 2013). Suas folhas suculentas são uma ótima fonte de proteínas (26% p/p) e apresenta níveis importantes de minerais, fibras alimentares, vitaminas A e C, além de ácido fólico (SOUZA *et al.*, 2016).

A taioba (*Xanthosoma taioba* E.G. Gonç.) é uma herbácea tuberosa, acaule, com altura variando entre 50-90 cm, nativa de Minas Gerais e possui folhas membranáceas medindo entre 20-35 cm de comprimento e pecíolo ereto e esponjoso de comprimento entre 30-50 cm. É fonte de minerais com o cálcio, magnésio, manganês, ferro e zinco, além de vitamina C e carotenos. As folhas, pecíolos e rizoma podem ser utilizado na alimentação humana, desde que sejam bem refogados para eliminação do oxalato de cálcio presente. Por muito tempo, acreditava-se que esta planta era pertencente à espécie *Xanthosoma sagittifolium* (L.) Schott, originária da América Central, até que um estudo mais detalhado demonstrou que a taioba brasileira é uma nova espécie (KINUPP; LORENZI, 2014).

As sementes de pimenta Jalapeño apresentam uma composição rica em nutrientes, contendo aproximadamente 43% de fibras, 20% de proteínas e 17% de lipídios (SANDOVAL-CASTRO *et al.*, 2014, 2017). O elevado teor de fibras dessas sementes ressalta seu potencial para serem recuperadas e utilizadas como ingredientes em alimentos processados (BOUAZIZ *et al.*, 2020; GARCIA *et al.*, 2020). Além disso, a possibilidade de recuperar as proteínas das sementes está alinhada com a crescente tendência global de aproveitar as proteínas vegetais como uma fonte nutritiva de destaque na dieta humana (SÁ *et al.*, 2020).

Neste contexto, a qualidade de um material biológico pode ser preservada mediante estudo de parâmetros como secagem e armazenamento. Informações sobre o teor de água de equilíbrio desses materiais é imprescindível, pois define as condições adequadas para o armazenamento de frutas e hortaliças (SOUSA *et al.*, 2014).

Isotermas de sorção de água são consideradas uma importante ferramenta da termodinâmica para determinar a interação entre os componentes de um alimento e a água. As isotermas são gráficos que relacionam o teor de água de equilíbrio e a umidade relativa do ambiente, em temperatura constante, e fornecem informações relevantes para o processamento de alimentos como a secagem, embalagem e armazenamento (KUMAR; MISHRA, 2006; TONON *et al.*, 2009). Diversos modelos matemáticos são utilizados para descrever as isotermas de sorção: modelos cinéticos baseados na monocamada (modelo de BET), modelos cinéticos baseados na multicamada (modelo de GAB), modelos semi-empíricos (Ferro-Fontan, Henderson, Halsey, etc) e modelos empíricos (Smith, Oswin, etc.) (CORRÊA *et al.*, 2016).

A secagem é uma operação unitária em que ocorre a aplicação de calor sob condições controladas a fim de remover a maior quantidade de água possível de um alimento, por evaporação, visando a redução de massa e volume e estender a vida de prateleira (FELLOWS, 2019). A secagem de produtos agrícolas pode ser descrita por modelos matemáticos teóricos, semiteóricos e empíricos. Os modelos teóricos consideram as transferências de calor e massa na interface produto-ar de secagem e no interior do produto. Já os modelos semiteóricos e os empíricos consideram somente a resistência externa à temperatura e a umidade relativa do ar (FARIA *et al.*, 2012).

Visando contribuir para diminuição da insegurança alimentar apresentando dados que auxiliam no processamento e armazenamento de alimentos pouco consumidos, neste trabalho objetivou-se determinar as isotermas de sorção, bem como calcular as propriedades termodinâmicas de ora-pro-nóbis, taioba e sementes de pimenta Jalapeño em diferentes temperaturas que simulem condições de armazenamento e de secagem. Ademais, objetivou-se ajustar modelos matemáticos que descrevam a cinética de secagem e viabilizem os cálculos dos coeficientes de difusão e da energia de ativação para os materiais analisados.

OBJETIVOS

Objetivos gerais

Determinar as isotermas de sorção, bem como calcular as propriedades termodinâmicas de ora-pro-nóbis, taioba e sementes de pimenta jalapeño em diferentes temperaturas que simulem condições de armazenamento e de secagem. Ademais, objetiva ajustar modelos matemáticos que descrevam a cinética de secagem e viabilizem os cálculos dos coeficientes de difusão e da energia de ativação.

Objetivos específicos

- Determinar a composição proximal (o teor de água, o teor de proteína, o teor de cinzas, o teor de lipídeos e o teor de carboidratos) de cada planta;
- Determinar as isotermas de sorção das folhas de ora-pro-nóbis e das folhas, pecíolo e rizoma de taioba nas temperaturas de armazenamento (5 , 10, 20, 30 e 40 ºC);
- Determinar as isotermas de sorção das folhas de ora-pro-nóbis e das folhas, pecíolo e rizoma de taioba nas temperaturas de secagem (40 ºC, 50 ºC, 60 ºC, 70 ºC e 80 ºC);
- Determinar as isotermas de sorção das plantas nas temperaturas de armazenamento (8 ºC, 16 ºC, 24 ºC, 32 ºC e 40 ºC);
- Determinar as isotermas de sorção das plantas nas temperaturas de secagem (40 ºC, 48 ºC, 56 ºC, 64 ºC e 72 ºC);
- Determinar as curvas de cinética de secagem das plantas por meio de modelos empíricos e semiempíricos nas temperaturas de 40 ºC, 50 ºC, 60 ºC, 70 ºC e 80 ºC;
- Determinar o coeficiente de difusão efetivo;
- Avaliar a influência da temperatura no coeficiente de difusão efetivo
- Determinar as propriedades termodinâmicas utilizando as isotermas de sorção e curva de perda de água (calor isostérico de sorção, entropia diferencial, energia livre de Gibbs e temperatura isocinética);
- Avaliar a teoria da compensação entalpia-entropia;

1 CAPÍTULO 1 - REVISÃO DE LITERATURA

1.1 Segurança alimentar e Plantas alimentícias não convencionais

O termo segurança alimentar passou a ser utilizado na Europa durante a Primeira Guerra Mundial. Entretanto, este termo só ganhou força no período pós Segunda Guerra Mundial, com a constituição da Organização das Nações Unidas (ONU) em 1945. Desde então o conceito de Segurança Alimentar e Nutricional (SAN) está em constante construção (ABRANDH, 2013). No Brasil, a discussão relacionada à segurança e soberania alimentar e nutricional (SAN) da população humana se intensificou a partir da década de 1980 (BURITY *et al.*, 2010).

A segurança alimentar é afetada por aspectos econômicos, sociais e ambientais. Nos últimos anos, diversos fatores têm pressionado os sistemas de alimentos, dentre eles o crescimento populacional. A demanda global por alimentos tende a aumentar, uma vez que a população mundial estimada para 2050 é de 9 bilhões pessoas, que devem ter direito à saúde garantido mesmo com a diminuição dos recursos naturais (CAMPI *et al.*, 2021; COLE *et al.*, 2018).

De acordo com a Organização das Nações Unidas para alimentação e agricultura - FAO, (1996), a segurança alimentar é um cenário no qual "as pessoas tem acesso físico e econômico à alimentos em quantidades suficientes, seguros e nutritivos que satisfaçam suas preferências e necessidades alimentares para uma vida ativa e saudável". Visando este cenário, há quatro dimensões há serem avaliadas: disponibilidade física, acesso físico e econômico, utilização e estabilidade ao longo do tempo das três dimensões anteriores.

Antes da pandemia de COVID-19, o problema da insegurança alimentar não estava indo de encontro à uma solução até 2030. A prevalência de desnutrição que permaneceu constante nos últimos cinco anos, aumentou 1,5% em 2020 e atingiu um nível de 9,9%, tornando este objetivo ainda mais desafiador (FAO *et al.*, 2021). No Brasil, nos últimos dois anos, o número de pessoas vivendo em severa insegurança alimentar saltou de 10,3 para 19,1 milhões. Neste período, a fome se tornou realidade para aproximadamente 9 milhões de brasileiros (PENSSAN, 2021).

A lei n° 11.346 de 15 de setembro de 2006, que cria o Sistema Nacional de Segurança Alimentar e Nutricional – SISAN com vistas em assegurar o direito humano à alimentação adequada e dá outras providências, estabelece no artigo 2º que

> "A alimentação adequada é direito fundamental do ser humano, inerente à dignidade da pessoa humana e indispensável à realização dos direitos consagrados na Constituição Federal, devendo o poder público adotar as políticas e ações que se façam necessárias para promover e garantir a segurança alimentar e nutricional da população."

Logo, é dever do Estado fomentar pesquisas buscando alternativas para solução da insegurança alimentar.

O Brasil possui uma rica diversidade brasileira que é amplamente reconhecida e estudada por ter potencial alimentício, compostos bioativos, princípios ativos de medicamento e outras moléculas que podem ser empregadas em diversas áreas tecnológicas (BIONDO *et al.*, 2018).

Muitas plantas são denominadas "daninhas", "invasoras", "inços" e até nocivas, somente devido ao fato de se desenvolverem em meio às culturas tradicionais ou em locais em que as pessoas acham que não podem ou não devem ocorrer. No entanto, muitas destas espécies têm grande importância alimentícia (KINUPP; LORENZI, 2014).

Plantas alimentícias não convencionais (PANC) são aquelas presentes em determinadas localidades ou regiões exercendo influência na alimentação de uma população tradicional, entretanto não estão organizadas enquanto cadeia produtiva propriamente dita (BRASIL, 2010). As PANC geram autonomia para as pessoas que desejam buscar os nutrientes que necessitam e os sabores que mais lhe agradam. Em conjunto, integradas com as comunidades humanas, culturas biodiversas, esta autonomia é também fator de autoafirmação e emancipação, no que se pode chamar de soberania alimentar e ecológica (KELEN *et al.,* 2015).

No entanto, é importante destacar que algumas PANC são consideradas regulares por determinadas populações em áreas geográficas específicas. Portanto, as mudanças nos hábitos alimentares das pessoas, principalmente na área urbana, possivelmente impactaram negativamente o consumo e o reconhecimento de PANC. Todavia, sua qualidade nutricional e facilidade de produção devem ser valorizadas e incentivadas como uma alternativa para oferecer alimentos mais sustentáveis e saudáveis para a alimentação da população, caminhando em consonância com as metas globais da Agenda 2030 (MARIUTTI *et al.,* 2021). Ademais, partes não usualmente consumidas de hortaliças convencionais também podem ser consideradas PANC, como é o caso das folhas de chuchu, abóbora, batata-doce e tantas outras (SARTORI *et al.*, 2020).

Estima-se que 27 mil espécies de plantas com potencial alimentício são plantas nativas e exóticas, cultivadas ou silvestres. Destas, 57% podem contribuir significativamente para melhorar a segurança alimentar, particularmente, em áreas duramente afetadas pela pandemia (CRUZ-GARCIA, 2017; IRANI *et al.*, 2018). Estudos recentes apontam que as PANC apresentam fator nutricional superior à algumas hortaliças tradicionais e possuem aporte relevante na ingestão diária de vitaminas e minerais essenciais à manutenção da boa saúde humana. Outros estudos descrevem que algumas PANC podem contribuir de maneira positiva ao trato gastrointestinal, pois atuam na microbiota intestinal que desempenha função relevante no equilíbrio intestinal (LIBERATO *et al.*, 2019; PASCHOAL *et al.*, 2015; SARTORI *et al.*, 2020).

A ora-pro-nóbis, taioba e mangarito são exemplos de PANC. Essas plantas são ingredientes importantes na culinária de diferentes regiões brasileiras, fazendo parte da identidade gastronômica de determinadas localidades, como o estado de Minas Gerais, onde eram amplamente consumidos antes do êxodo rural. Em algumas cidades e regiões, ainda são tradicionalmente consumidos em saladas ou refogados, fáceis de preparar na maioria das vezes. No entanto, o tipo de preparo culinário depende da parte comestível da PANC, como folhas, frutos, flores, sementes, vagens, raízes, galhos, brotos, que podem ser consumidos in natura ou usados para fazer sucos, ensopados, saladas, doces, geleias, sorvetes, refogados, bolos, entre outros. Há muitas maneiras de incorporar PANC na dieta; no entanto, não são estabelecidas políticas públicas para popularizar o consumo de PANC e nem atividades de educação nutricional para incentivar seu cultivo e uso pela população (MARIUTTI *et al.*, 2021).

1.2 Ora-pro-nóbis (*Pereskia aculeata* Miller)

A ora-pro-nóbis (*Pereskia aculeata* Miller) é uma planta trepadeira, que pertence à família *Cactaceae*, nativa da América Central e América tropical, e é naturalmente distribuída do Nordeste para o Sul do Brasil (SHARIF et al., 2013). O cultivo e propagação desta planta é fácil devido à baixa demanda hídrica e baixa incidência de doenças, consequentemente, baixo custo de produção. A propagação pode ser feita vegetativamente via estaquia caulinar que é bastante simples, rápida, e permite a produção de grande quantidade de mudas em um pequeno intervalo de tempo, usando menor número de plantas matrizes, em área reduzida, além da multiplicação uniforme de genótipos de interesse (HARTMANN *et al.*, 2002; MADEIRA; SILVEIRA, 2010).

Na Figura 1 está apresentada uma foto de uma planta inteira de ora-pró-nobis e detalhes das folhas e caules. A folha é simples, elíptica e possui epiderme uniestratificada, estômatos paracíticos em ambas as faces, mesofilo que tende a ser dorsiventral, contendo numerosas drusas de oxalato de cálcio e células isodiamétricas grandes com conteúdo mucilaginoso. A nervura central é percorrida por um feixe vascular colateral em arco aberto. O pecíolo tem secção plano-convexa e um feixe colateral em formato de arco. O caule, em estrutura secundária incipiente, possui epiderme unisseriada, colênquima angular, parênquima cortical com muitos amiloplastos, calotas de fibras perivasculares e organização vascular colateral. No córtex e na medula, são observadas numerosas cavidades com conteúdo mucilaginoso e drusas de oxalato de cálcio, estas também presentes no floema (DUARTE; HAYASHI, 2005).

Figura 1 – Planta inteira de ora-pro-nóbis (*Pereskia aculeata* Miller) (a) e detalhes das folhas e caules (b).
Fonte: Google Imagens

Possui flores, espinhos e folhas ricas em substâncias de alto valor biológico, possuindo grande potencial alimentício e medicinal. As flores e frutos de ora-pro-nóbis são apresentadas na Figura 2. A floração ocorre entre os meses de janeiro e abril, com flores pequenas de cor branca, enquanto a formação dos frutos ocorre apenas de junho a julho, apresentando uma coloração amarelada e formato arredondado (RODRIGUES *et al.*, 2019).

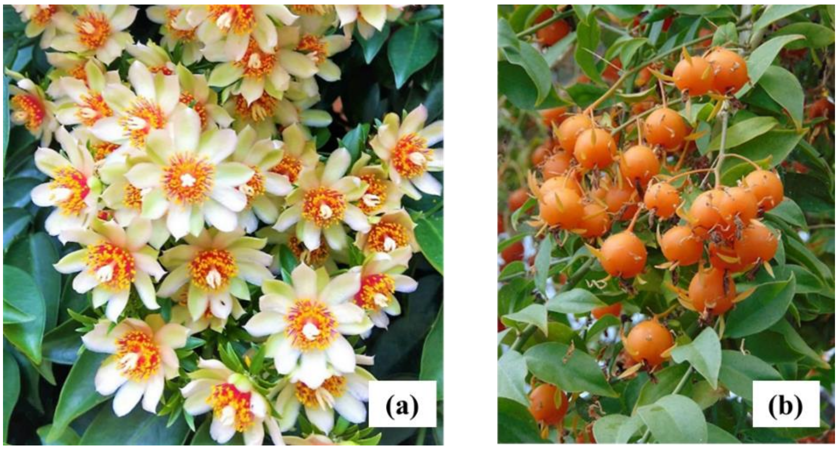

Figura 2 – Flores (a) e frutos (b) de ora-pro-nóbis.
Fonte: Google Imagens

O consumo de cactáceas tem aumentado devido à excelente qualidade nutricional das plantas dessa família. Os cactos sintetizam grandes quantidades de mucilagem, um complexo de carboidratos que possui alta capacidade de absorção de água e importantes efeitos biológicos como imunomodulação, atividade hipoglicêmica e interação com a microbiota intestinal podendo contribuir com uma melhor saúde do intestino humano (AGOSTINI-COSTA, 2020; MARTIN *et al.*, 2017; XU *et al.*, 2016). Portanto, as folhas de ora-pro-nóbis são uma excelente fonte de fibras e também de proteínas (28% b.s.), sendo que aproximadamente 60% deste total de proteínas é composto por aminoácidos essenciais, principalmente triptofano, leucina, lisina, fenilalanina e tirosina. Estas proteínas atingiram os requisitos estabelecidos pela FAO para crianças de 2 a 5 anos de idade pois a digestibilidade in vitro é de 76% (TAKEITI *et al.*, 2009). Ademais, minerais como potássio, cálcio, magnésio, fósforo, manganês, ferro, zinco e cobre também são encontrados (DE ALMEIDA *et al.*, 2014).

GARCIA *et al.*, (2019) avaliaram o perfil fitoquímico e atividades biológicas de extratos de folhas de OPN que apresentaram potencial antimicrobiano promissor contra bactérias gram-positivas e gram-negativas e ausência verificada de hepatotoxicidade em células PLP2. Neste estudo, os autores ainda relataram a presença de 10 compostos fenólicos sendo dois ácidos fenólicos (derivados do ácido cafeico) e oito flavonóides (derivados de quercetina, kaempferol e glicosídeo de isorhamnetina). O ácido cafetárico foi o principal constituinte fenólico do extrato, respondendo por mais de 49% do conteúdo fenólico, seguido pela quercetina-3-O-rutinosídeo (14,99%) e isorhamnetina- O -pentosídeo- O-rutinoside (9,56%). Além do mais, o extrato da folha de ora-pro-nóbis apresentou valores relevantes de capacidade antioxidante nos ensaios DPPH e ABTS, com atividades superiores ao Trolox.

Nos últimos anos, alguns estudos têm sido realizados objetivando desenvolver produtos alimentícios adicionados de ora-pro-nóbis. Durante um evento tradicional na Zona Rural de Uberlândia, a Semana da Família Rural, QUEIROZ *et al.*, (2015) avaliaram a aceitação sensorial de alimentos processados com folhas de ora-pro-nóbis *in natura* ou previamente secas. Os autores aplicaram um teste de escala hedônica de 5 pontos (n=232) e obtiveram índice de aceitação superior a 90% em todos os alimentos adicionados de folhas de OPN, sendo eles: biscoito de queijo, bolo de limão, bolo de chocolate, bombom, doce de abóbora, doce de banana, hambúrguer de frango, hambúrguer de suíno, pão de cebola e torta de legumes.

Portanto, a produção e consumo das folhas de *P. aculeata* pela população é de suma importância devido seu potencial como fonte sustentável de nutracêuticos e ingredientes alimentícios promissores para serem utilizados para elevar a qualidade nutricional e auxiliar na conservação de alimentos (GARCIA *et al.*, 2019).

1.3 Taioba (*Xanthosoma taioba* E.C.Gonç)

Possivelmente, a América Central e as Antilhas foram relevantes na seleção e dispersão das espécies e variedades cultivadas, sendo a primeira denotação da espécie de cultivo relatada como *Xanthosoma sagittifolium*. Entretanto, há outras espécies de *Xanthosoma* empregadas na alimentação como a *Xanthosoma maffafa* oriunda da África e a *Xanthosoma robustum*, da Flórida. A taioba roxa (*Xanthosoma violaceum*) e a taioba comum (*Xanthosoma taioba*) são as mais conhecidas no Brasil. As espécies de taioba são comumente discutidas ou até mesmo confundida com o taro (*Colocasia esculenta*) (GOMES *et al.*, 2014).

A taioba é facilmente cultivada em clima quente, interrompendo a produção das folhas em baixas temperaturas. Devido a isso, o cultivo em regiões de altitude elevada é muito difícil. A planta demanda de solo sempre úmido, rico em húmus e de pH variando entre 5,5-6,5. No Brasil, seu ciclo completo (plantio à colheita) dura de 4 a 5 meses, enquanto que em outros países pode levar até 10 meses (ABRAMO, 1990; LETERME *et al.*, 2005).

É uma herbácea que pode atingir até um metro de altura. Possui caules eretos e cilíndricos que medem entre 3 e 7 cm de diâmetro, densamente recobertos por fibras marrons, resultando em rizomas pequenos. Cada planta possui de 2 a 4 folhas ligadas ao caule por um pecíolo 25 a 65 cm de comprimento, verde, cerosos e embainhados até cerca de metade do comprimento. As lâminas foliares tem entre 18 e 25 cm de largura e altura variando entre 50 e 55 cm. Apresenta de uma a três inflorescências por axila foliar, pedúnculo de 16 a 17 cm de altura e 1,5 a 2 cm de largura, espata de 20 a 24 cm de comprimento com características semelhantes às do pecíolo (GONÇALVES, 2011).

Na Figura 3 está apresentada a morfologia de uma taioba típica e na Figura 4, uma foto de taiobas cultivadas pelo Movimento Planta e Vida em Rio Verde - Goiás. As principais características que as diferem das plantas da mesma família são formato sagitado com linha contornando toda sua borda e as folhas fundem-se exatamente no talo, com seiva de aparência esbranquiçada (LIMA; KRUPEK, 2016). Estas características auxiliam na identificação correta da planta cujas folhas, pecíolos e rizoma podem ser utilizados na alimentação humana, desde que sejam bem refogados para eliminação do oxalato de cálcio presente. É fonte de minerais com o cálcio, magnésio, manganês, ferro e zinco, além de vitamina C e carotenos (KINUPP; LORENZI, 2014).

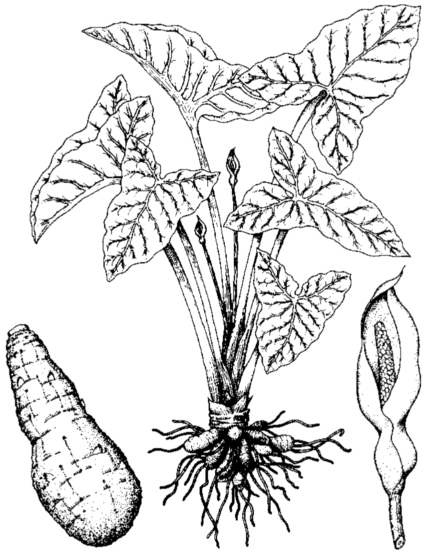

Figura 3 - Morfologia geral da taioba (X*anthosoma* sp.) típica.
Fonte: (GIACOMETTI; LEÓN, 1994).

Figura 4 - *Xanthosoma taioba* cultivada no Movimento Planta e Vida em Rio Verde – GO
Fonte: Acervo pessoal

A taioba é rica em fibras solúveis e insolúveis, sendo que estas fibras insolúveis estão presentes em uma maior quantidade na planta. Portanto, a planta pode contribuir para a regulação intestinal, pois não é completamente digerida pelo trato gastrointestinal. Além do mais, a passagem pelo estômago é mais demorada, fornecendo uma sensação de saciedade, e também pode auxiliar na redução do colesterol (SEGANFREDO et al., 2001).

Assim como outras hortaliças, a taioba não é fonte de óleo por apresentar baixos teores de extrato etéreo, revelando-se como uma alternativa para dietas vegetarianas e que se baseiam em alimentos com baixos níveis de lipídeos e calorias. O valor energético é reduzido, sendo uma boa opção para inclusão em dietas hipocalóricas (PINTO *et al.*, 2001).

Estudos realizados por JORDAN *et al.* (2021), ARAÚJO *et al.* (2019) e GOMES *et al.* (2014) destacaram a excelente atividade antioxidante e a presença de vários compostos bioativos, o que torna esta planta promissora no tocante à propriedades funcionais e nutracêuticas. Os tubersos (rizomas) e tubersilhos (batatinhas) da taioba são seu principal reservatório energético, destacando-se o seu alto teor de amido. São considerados, também, fonte de vitaminas: tiamina, riboflavina, niacina e ácido ascórbico (JACKIX, 2015).

As folhas e talos podem ser utilizados em preparos como em refogados, omeletes, ensopados também devem ser cozidos, pois crus apresentam o efeito tóxico do ácido oxálico. Os rizomas tuberosos podem ser consumidos cozidos ou moídos, em purês ou frituras (KELEN *et al.*, 2015).

1.4 Sementes de pimenta Jalapeño (*Capsicum annuum* var. *annuum*)

A pimenta pertence ao gênero *Capsicum* é um dos vegetais, condimentos e especiarias mais antigos e populares do mundo sendo utilizada em aromatizantes, corantes naturais e em medicamentos tradicionais. Existem cerca de 25 espécies deste gênero e o centro de origem é a América Latina (HERNÁNDEZ-PÉREZ *et al.*, 2020) destacando-se a variedade Jalapeño que é a mais apreciada na América do Norte e também reconhecida como uma das melhores para a produção de molhos. Os frutos da pimenta Jalapeño (Figura 5) variam de 5,0 a 8,0 cm de comprimento e 2,5 a 3,0 cm de largura, com coloração que vai do verde claro ao verde escuro quando estão verdes, e vermelha quando maduras. Suas paredes são espessas, com estrias visíveis na superfície. Geralmente têm formato cônico, com uma pungência moderada e um aroma distintivo, sendo consumidos frescos, desidratados ou em pó. A espessura da polpa dos frutos é distinta das outras variedades de pimenta, resultando em um volume maior de polpa (CARVALHO *et al.*, 2006).

Figura 5 - Pimenta jalapeño (*Capsicum annuum*)
Fonte: Google imagens

No que diz respeito à produção nacional mexicana de *Capsicum annuum,* os estados de Chihuahua, Sinaloa, Zacatecas, San Luis Potosí e Sonora foram os maiores produtores em volumes totais com 722, 648, 458 e 327 mil toneladas, respectivamente. Em 2020, esses estados contribuíram com 64,89% da produção total nacional de pimenta Jalapeño (OECD; FAO, 2020). No Brasil, o cultivo teve início na década de 1990, nas regiões noroeste de Minas Gerais e de São Paulo. É amplamente cultivada na área de Catalão, no estado de Goiás e geralmente, as plantações estão localizadas nas proximidades das indústrias de processamento de molhos de pimenta (RIBEIRO *et al.*, 2021). Aproximadamente 20% da pimenta é consumida in natura e 60% da produção é destinada a produtos processados como temperos, enlatados e molhos (NIP, 2005; SANDOVAL-CASTRO *et al.*, 2017). Após o processamento, o subproduto da pimenta Jalapeño é uma mistura de 95% de sementes e 5% de cascas, talos e polpa não utilizada (VALDEZ-MORALES *et al.*, 2021) que são gerados em diferentes etapas do processamento industrial.

As sementes de pimenta Jalapeño são fontes de fibra (≃ 43%, d.b.), proteínas (≃ 20%, d.b.) e lipídios (≃ 17%, d.b.) (SANDOVAL-CASTRO *et al.*, 2014, 2017). Seu alto teor de fibras demonstra o potencial dessas sementes para serem recuperadas e incorporadas como ingredientes em alimentos processados (BOUAZIZ *et al.*, 2020; GARCIA *et al.*, 2020). O teor de proteína parece ser recuperável, o que é consistente com as tendências globais de utilização de proteínas vegetais como excelente fonte nutritiva para a dieta humana (SÁ *et al.*, 2020). Compostos bioativos com capacidade antioxidante (SANDOVAL-CASTRO *et al.*, 2017) também foram relatados. Além disso, o óleo de semente de pimenta Jalapeño é fonte de importantes nutracêuticos lipofílicos, como β-caroteno, ácidos graxos essenciais, capsaicina, αtocoferol e diidrocapsaicina (LU *et al.*, 2019; MA *et al.*, 2019; SANDOVAL-CASTRO *et al.*, 2017) e possui sabor agradável semelhante ao óleo de girassol (JARRET *et al.*, 2013).

1.5 Água nos alimentos

O principal constituinte de grande parte dos alimentos é a água. Esta desempenha um papel fundamental nos processos físicos e químicos dos alimentos (DAMODARAN *et al.*, 2010). Geralmente o teor de água corresponde a água contida no alimento, que pode ser classificada em: umidade adsorvida, referente a água ligada, encontrada no interior do alimento, sem combinar-se quimicamente com o mesmo e umidade de superfície, que se refere a água livre ou presente na superfície externa do alimento e é facilmente evaporada. o teor de água corresponde a perda em massa sofrida pelo produto quando aquecido em condições nas quais a água é removida (IAL, 2008).

A água ligada não se comporta da mesma maneira que a água pura e pode ser definida como a água em contato com solutos e outros constituintes não aquosos, que possui mobilidade reduzida e não congela a -40 ºC. Em função dos vários graus de ligação da água, a água ligada pode ser classificada em: água constitucional que corresponde a uma pequena parte da água no alimento com alto teor de água. Representa a primeira camada de água adjacente aos compostos não aquosos do alimento e está mais fortemente ligada aos compostos não aquosos do alimento por interações iônicas; água vicinal que corresponde à camada seguinte de água adjacente à água constitucional e ocupa os sítios mais próximos da maioria dos grupos hidrofílicos presentes nos constituintes não aquosos; água de multicamadas que corresponde à água ligada mais fracamente que a água vicinal. Apesar de estar fracamente ligada aos solutos, a intensidade da força de ligação aos constituintes não aquosos é suficiente para impedir que ela se comporte como água pura (RIBEIRO; SERAVALLI, 2007).

A quantidade de água nos alimentos e a velocidade de reações são comumente relacionados entre si, porém, não indica adequadamente a estabilidade de um alimento uma vez alimentos com o mesmo teor de água tem diferenças na estabilidade. Este comportamento se deve às diferenças de intensidade de ligação entre a água e constituintes não aquosos (DAMODARAN *et al.*, 2010).

É possível utilizar a termodinâmica para descrever o estado da água em uma matriz alimentícia sob uma variedade de condições externas, incluindo temperaturas de congelamento e ambiente e altas pressões. Atividade de água (a_w) é o termo utilizado para descrever o comportamento da água em materiais biológicos (REID, 2020). Segundo LEWIS; RANDALL, (1961), atividade é, em uma dada temperatura, a razão entre a fugacidade de uma substância (f) e sua fugacidade em um estado padrão (f^0), conforme Equação (1).

$$a = \left(\frac{f}{f^0}\right)_T \tag{1}$$

Fugacidade é a medida da tendência de escape de uma substância dada em unidade de pressão. O estado padrão se refere a amostra caracterizada sob condições bem definidas e convencionou-se a utilizar os dados desta condição como referência. Os dados do estado padrão devem ser aqueles obtidos na mesma temperatura em que o sistema está submetido. Estas definições são provenientes do estudo da termodinâmica de sistemas em equilíbrio. Logo, existem relações entre a atividade e outras propriedades termodinâmicas tais como energia livre, entalpia, potencial químico e pressão osmótica. Na ciência de alimentos é comum substituir a fugacidade pela pressão vapor de equilíbrio uma vez que os valores destas propriedades são aproximadamente iguais (REID, 2020).

Portanto, a atividade de água do sistema vapor d'água-matriz alimentícia pode ser definida pela Equação (2),

$$a_w = \left(\frac{p_w}{p_w^{eq}}\right)_T = \frac{\%\,UR}{100} \tag{2}$$

em que p_w é a pressão parcial da água, p_w^{eq} é a pressão de vapor da água no equilíbrio e %UR é a umidade relativa percentual da vizinhança (RAO *et al.*, 2014).

No estudo da conservação de alimentos, a estabilidade microbiológica de alimentos armazenados sob temperatura constante, depende mais da atividade de água no equilíbrio do que do teor de água total (CAURIE, 2007). A atividade de água descreve o estado da água e indica a sua disponibilidade para participar de reações de deterioração, químicas ou bioquímicas, ou ainda viabilizar a atividade microbiana. O conhecimento das relações de equilíbrio entre a matriz alimentícia e a atmosfera em que está submetida uma vez que a sorção de gases e vapor d'água afeta a qualidade e a conservação de um alimento. Em secagem, a atividade de água é relacionada com a teor de água de equilíbrio de um material biológico (TELIS; MAURO, 2016).

Na Figura 6 está apresentado um gráfico que relaciona as taxas das reações de oxidação lipídica, escurecimento não enzimático (reação de Maillard), reações hidrolíticas, atividade enzimática e crescimento microbiano com a atividade de água de um alimento.

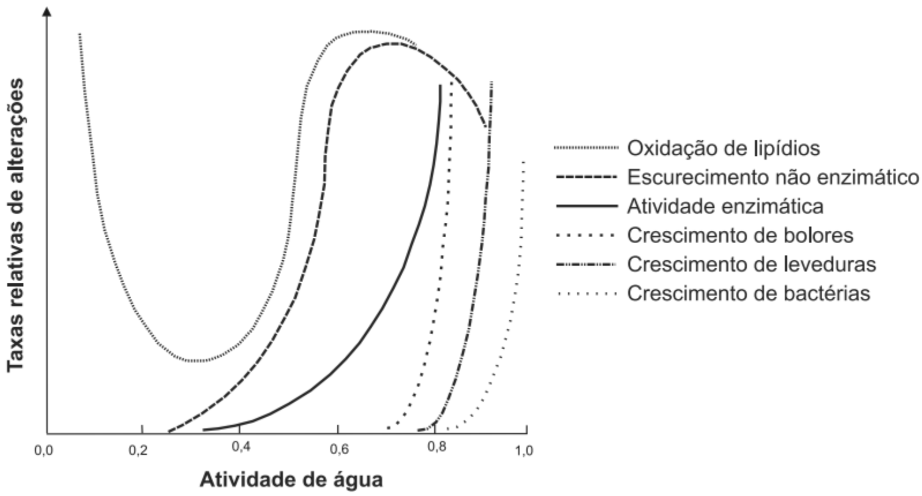

Figura 6 - Taxas relativas das principais alterações de alimentos em razão da atividade de água
Fonte: (AZEREDO, 2012)

De modo geral, as reações apresentadas na Figura 6 apresentam velocidade relativa expressivamente reduzida à medida que a_w tende a 0,2, exceto a oxidação de lipídios. A oxidação lipídica, por sua vez, é a única reação que ocorre em a_w abaixo de 0,20, e tem um aumento exponencial entre a faixa de 0,25 e 0,80. A velocidade relativa das reações de oxidação de lipídios é reduzida ao mínimo possível quando a_w = 0,3, e posteriormente, eleva-se bruscamente (VAN DER BERG, 1984).

Mesmo em atividades de água muito baixas, as reações químicas e enzimáticas podem acontecer. As reações de escurecimento não enzimático são favorecidas quando a atividade de água varia entre 0,20 e 0,80 (Figura 6). O aumento da atividade de água favorece as reações químicas e enzimáticas. A estabilidade das vitaminas também é afetada pela atividade de água do alimento. A degradação das vitaminas não deteriora o alimento, porém prejudica seu valor nutricional. As vitaminas B1 (tiamina), B2 (riboflavina) e C (ácido ascórbico) sofrem influência do valor de a_w do alimento. Cada vitamina tem uma faixa de valores de a_w em que é mais estável e uma faixa de valores em que sofre maior degradação. Esses valores são de difícil determinação uma vez que fatores como a composição da matriz alimentar em que está presente, temperatura e pH influenciam bastante na mensuração (BARBOSA-CÁNOVAS *et al.*, 2020; HARDMAN, 1987).

O crescimento microbiano é fortemente dependente da a_w, uma vez que cada microrganismo requer uma a_w mínima para o seu desenvolvimento. Grande parte dos microrganismos patógenos não se multiplicar em $a_w < 0,86$, ainda que outros fatores intrínsecos, como pH e disponibilidade de nutrientes e extrínsecos, como a temperatura, sejam ideais (BARBOSA-CÁNOVAS *et al.*, 2003; KAREL; LUND, 2003). Os fungos filamentosos são os microrganismos mais resistentes à redução da atividade de água, portanto, um dos principais responsáveis pela deterioração de alimentos na faixa de a_w entre 0,61 e 0,70. Nessa faixa de a_w não há competição com bactérias (BEUCHAT, 1983).

O valor mínimo de a_w requerido para o crescimento microbiano pode ser aumentado ou diminuído por fatores como mudança de pH, adição de sal, adição de agentes antimicrobianos, tratamento térmico, condições e tempo de estocagem (RAHMAN, 2007). Em geral, o valor ótimo para o crescimento dos microrganismos está entre 0,90 e 0,99, abaixo disso, o crescimento é moderado, retardado ou inibido (ARAÚJO *et al.*, 2005).

Um alimento com a_w por volta de 0,30 é muito estável quanto às reações de oxidação lipídica, reações de escurecimento não enzimático, reações hidrolíticas, atividade enzimática e crescimento de microrganismos (CELESTINO, 2010).

1.6 Isotermas de sorção

A curva do teor de água de um alimento (expressa como massa de água por unidade de massa de matéria seca) versus atividade de água, sob temperatura constante, é conhecida como isoterma de sorção de água (Figura 7). Estas curvas são utilizadas para estudar e controlar processos de concentração e desidratação, formular misturas alimentícias a fim de evitar a transferência de água entre os ingredientes, determinar as propriedades de barreira de umidade necessárias ao material de embalagem necessário à proteção de um sistema em particular, determinar o teor de água que reduzirá o crescimento microbiano de interesse em um sistema e, prever a estabilidade física e química dos alimentos em função de mudanças em seu teor de água (DAMODARAN *et al.*, 2010).

A isoterma de sorção pode ser determinada em duas direções: adsorção e dessorção. A primeira é obtida quando um material mais seco é colocado em um ambiente com umidade relativa mais altas. O ganho de massa, devido ao ganho de água, é medido após atingir o equilíbrio. A segunda é obtida colocando-se um material inicialmente úmido sob umidades relativas decrescentes, e, nesse caso, medindo-se a perda de massa após o equilíbrio (LABUZA, 1968).

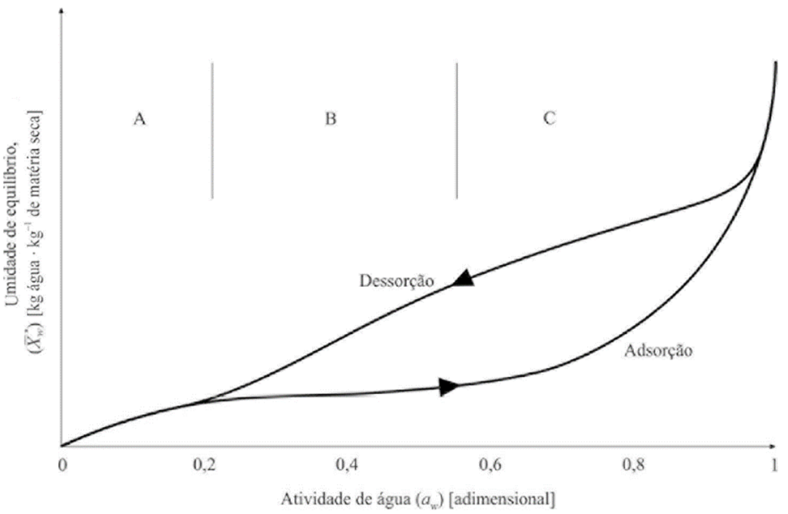

Figura 7 - Isotermas de adsorção e dessorção
Fonte: (TELIS; MAURO, 2016).

Intervalos de valores da atividade de água do material biológico podem ser utilizados para dividir as isotermas de sorção em três regiões. A primeira região é limitada a $a_w < 0,2$ e corresponde a água da monocamada, que está fortemente aderida a sítios polares de sorção. A segunda região, $0,2 < a_w < 0,6$, está relacionada à água ligada em macromoléculas mais distantes da superfície da matriz alimentícia. Por fim, a terceira região ($a_w < 0,6$) está relacionada à água relativamente livre para atuar como solvente em reações químicas (TELIS; MAURO, 2016).

Conforme apresentado na Figura 7, a isoterma de adsorção não coincide com a isoterma de dessorção, indicando a presença de histerese. A histerese está relacionada com a natureza e o estado dos componentes de um alimento. Pode refletir seus rearranjos estruturais e conformacionais, que alteram a acessibilidade de sítios polares energeticamente favoráveis e, portanto, podem dificultar o movimento da água. Não há modelos que descrevam quantitativamente o ciclo de histerese dos alimentos, e provavelmente não haverá solução final para esse problema por muito tempo (RAO *et al.*, 2014).

Os métodos experimentais para obtenção das isotermas de sorção são divididos em dinâmico e estático. Os métodos dinâmicos baseiam-se na mudança contínua da umidade relativa do ar ou da temperatura. As amostras são colocadas em uma micro balança e uma corrente de ar com umidade relativa e temperatura constante flui continuamente sobre eles. A exposição constante ao fluxo de ar e pequena massa da amostra reduzem o tempo de determinação de dias para horas, viabilizando a medição de pontos em altos níveis de a_w sem o risco de crescimento microbiano ou alterações físico-químicas na amostra. Por outro lado, nos métodos estáticos as amostras são mantidas em recipientes herméticos e fechados em contato com ar em umidade relativa constante e temperatura até que o equilíbrio entre a amostra e o ar sejam alcançados. Esses métodos podem ser classificados como higrométricos, manométrico e gravimétrico (CABALLERO-CERÓN *et al.*, 2015).

As isotermas de sorção podem ser classificadas segundo sua forma (Figura 8). A curva tipo I é conhecida como isoterma de Langmuir, obtida supondo adsorção monomolecular de um gás por sólidos porosos em um volume finito de vazios. A curva do tipo II é chamada de sigmoide ou formato de S e possui tendência assintótica à medida que a atividade de água se aproxima de 1. Já a curva do tipo III é conhecida como isoterma de Flory-Higgs. As demais curvas não possuem um nome especiais e os tipos II e III são as formas mais comuns em produtos alimentícios (BASU *et al.*, 2006; BRUNAUER *et al.*, 1940; MATHLOUTHI; ROGÉ, 2003).

Diversos modelos matemáticos são utilizados para descrever as isotermas de sorção. Dentre eles, os modelos de GAB (Guggenheim-Anderson-de Boer), Peleg, Halsey, Oswin e Henderson são os mais utilizados.

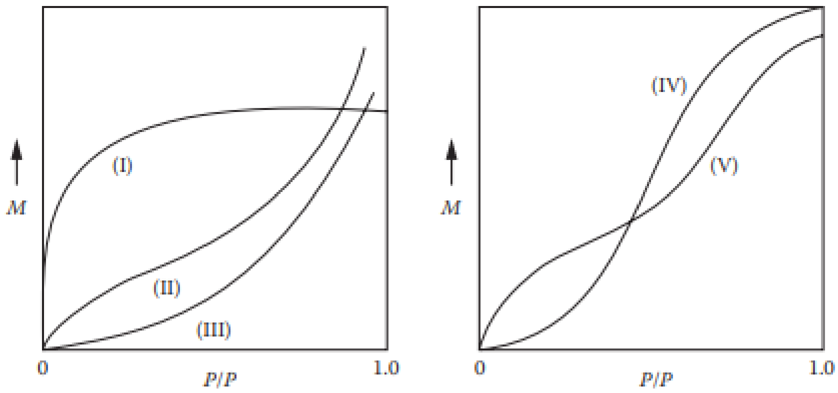

Figura 8 - Os cinco tipos de isotermas de sorção de van der Waals.
Fonte: (BRUNAUER et al., 1940).

1.6.1 Modelo de GAB

Em 1946, Anderson modificou o modelo de BET (Brunauer-Emmett-Teller) supondo que o calor de adsorção da segunda até a nona camada de água é menor que o calor latente de liquefação. Posteriormente, a equação de Anderson foi derivada cineticamente e estatisticamente por de Boer e Guggenheim, respectivamente, originando a equação (3) de GAB (LEWICKI, 2008).

$$X_{eq} = \frac{X_m C k a_w}{(1 - k a_w)(1 + (C - 1) k a_w)} \quad (3)$$

em que C é uma constante adimensional relacionada ao calor de sorção na região da monocamada e k é outra constante adimensional associada ao calor de sorção das multicamadas. Os parâmetros C e k podem ser calculados por uma equação do tipo Arrhenius.

$$C = C' exp\left(\frac{-\Delta H_c}{RT}\right) \quad (4)$$

$$k = k' exp\left(\frac{-\Delta H_k}{RT}\right) \quad (5)$$

em que $\Delta H_c = \Delta H_m - \Delta H_q$; $\Delta H_k = \Delta H_l - \Delta H_q$ (kJ mol^{-1}); ΔH_l é o calor de condensação da água pura (kJ mol^{-1}); ΔH_m é o calor de sorção total da monocamada (kJ mol^{-1}); ΔH_q é o calor de sorção total da multicamada que recobre a monocamada (kJ mol^{-1}); C' e k' são constantes das características entrópicas (BASU *et al.*, 2006). X_m é o teor de água da monocamada e é considerado independente da temperatura, contudo, em alguns casos diminui com o aumento da temperatura. Esse decréscimo pode estar relacionado a redução dos sítios de ligação água-matriz sólida como resultado da mudanças físicas e químicas causadas pela temperatura. A equação (6) apresenta a relação de X_m com a temperatura.

$$X_m = X_{m,0} exp\left(\frac{\Delta H_X}{RT}\right) \quad (6)$$

em que $X_{m,0}$ e ΔH_x (kJ mol^{-1}) são constantes (CABALLERO-CERÓN *et al.*, 2015).

1.6.2 Modelo de Peleg

A Equação (7) é um modelo semiempírico que possui 4 constantes (k_1, k_2, n_1, n_2) e pode descrever as isotermas com forma sigmoide ou não.

$$X_{eq} = k_1 a_w^{n_1} + k_2 a_w^{n_2} \quad (7)$$

As constantes relacionadas ao expoente da atividade possuem restrições, sendo que $n_1 < 1$ e $n_2 > 1$. Este modelo não é baseado na suposição da existência de uma monocamada bem delimitada de água adsorvida, porém, a plotagem de $a_w /[X_{eq}(1 - a_w)]$ vs a_w resulta em um gráfico quase linear, semelhante ao utilizado para calcular o teor de água da monocamada via modelo de BET (PELEG, 1993).

1.6.3 Modelo de Oswin

Este modelo é baseado na expansão das séries de Pearson para curvas sigmoides aplicadas às isotermas do tipo II. Este modelo é um dos mais apropriados para descrever as isotermas de sorção de alimentos amiláceos e apresenta ajuste razoável à dados de carnes e vegetais (BOQUET *et al.*, 1978).

$$X_{eq} = M\left(\frac{a_w}{1-a_w}\right)^{N} \quad (8)$$

em que M e N são constantes do modelo. O parâmetro M apresenta comportamento linear quando plotado em função da temperatura e em razão disso, o modelo de Oswin pode tomar duas formas algébricas como apresentado nas equações (9) e (10)

$$X_{eq} = (A+BT)\left(\frac{a_w}{1-a_w}\right)^{N} \quad (9)$$

$$a_w = \left[\left(\frac{X_{eq}}{A+BT}\right)^{-C} + 1\right]^{-1} \quad (10)$$

em que C = 1/N.

1.6.4 *Modelo de Halsey*

O modelo proposto por HALSEY (1948) descreve a condensação das multicamadas, considerando que a energia potencial da molécula de água varia inversamente ao h_2-ésimo da sua distância da superfície (BASU *et al.*, 2006).

$$X_{eq} = (-h_1\, ln(a_w))^{-\frac{1}{h_2}} \quad (11)$$

1.6.5 *Modelo de Henderson*

Uma relação empírica entre a água adsorvida e a atividade de água é utilizada para descrever as isotermas de sorção de produtos alimentícios via modelo de HENDERSON (1952).

$$X_{eq} = \left(-\frac{1}{H_1}\, ln\, a_w\right)^{\frac{1}{H_2}} \quad (12)$$

Os modelos matemáticos visam a predição do teor de água de equilíbrio de um material a uma dada atividade de água, ou vice-versa, sob uma temperatura. Portanto, eles viabilizam a determinação das melhores condições de armazenamento de produtos, shelf-life e otimização de processos de secagem. Ademais, podem atuam como ferramentas para estimativa de parâmetros termodinâmicos que contribuem para a melhor compreensão das alterações físicas e químicas que ocorrem em produtos desidratados (ERBAŞ *et al.*, 2016).

1.7 Propriedades termodinâmicas de sorção de água

A determinação das propriedades termodinâmicas de sorção auxiliam na elucidação do fenômeno de interações moleculares entre a água e o sorvente (AGUERRE *et al.*, 1986; BERISTAIN *et al.*, 1996), bem como são necessárias para o design de equipamentos.

Entretanto, há bastante discordância no que tange a validade das quantidades termodinâmicas calculadas para sistemas alimentícios pois assume-se um equilíbrio verdadeiro e logo, que todas as mudanças ocorridas no sistema são reversíveis. Contudo, a presença da histerese é a manifestação da irreversibilidade. Por outro lado, os dados de sorção oferecem limites inferiores e superiores para uma isoterma "verdadeira" e consequentemente, também limita as quantidades termodinâmicas (RIZVI, 2014).

As moléculas de água da monocamada estão fortemente ligadas à matriz sólida alimentícia. À medida que o teor de água do alimento se aproxima do teor de água da monocamada, a diferença entre a entalpia de vaporização de água adsorvida e o calor latente de vaporização da água pura aumenta. O calor de vaporização da água adsorvida é chamado de calor isostérico de sorção e é utilizado no projeto de sistemas de desidratação, uma vez que este informa o requerimento de energia para evaporar a água. Em sistemas termodinâmicos alimentícios, esta propriedade pode ser calculada via equação de Clausius-Clayperon (13) (ESCOBEDO-AVELLANEDA *et al.*, 2020).

$$\left.\frac{\partial(\ln a_w)}{\partial(1/T)}\right|_{X_{eq}} = -\frac{Q_{st}-\lambda}{R} = -\frac{q_{st}}{R} \quad (13)$$

em que a_w é a atividade de água, T é a temperatura, Q_{st} é o calor isostérico de sorção, q_{st} é o calor isostérico líquido de sorção e R é a constante universal dos gases.

O calor isostérico de sorção depende fortemente do teor de água do alimento. Na Figura 9 observa-se que à medida que o teor de água aumenta e a_w se aproxima de 1,0, tendendo ao calor de vaporização da água pura (λ_{vap}). Os valores são mais altos em baixos valores de teor de água (<20%) porque as moléculas de água nesta zona se ligam diretamente aos componentes do alimento. Em produtos com alto teor de açúcar, os valores de q_{st} são maiores do que em produtos de conteúdo de fibra porque no primeiro, as moléculas de água formam ligações de hidrogênio com moléculas de açúcar e mais energia será necessária para quebrá-las (GABAS *et al.*, 1999).

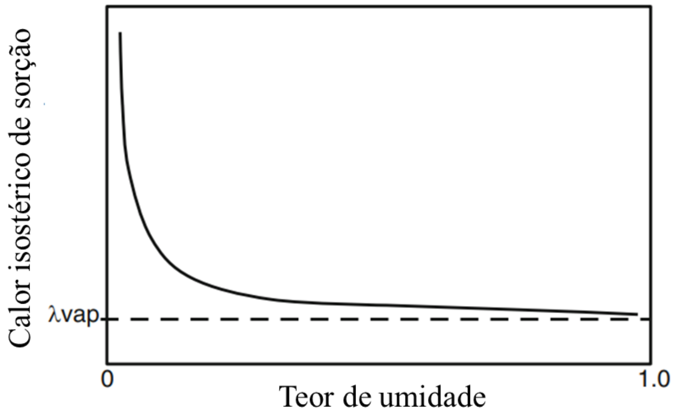

Figura 9 - Calor isostérico de sorção em função do teor de água.
Fonte: Adaptado de CABALLERO-CERÓN et al., (2015)

As variações de entalpia (ΔH) estão associadas as mudanças de energia devido à interação molecular entre moléculas de água e sorvente durante os processos de sorção, enquanto as variações de entropia (ΔS) podem estar associadas às forças de ligação e/ou forças de repulsão no sistema (APOSTOLOPOULOS; GILBERT, 1990; BERISTAIN *et al.*, 1996). A atividade de água se relaciona com as variações de entalpia e entropia segundo a Equação 14.

$$\ln a_w = \frac{\Delta H}{RT} - \frac{\Delta S}{R} \quad (14)$$

A energia livre de Gibbs (ΔG) está relacionada à afinidade da água à matriz e fornece informação sobre a espontaneidade do processo de sorção (APOSTOLOPOULOS; GILBERT, 1990; BERISTAIN *et al.*, 1996). A atividade de água se relaciona com a energia livre de Gibbs segundo a Equação 15.

$$\Delta G = RT \ln a_w \quad (15)$$

Quando se agrupa a Equação 14 na Equação 15, obtém-se uma relação linear para o cálculo da energia livre de Gibbs em função da entalpia e da entropia, dada pela Equação 16, conhecida como equação de Van't Hoff. Esta equação também é muito utilizada para verificar compensações cinéticas e termodinâmicas em muitos processos químicos, físicos, biológicos e alimentares.

$$\Delta H = \mathrm{T}\Delta S + \Delta G \quad (16)$$

A compensação cinética pode ser avaliada para qualquer processo e, quando ocorre, fornece informações sobre o mecanismo da reação e se a reação é controlada por entalpia ou entropia. Um processo é controlado pela entalpia, quando uma mudança na variável ambiental (neste caso, a atividade de água) causaria uma sensibilidade à temperatura superior a agitação. Por outro lado, se o mesmo processo é controlado pela entropia, a mesma mudança na variável ambiental resultaria uma sensibilidade à agitação superior a temperatura (GARVÍN *et al.*, 2017). A energia livre de Gibbs também pode ser utilizada para avaliar a espontaneidade do processo, sendo espontâneo quando $\Delta G < 0$ e não espontâneo quando $\Delta G > 0$ (MCMINN *et al.*, 2005).

Uma consequência matemática da compensação cinética é a temperatura isocinética, definida como a temperatura na qual a constante cinética deve ser a mesma independentemente da variável ambiental (pH, pressão, atividade de água). A compensação termodinâmica pode ser encontrada para qualquer processo que envolva um equilíbrio e consiste na relação linear entre a variação de entalpia e entropia, ambas previamente obtidas a partir da equação de Van't Hoff para diferentes valores de uma variável ambiental. Uma consequência matemática da compensação termodinâmica é a temperatura de isoequilíbrio, definida como a temperatura na qual a constante de equilíbrio deve ser a mesma independentemente da variável ambiental. De acordo com a teoria do estado de transição, algumas constantes cinéticas podem ser relacionadas à constante de equilíbrio do estágio de equilíbrio inicial entre os reagentes e o estado de transição. Para estes casos, pode-se concluir que ambas as compensações estão relacionadas matematicamente e, portanto, não só a existência de um tipo de compensação implica a existência do outro, mas as temperaturas isocinética e isoequilíbrio devem ser as mesmas, ou pelo menos muito próximas uns aos outros (GARVÍN *et al.*, 2017).

A temperatura isocinética (T_B) estimada pela Equação de Van’t Hoff é comparada a uma média harmônica (T_{hm}), obtida pela Equação 17, com o objetivo de determinar se o fenômeno de sorção é controlado pela entalpia ou pela entropia. Quando a $T_B > T_{hm}$, a sorção controlada pela entalpia e quando $T_B > T_{hm}$, a sorção é guiada pela entropia (AGUERRE *et al.*, 1986; GABAS *et al.*, 1999).

$$T_{hm} = \frac{n}{\sum_{i=1}^{n}\left(\frac{1}{T}\right)} \tag{17}$$

1.8 Desidratação de alimentos: Secagem

A desidratação é um tradicional método de conservação de alimentos, também é utilizada para a produção de alimentos especiais, ingredientes alimentares e resíduos de alimentos (SARAVACOS; KOSTAROPOULOS, 2016).

A desidratação de alimentos pode ser realizada por duas maneiras: secagem e liofilização. A secagem é definida como uma operação unitária que transforma um material sólido, semissólido ou líquido, em um produto sólido com teor de água relativamente baixo. Esta operação unitária também implica na transferência de água do material para uma fase gasosa não saturada. Geralmente, a remoção de água acontece via evaporação que é realizada fornecendo energia térmica a fim de provocar a mudança de fase da água líquida para vapor. Já a liofilização o vapor de água é o resultado da sublimação do gelo (TELIS; MAURO, 2016).

A desidratação dos alimentos é realizada por transferência de calor externa e interna, ou seja, do ambiente para a superfície do alimento e da superfície para o interior. Simultaneamente, o aumento da temperatura induz a transferência de água interna através do interior do alimento para a superfície. A transferência de calor externa pode ocorrer por meio de qualquer um dos três mecanismos de transferência, seja o processo adiabático ou não adiabático. Na secagem adiabática, a transferência por convecção ocorre principalmente quando uma corrente de ar quente flui externamente sobre a estrutura do alimento, enquanto a transferência por condução é mais comum dentro do produto devido a um gradiente interno de temperatura (BARBOSA-CÁNOVAS; JULIANO, 2020).

A transferência de calor do ambiente circundante faz com que a água interna seja transportada para a superfície do produto na forma líquida e depois evaporada, ou evaporada internamente em uma interface líquido-vapor e depois transportada como vapor para a superfície (OKOS *et al.*, 1992). Por exemplo, quando um alimento encontra ar quente e seco, o ar úmido que forma um filme ao redor da superfície do alimento é levado pela corrente de ar em movimento. A remoção do vapor de água estabelece um gradiente de pressão do interior do alimento para o ar seco, que fornece a força motriz por trás da remoção da água. O filme é de espessura variável dependendo da velocidade do ar que recebe. Quanto mais espesso o filme, menor é o coeficiente de transferência de calor e menor a quantidade de água removida (BARBOSA-CÁNOVAS; JULIANO, 2020).

O movimento da água nos alimentos pode ocorrer por quatro mecanismos de transporte e suas combinações: escoamento capilar – devido a gradientes de pressão de sucção capilar, especialmente em leitos de pó e sólidos porosos onde a tensão superficial do material está envolvida; difusão líquida – devido aos gradientes de concentração entre as profundidades do alimento e a superfície; o mecanismo mais comumente considerado para modelagem de processos de secagem.; difusão de vapor – devido a gradientes parciais de pressão de vapor; escoamento viscoso – devido a gradientes de pressão total, causados por pressão externa ou altas temperaturas (CRAPISTE; ROTSTEIN, 1997; GEANKOPLIS, 1993).

Uma grande variedade de equipamentos industriais de secagem de alimentos é utilizada e foi desenvolvida principalmente, de modo empírico, mas continuamente aprimorado pelos recentes avanços na tecnologia de secagem e engenharia de alimentos. Além dos requisitos básicos de engenharia de processo, os secadores de alimentos devem atender aos rigorosos padrões de qualidade e segurança de alimentos (SARAVACOS; KOSTAROPOULOS, 2016).

As operações de secagem reduzem o teor de água dos alimentos para evitar o crescimento microbiano e a deterioração, aumentar a vida de prateleira, minimizar a quantidade de embalagens e melhorar o armazenamento facilitando o transporte. Pesquisadores mostraram que confiar apenas em práticas experimentais de secagem sem considerações matemáticas para a cinética de secagem, pode afetar a eficiência dos secadores, aumentar o custo de produção e reduzir a qualidade do produto seco. Um modelo eficaz é necessário para o projeto, otimização, integração e controle de energia; portanto, o uso de modelos matemáticos para encontrar a cinética de secagem de produtos vegetais é muito importante (INYANG *et al.*, 2018).

1.9 Cinética de secagem

A cinética de secagem é uma função das características do material (propriedades físicas, dimensões) e das propriedades do ambiente de secagem, incluindo temperatura, umidade e velocidade do ar, pressão da câmara, potência de micro-ondas, ultrassom intensidade e outros fatores dependendo do método de secagem utilizado (MICHAILIDIS; KROKIDA, 2014).

O teor de água de um alimento, durante um processo de secagem, apresenta o comportamento mostrado pela curva da Figura 10. O segmento AB corresponde ao período de adaptação do alimento às condições de secagem e sua temperatura atinge um valor constante. Durante o período BC, denominado período de secagem constante, a água forma um filme contínuo na superfície exposta do alimento, que se comporta como se não existisse sólido, ou seja, a água do alimento não encontra resistência para “sair” dele. O ponto C marca o fim do período de secagem constante, e o alimento atinge o teor de água conhecido como teor de água crítico. A partir desse momento, há um aumento na resistência interna e o movimento de líquido do interior para a superfície do sólido não é capaz de compensar o líquido que está sendo evaporado, iniciando-se o primeiro período de taxa decrescente (CELESTINO, 2010).

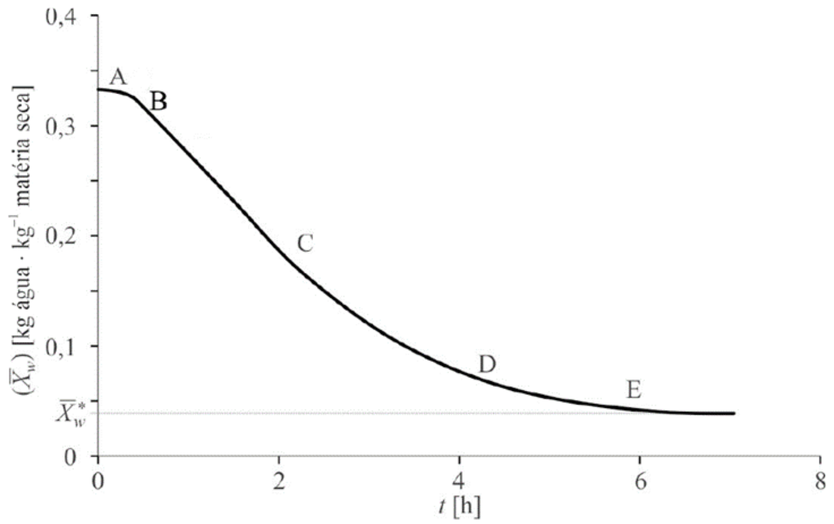

Figura 10 - Curva típica de secagem
Fonte: (TELIS; MAURO, 2016)

No período CD, primeiro período de taxa decrescente, a superfície do alimento se torna cada vez mais seca pois há cada vez menos líquido está na superfície do sólido para evaporar, podendo haver rachaduras na superfície do alimento. O ponto D marca o início do segundo período de taxa decrescente, em que o teor de água do alimento diminui até atingir a teor de água de equilíbrio para as condições de temperatura e umidade relativa do ar. Quando o teor mínimo de água (teor de água de equilíbrio) é atingido, encerra-se o processo de secagem. Alcança-se o teor de água de equilíbrio quando o alimento é mantido por longo período em determinada condição de temperatura e umidade relativa do ar que o envolve. Nessa condição, a pressão parcial de vapor da água na superfície do produto é igual à pressão parcial de vapor de água contida no ar (CELESTINO, 2010).

O mecanismo descrito anteriormente pode ser mais bem compreendido com auxílio da Figura 11 em que está apresentada a taxa de secagem em função do teor de água de um alimento.

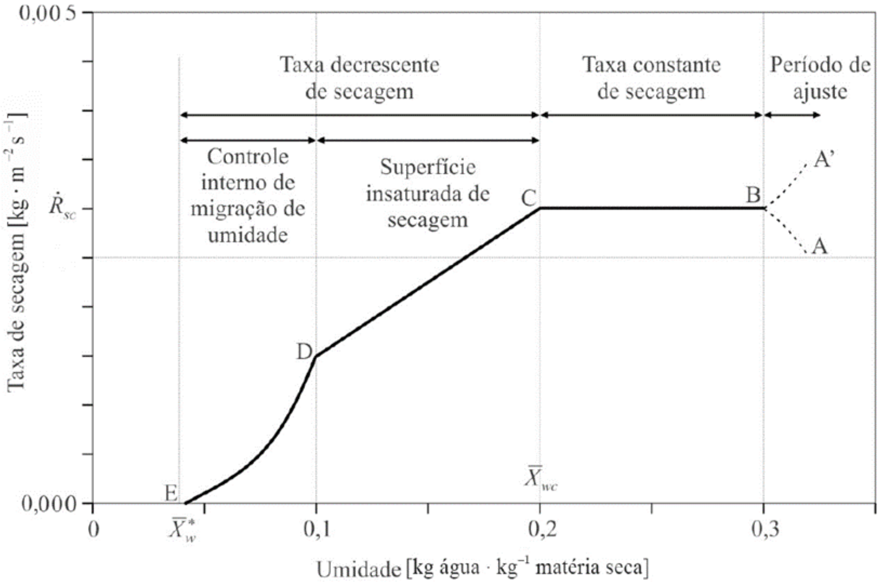

Figura 11 - Taxa de secagem em função do teor de água.
Fonte: (TELIS; MAURO, 2016)

Uma vez que o principal mecanismo na secagem de sólidos é a difusão de água, a lei de Fick (Equação 18) pode ser aplicada a um sistema unidimensional.

$$\frac{\partial X}{\partial t} = D_{eff}\,\frac{\partial^2 X}{\partial^2 x^2} \tag{18}$$

em que X é o teor de água (g H_2O/g sólidos secos), t é o tempo (segundos), D_{eff} é o coeficiente de difusão efetivo (m^2/s), e x é a distância (metros).

De acordo com a lei de Fick, D_{eff} é considerado constante e difusão unidirecional, assumindo que a resistência à transferência de massa e a mudança de volume na perda ou ganho de água são considerados desprezíveis (LABUZA; ALTUNAKAR, 2020a). CRANK, (1975) propôs uma solução para a Equação 18 considerando a geometria da matriz sólida. Portanto, a equação diferencial de Fick pode assumir diferentes formas regulares, algumas das quais são usadas para determinar D_{eff} experimentalmente. As Equações 19, 20, 21, são a soluções da lei de Fick para placa plana, esfera e cilindro infinito, respectivamente.

$$RX = \frac{\bar{X} - X_{eq}}{X_0 - X_{eq}} = \frac{8}{\pi^2}\sum_{n=0}^{\infty}\frac{1}{(2n+1)^2}\,exp\left(\frac{-(2n+1)^2\,\pi^2 D_{eff}t}{4l^2}\right) \tag{19}$$

$$RX = \frac{\bar{X} - X_{eq}}{X_0 - X_{eq}} = \frac{6}{\pi^2}\sum_{n=0}^{\infty}\frac{1}{n^2}\,exp\left(\frac{-n^2\,\pi^2 D_{eff}t}{r^2}\right) \tag{20}$$

$$RX = \frac{\bar{X} - X_{eq}}{X_0 - X_{eq}} = \frac{4}{r_a^2}\sum_{n=0}^{\infty}\frac{1}{\beta_n^2}\,exp\left(-\beta_n^2 D_{eff}t\right) \tag{21}$$

em que: RX é a razão de teor de água (adimensional), $\bar{X}$ é o teor de água médio do produto, X_0 é o teor de água inicial, D_{eff} é o coeficiente de difusão, t é o tempo, l é a meia espessura da placa, r é o raio da esfera, β são as raízes da função de Bessel de ordem zero e r_a é o raio do cilindro.

A dependência do coeficiente de difusão (D_{eff}) em relação a temperatura é comumente representada em função da expressão de Arrhenius (BARBOSA-CÁNOVAS; VEGA-MERCADO, 1996; CRAPISTE; ROTSTEIN, 1997).

$$D_{eff} = D_0(X)\ exp\left[\frac{\Delta E_a(X)}{RT}\right] \quad (22)$$

em que $D_0(X)$ é um termo de difusividade dependente de umidade, ΔE_a (X) (cal/mol) é a energia de ativação do processo de difusão, X é o teor de água fixo, R é a constante do gás (1,987 cal/mol·K) e T (K) é a temperatura.

A cinética de secagem substitui os complexos modelos matemáticos para a descrição dos fenômenos simultâneos de transporte de calor e massa no camadas internas do material de secagem e na interface com o espaço circundante (MICHAILIDIS; KROKIDA, 2014). Os modelos de cinética de secagem não consideram os efeitos das interações por outros parâmetros além do tempo de secagem (INYANG *et al.*, 2018).

Há vários modelos matemáticos, teóricos, semiteóricos ou semiempíricos e empíricos, comumente utilizados para descrever o comportamento da razão de teor de água de um alimento em função do tempo. Na Tabela 1 estão apresentados diversos modelos matemáticos empregados para descrever a cinética de secagem de produtos agrícolas.

Tabela 1 - Modelos matemáticos empregados em cinética de secagem de produtos alimentícios

Modelo	Equação
Lewis/Newton	$RX = exp(-kt)$
Page	$RX = exp(-kt^n)$
Page modificado	$RX = exp[(-kt)^n]$
Henderson e Pabis	$RX = a \cdot exp(-kt)$
Logaritmo	$RX = a \cdot exp(-kt) + c$
Dois termos	$RX = a \cdot exp(-k_0 t) + b \cdot exp(-k_1 t)$
Aproximação da difusão	$RX = a \cdot exp(-kt) + (1-a)exp(-kbt)$

Wang e Singh	$RX = M_0 + at + bt^2$
Weibull	$RX = exp\left[-\left(\frac{t}{a}\right)^b\right]$
Midilli	$RX = a \cdot exp(-kt^n) + bt$
Silva	$RX = exp(-at - bt^{0,5})$

em que RX é a razão de umidade, t é o tempo e a, b, k, k_0, k_1 e n são constantes dos modelos

Os modelos teóricos são derivados da segunda lei da difusão de Fick, enquanto os semiteóricos são geralmente derivados da segunda lei de Fick e suas modificações e também da lei de resfriamento de Newton. Por outro lado, os modelos empíricos de secagem objetivam apenas uma relação direta entre a razão de teor de água e o tempo de secagem (ERBAY; ICIER, 2010; FERNANDO; AMARASINGHE, 2016; PANCHARIYA *et al.*, 2002).

1.10 REFERÊNCIAS

ABRAMO, M. A. **Taioba, cará e inhame: o grande potencial inexplorado**. São Paulo: Ícone, 1990. 1990.

ABRANDH. **O Direito Humano à Alimentação Adequada e o Sistema Nacional de Segurança Alimentar e Nutricional**. Brasília: ABRANDH, 2013. 2013. Disponível em: http://www.mds.gov.br/webarquivos/publicacao/seguranca_alimentar/DHAA_SAN.pdf.

AGOSTINI-COSTA, T. S. Bioactive compounds and health benefits of Pereskioideae and Cactoideae: A review. **Food Chemistry**, [*s. l.*], v. 327, n. April, 2020.

AGUERRE, R. J.; SUÁREZ, C.; VIOLLAZ, P. E. Enthalpy-Entropy Compensation in Sorption Phenomena: Application to the Prediction of the Effect of Temperature on Food Isotherms. **Journal of Food Science**, [*s. l.*], v. 51, n. 6, p. 1547–1549, 1986. Disponível em: https://onlinelibrary.wiley.com/doi/10.1111/j.1365-2621.1986.tb13856.x.

APOSTOLOPOULOS, D.; GILBERT, S. G. Water Sorption of Coffee Solubles by Frontal Inverse Gas Chromatography: Thermodynamic Considerations. **Journal of Food Science**, [*s. l.*], v. 55, n. 2, p. 475–487, 1990.

ARAÚJO, S. de S.; ARAÚJO, P. de S.; GIUNCO, A. J.; SILVA, S. M.; ARGANDOÑA, E. J. S. Bromatology, food chemistry and antioxidant activity of Xanthosoma sagittifolium (L.) Schott. **Emirates Journal of Food and Agriculture**, [*s. l.*], v. 31, n. 3, p. 188–195, 2019.

ARAÚJO, L. F.; OLIVEIRA, L. S. C.; PERAZZO NETO, A.; ALSINA, O. L. S.; SILVA, F.

L. H. Equilíbrio higroscópico da palma forrageira: relação com a umidade ótima para fermentação sólida. **Revista Brasileira de Engenharia Agrícola e Ambiental**, [*s. l.*], v. 9, n. 3, p. 379–384, 2005.

AZEREDO, H. M. C. De. **Fundamentos de estabilidade de alimentos**. Embrapa Ined. Brasília: Embrapa, 2012. Disponível em: http://scholar.google.com/scholar?hl=en&btnG=Search&q=intitle:Fundamentos+de+estabilidade+de+alimentos#0.

BARBOSA-CÁNOVAS, G. V.; FERNÁNDEZ-MOLINA, J. J.; ALZAMORA, S. M.; TAPIA, M. S.; LÓPEZ-MALO, A.; CHANES, J. W. **Handling and Preservation of Fruits and Vegetables by Combined Methods for Rural Areas**. Rome: FAO, 2003. 2003.

BARBOSA-CÁNOVAS, G. V.; FONTANA, A. J.; SCHMIDT, S. J.; LABUZA, T. P. **Water Activity in Foods**. 2nd. ed. Chicago: John Wiley & Sons, 2020. 2020. Disponível em: https://onlinelibrary.wiley.com/doi/book/10.1002/9781118765982.

BARBOSA-CÁNOVAS, G. V.; JULIANO, P. Desorption Phenomena in Food Dehydration Processes. *In*: BARBOSA-CÁNOVAS, Gustavo V.; FONTANA JR., Anthony J.; SCHMIDT, Shelly J.; LABUZA, Theodore P. (org.). **Water Activity in Foods**. 2nd. ed. Chicago: John Wiley & Sons, 2020. p. 425–452. Disponível em: https://onlinelibrary.wiley.com/doi/abs/10.1002/9781118765982.ch17.

BARBOSA-CÁNOVAS, G. V.; VEGA-MERCADO, H. **Dehydration of Foods**. New York: Chapman & Hall, 1996. 1996.

BASU, S.; SHIVHARE, U. S.; MUJUMDAR, A. S. Models for sorption isotherms for foods: A review. **Drying Technology**, [*s. l.*], v. 24, n. 8, p. 917–930, 2006.

BERISTAIN, C. I.; GARCIA, H. S.; AZUARA, E. Enthalpy-entropy compensation in food vapor adsorption. **Journal of Food Engineering**, [*s. l.*], v. 30, n. 3–4, p. 405–415, 1996.

BEUCHAT, L. R. Influence of Water Activity on Growth, Metabolic Activities and Survival of Yeasts and Molds. **Journal of Food Protection**, [*s. l.*], v. 46, n. 2, p. 135–141, 1983. Disponível em: https://meridian.allenpress.com/jfp/article/46/2/135/165746/Influence-of-Water-Activity-on-Growth-Metabolic.

BIONDO, E.; FLECK, M.; KOLCHINSKI, E. M.; SANT’ANNA, V. Diversidade e potencial de utilização de plantas alimentícias não convencionais no Vale do Taquari,RS. **Revista Eletrônica Científica da UERGS**, [*s. l.*], v. 4, n. 1, p. 61–90, 2018.

BOQUET, R.; CHIRIFE, J.; IGLESIAS, H. A. Equations for fitting water sorption isotherms of foods: II. Evaluation of various two-parameter models. **International Journal of Food Science & Technology**, [*s. l.*], v. 13, n. 4, p. 319–327, 1978.

BOUAZIZ, M. A.; BCHIR, B.; BEN SALAH, T.; MOKNI, A.; BEN HLIMA, H.; SMAOUI, S.; ATTIA, H.; BESBES, S. Use of Endemic Date Palm (Phoenix dactylifera L.) Seeds as an Insoluble Dietary Fiber: Effect on Turkey Meat Quality. **Journal of Food Quality**, [*s. l.*], v. 2020, 2020.

BRASIL, MINISTÉRIO DA AGRICULTURA, P. e A. **Hortaliças não-convencionais: (tradicionais)**. Brasília: MAPA/ACS, 2010. 2010. Disponível em: https://www.abcsem.com.br/docs/cartilha_hortalicas.pdf.

BRUNAUER, S.; DEMING, L. S.; DEMING, W. E.; TELLER, E. On the theory of the van der Waals adsorption of gases. **Journal of the American Chemical Society**, [*s. l.*], v. 62, n. 7, p. 1723–1732, 1940.

BURITY, V.; FRANCESCHINI, T.; VALENTE, F.; RECINE, E.; LEÃO, M.; CARVALHO, M. F. **Direito Humano à Alimentação Adequada no Contexto da Segurança Alimentar e Nutricional**. Brasília: ABRANDH, 2010.

CABALLERO-CERÓN, C.; GUERRERO-BELTRÁN, J. A.; MÚJICA-PAZ, H.; TORRES, J. A.; WELTI-CHANES, J. Moisture Sorption Isotherms of Foods: Experimental Methodology, Mathematical Analysis, and Practical Applications. *In*: WATER STRESS IN BIOLOGICAL, CHEMICAL, PHARMACEUTICAL AND FOOD SYSTEMS. [*S. l.: s. n.*], 2015. p. 187–214. Disponível em: http://link.springer.com/10.1007/978-1-4939-2578-0_15.

CAMPI, M.; DUEÑAS, M.; FAGIOLO, G. Specialization in food production affects global food security and food systems sustainability. **World Development**, [*s. l.*], v. 141, p. 105411, 2021. Disponível em: https://doi.org/10.1016/j.worlddev.2021.105411.

CARVALHO, S. I. C.; BIANCHETTI, L. B.; RIBEIRO, C. S. C.; LOPES, C. A. **Pimentas do gênero Capsicum no Brasil.** Brasília: Embrapa Hortaliças, 2006. 2006.

CAURIE, M. Hysteresis phenomenon in foods. **International Journal of Food Science and Technology**, [*s. l.*], v. 42, n. 1, p. 45–49, 2007.

CELESTINO, S. M. C. **Princípios de secagem de alimentos**. Planaltina: Embrapa Cerrados, 2010. 2010.

COLE, M. B.; AUGUSTIN, M. A.; ROBERTSON, M. J.; MANNERS, J. M. The science of food security. **npj Science of Food**, [*s. l.*], v. 2, n. 1, p. 1–8, 2018. Disponível em: http://dx.doi.org/10.1038/s41538-018-0021-9.

CORRÊA, P. C.; OLIVEIRA, G. H. H. de; OLIVEIRA, A. P. L. R. de; GONELI, A. L. D.; SILVA, M. G. Condições ambientais seguras para o armazenamento de folhas de fumo. **Revista de Ciências Agrarias - Amazon Journal of Agricultural and Environmental Sciences**, [*s. l.*], v. 59, n. 2, p. 106–112, 2016. Disponível em: http://doi.editoracubo.com.br/10.4322/rca.2105.

CRANK, J. **The Mathematics of Diffusion**. 2. ed. Oxford, UK: Clarendon Press, 1975.

CRAPISTE, G. H.; ROTSTEIN, E. Design and performance evaluation of dryers. *In*: HANDBOOK OF FOOD ENGINEERING PRACTICE. Boca Raton: CRC Press, 1997.

CRUZ-GARCIA, G. S. Management and Motivations to Manage “Wild” Food Plants. A Case Study in a Mestizo Village in the Amazon Deforestation Frontier. **Frontiers in Ecology and Evolution**, [*s. l.*], v. 5, 2017. Disponível em: http://journal.frontiersin.org/article/10.3389/fevo.2017.00127/full.

DAMODARAN, S.; PARKIN, K. L.; FENNEMA, O. R. **Química de alimentos de Fennema**. 4. ed. Porto Alegre: Artmed, 2010. 2010.

DE ALMEIDA, M. E. F.; JUNQUEIRA, A. M. B.; SIMÃO, A. A.; CORRÊA, A. D. Caracterização química das hortaliças não-convencionais conhecidas como ora-pro-nobis. **Bioscience Journal**, [*s. l.*], v. 30, n. 3 SUPPL. 1, p. 431–439, 2014.

DUARTE, M. R.; HAYASHI, S. S. Estudo anatômico de folha e caule de Pereskia aculeata Mill. (Cactaceae). **Revista Brasileira de Farmacognosia**, [*s. l.*], v. 15, n. 2, p. 103–109, 2005.

ERBAŞ, M.; AYKIN, E.; ARSLAN, S.; DURAK, A. N. Adsorption behaviour of bulgur. **Food Chemistry**, [*s. l.*], v. 195, p. 87–90, 2016. Disponível em: https://linkinghub.elsevier.com/retrieve/pii/S0308814615009425.

ERBAY, Z.; ICIER, F. A Review of Thin Layer Drying of Foods: Theory, Modeling, and Experimental Results. **Critical Reviews in Food Science and Nutrition**, [*s. l.*], v. 50, n. 5, p. 441–464, 2010. Disponível em: https://www.tandfonline.com/doi/full/10.1080/10408390802437063.

ESCOBEDO-AVELLANEDA, Z.; RODRÍGUEZ-MARTÍNEZ, V.; SERMENT-MORENO,

V.; VELÁZQUEZ, G.; WELTI-CHANES, J.; TORRES, J. A. Selected Applications of Water Activity Management in the Food Industry. *In*: BARBOSA-CÁNOVAS, Gustavo V.; FONTANA JR., Anthony J.; SCHMIDT, Shelly J.; LABUZA, Theodore P. (org.). **Water Activity in Foods**. 2nd. ed. Chicago: John Wiley & Sons, 2020. p. 465–482. Disponível em: https://onlinelibrary.wiley.com/doi/abs/10.1002/9781118765982.ch19.

FAO. **Rome Declaration on World Food SecurityWorld Food Summit**. Roma: [*s. n.*], 1996.

FAO; IFAD; UNICEF; WFP; WHO. **In brief to The state of food security and nutrition in the world. Transforming food systems for food security, improved nutrition and affordable healthy diets for all**. Rome: [*s. n.*], 2021.

FARIA, R. Q. de; TEIXEIRA, I. R.; DEVILLA, I. A.; ASCHERI, D. P. R.; RESENDE, O. Cinética de secagem de sementes de crambe. **Revista Brasileira de Engenharia Agrícola e Ambiental**, [*s. l.*], v. 16, n. 5, p. 573–583, 2012. Disponível em: http://www.scielo.br/scielo.php?script=sci_arttext&pid=S1415-43662012000500014&lng=pt&tlng=pt.

FELLOWS, P. J. **Tecnologia do processamento de alimentos: princípios e práticas**. 4. ed. Porto Alegre: Artmed, 2019. 2019.

FERNANDO, J. A. K. M.; AMARASINGHE, A. D. U. S. Drying kinetics and mathematical modeling of hot air drying of coconut coir pith. **SpringerPlus**, [*s. l.*], v. 5, n. 1, p. 807, 2016. Disponível em: http://springerplus.springeropen.com/articles/10.1186/s40064-016-2387-y.

GABAS, A. L.; TELIS-ROMERO, J.; MENEGALLI, F. C. Thermodynamic model for water sorption by grape skin and pulp. **Drying Technology**, [*s. l.*], v. 17, n. 4–5, p. 962–974, 1999. Disponível em: http://www.tandfonline.com/doi/abs/10.1080/07373939908917584.

GARCIA, J. A. A.; CORRÊA, R. C. G.; BARROS, L.; PEREIRA, C.; ABREU, R. M. V.; ALVES, M. J.; CALHELHA, R. C.; BRACHT, A.; PERALTA, R. M.; FERREIRA, I. C. F. R. Phytochemical profile and biological activities of "Ora-pro-nobis" leaves (Pereskia aculeata Miller), an underexploited superfood from the Brazilian Atlantic Forest. **Food Chemistry**, [*s. l.*], v. 294, n. May, p. 302–308, 2019. Disponível em: https://doi.org/10.1016/j.foodchem.2019.05.074.

GARCIA, M. V.; MILANI, M. S.; RIES, E. F. Production optimization of passion fruit peel flour and its incorporation into dietary food. **Food Science and Technology International**, [*s. l.*], v. 26, n. 2, p. 132–139, 2020.

GARVÍN, A.; IBARZ, R.; IBARZ, A. Kinetic and thermodynamic compensation. A current and practical review for foods. **Food Research International**, [*s. l.*], v. 96, p. 132–153, 2017.

GEANKOPLIS, C. J. Drying of process materials. *In*: TRANSPORT PROCESSES AND UNIT OPERATIONS. 3. ed. Englewood Cliffs: Prentice-Hal, 1993. p. 520–583.

GIACOMETTI, D. C.; LEÓN, J. Tannia, yautia (Xanthosoma sagittifolium). *In*: NEGLECTED CROPS: 1942 FROM A DIFFERENT PERSPECTIVE. Rome: FAO, 1994. p. 341.

GOMES, G. B.; RODARTE, M. F.; CAMPOS, R. F. B.; SANTOS, F. S. Caracterização do consumo da folha de taioba (Xanthosoma sagittifolium (L.) Schott) pela população da região pericentral do município de São Roque, SP. **Revista Eletrônica acadêmica IFSP – Campus São Roque**, [*s. l.*], v. 1, n. 3, p. 76–81, 2014.

GONÇALVES, E. G. The Commonly Cultivated Species of Xanthosoma Schott (Araceae), including Four New Species. **Aroideana**, [*s. l.*], v. 34, n. 1, p. 3–23, 2011.

HALSEY, G. Physical Adsorption on Non-Uniform Surfaces. **The Journal of Chemical Physics**, [*s. l.*], v. 16, n. 10, p. 931–937, 1948. Disponível em: http://aip.scitation.org/doi/10.1063/1.1746689.

HARDMAN, T. M. **Water and food quality**. 1. ed. London: Elsevier, 1987. 1987.

HARTMANN, H. T.; KESTER, D. E.; DAVIES, F. T.; GENEVE, R. L. **Plant propagation: principles and practices**. 7. ed. Upper Saddle River: Prentice Hall, 2002. 2002.

HENDERSON, S. M. A basic concept of equilibrium moisture. **Agricultural Engineering**, [*s. l.*], v. 33, p. 29–33, 1952.

HERNÁNDEZ-PÉREZ, T.; GÓMEZ-GARCÍA, M. del R.; VALVERDE, M. E.; PAREDES-LÓPEZ, O. Capsicum annuum (hot pepper): An ancient Latin-American crop with outstanding bioactive compounds and nutraceutical potential. A review. **Comprehensive Reviews in Food Science and Food Safety**, [*s. l.*], v. 19, n. 6, p. 2972–2993, 2020. Disponível em: https://ift.onlinelibrary.wiley.com/doi/10.1111/1541-4337.12634.

IAL. **Métodos físico-químicos para análise de alimentos**. São Paulo: Instituto Adolfo Lutz, 2008. 2008.

INYANG, U. E.; OBOH, I. O.; ETUK, B. R. Kinetic Models for Drying Techniques—Food Materials. **Advances in Chemical Engineering and Science**, [*s. l.*], v. 08, n. 02, p. 27–48, 2018.

IRANI, R.; KHALED, K. L.; DUTTA, C. Analysis of the Pattern of Complex Carbohydrates of Bamboo Shoot and Plantain Stem with Special Emphasis on its Impact on Metabolic Disorders. **International Journal of Engineering, Science and Mathematics**, [*s. l.*], v. 7, n. 4, 2018.

JACKIX, E. A. Propriedades funcionais de vegetais e efeitos da folha de taioba (Xanthosoma sagittifolium) sobre a saúde. **Revista Brasileira De Nutrição Funcional**, [*s. l.*], v. 1, n. 64, p. 31–38, 2015. Disponível em: https://www.vponline.com.br/portal/noticia/pdf/5f71eba60f24ee6af7e075c59cea3e3f.pdf.

JARRET, R. L.; LEVY, I. J.; POTTER, T. L.; CERMAK, S. C. Seed oil and fatty acid composition in Capsicum spp. **Journal of Food Composition and Analysis**, [*s. l.*], v. 30, n. 2, p. 102–108, 2013.

JORDAN, R. A.; SANJINEZ-ARGANDOÑA, E. J.; FERREIRA, O. M.; QUEQUETO, W. D.; SIQUEIRA, V. C.; MENDOZA, V. da S.; FLOZINO, G. K. M.; SANCHES, Í. S.; SANCHES, É. S.; ANTUNES, B. M. Efeito de sistemas e condições de secagem sobre o consumo específico de energia e os compostos bioativos da taioba (Xanthosoma sagittifolium Schott). **Research, Society and Development**, [*s. l.*], v. 10, n. 7, p. e21610716512, 2021. Disponível em: https://rsdjournal.org/index.php/rsd/article/view/16512.

KAREL, M.; LUND, D. B. **Physical Principles of Food Preservation**. New York: CRC Press, 2003. 2003.

KELEN, M. E. B.; NOUHUYS, I. S. V.; KEHL, L. C.; BRACK, P.; SILVA, D. B. **Plantas Alimentícias Não Convencionais (PANCs): Hortaliças espontâneas e nativas**. 1. ed. Porto Alegre: UFRGS, 2015. 2015. Disponível em: https://www.google.com.br/url?sa=t&rct=j&q=&esrc=s&source=web&cd=1&cad=rja&uact=8&ved=0ahUKEwinrcHsjLPQAhUFhpAKHS-ECMMQFgggMAA&url=https://www.ufrgs.br/viveiroscomunitarios/wp-content/uploads/2015/11/Cartilha-15.11-online.pdf&usg=AFQjCNGf3ptibnfFRlIEHi2-u.

KINUPP, V. F.; LORENZI, H. **Plantas alimentícias não convencionais (PANC) no Brasil: guia de identificação, aspectos nutricionais e receitas ilustradas.** 1. ed. Nova Odessa: Instituto Plantarum, 2014. 2014.

KUMAR, P.; MISHRA, H. N. Moisture sorption characteristics of mango-soy-fortified yogurt powder. **International Journal of Dairy Technology**, [*s. l.*], v. 59, n. 1, p. 22–28, 2006.

Disponível em: https://onlinelibrary.wiley.com/doi/10.1111/j.1471-0307.2006.00215.x.

LABUZA, T. P. Sorption phenomena in foods. **Food Technology**, [*s. l.*], v. 22, p. 15–24, 1968.

LABUZA, T. P.; ALTUNAKAR, B. Diffusion and Sorption Kinetics of Water in Foods. *In*: BARBOSA-CÁNOVAS, Gustavo V.; FONTANA JR., Anthony J.; SCHMIDT, Shelly J.; LABUZA, Theodore P. (org.). **Water Activity in Foods**. 2nd. ed. Chicago: John Wiley & Sons, 2020. p. 287–309. Disponível em: https://onlinelibrary.wiley.com/doi/abs/10.1002/9781118765982.ch12.

LETERME, P.; LONDOÑO, A. M.; ESTRADA, F.; SOUFFRANT, W. B.; BULDGEN, A. Chemical composition, nutritive value and voluntary intake of tropical tree foliage and cocoyam in pigs. **Journal of the Science of Food and Agriculture**, [*s. l.*], v. 85, n. 10, p. 1725–1732, 2005.

LEWICKI, P. P. Data and Models of Water Activity. II: Solid Foods. *In*: FOOD PROPERTIES HANDBOOK. 2. ed. Boca Raton: Taylor & Francis Group, 2008.

LEWIS, G. N.; RANDALL, M. **Thermodynamics**. New York: McGraw Hill, 1961. 1961.

LIBERATO, P. da S.; LIMA, D. V. T. de; SILVA, G. M. B. da. PANCs - PLANTAS ALIMENTÍCIAS NÃO CONVENCIONAIS E SEUS BENEFÍCIOS NUTRICIONAIS. **ENVIRONMENTAL SMOKE**, [*s. l.*], v. 2, n. 2, p. 102–111, 2019. Disponível em: https://environmentalsmoke.com.br/index.php/EnvSmoke/article/view/64.

LIMA, A. S. G.; KRUPEK, R. A. Caracterização morfológica, anatômica, e toxinas endógenas em Colocasia esculenta (L.) Schott e Xanthosoma sagittifolium (L.) Schott. **Luminária**, [*s. l.*], v. 18, n. 1, p. 31–40, 2016.

LU, Z. X.; HE, J. F.; ZHANG, Y. C.; BING, D. J. Composition, physicochemical properties of pea protein and its application in functional foods. **https://doi.org/10.1080/10408398.2019.1651248**, [*s. l.*], v. 60, n. 15, p. 2593–2605, 2019.

MA, Y.; WU, X.; ZHAO, L.; WANG, Y.; LIAO, X. Comparison of the compounds and characteristics of pepper seed oil by pressure-assisted, ultrasound-assisted and conventional solvent extraction. **Innovative Food Science & Emerging Technologies**, [*s. l.*], v. 54, p. 78–86, 2019.

MADEIRA, N. R.; SILVEIRA, G. S. R. **Ora-pro-nóbis**. São Paulo: Globo Rural, 2010. 2010.

MARIUTTI, L. R. B.; REBELO, K. S.; BISCONSIN-JUNIOR, A.; DE MORAIS, J. S.;

MAGNANI, M.; MALDONADE, I. R.; MADEIRA, N. R.; TIENGO, A.; MARÓSTICA, M. R.; CAZARIN, C. B. B. The use of alternative food sources to improve health and guarantee access and food intake. **Food Research International**, [*s. l.*], v. 149, n. September, 2021.

MARTIN, A. A.; DE FREITAS, R. A.; SASSAKI, G. L.; EVANGELISTA, P. H. L.; SIERAKOWSKI, M. R. Chemical structure and physical-chemical properties of mucilage from the leaves of Pereskia aculeata. **Food Hydrocolloids**, [*s. l.*], v. 70, p. 20–28, 2017. Disponível em: https://linkinghub.elsevier.com/retrieve/pii/S0268005X16306658.

MATHLOUTHI, M.; ROGÉ, B. Water vapour sorption isotherms and the caking of food powders. **Food Chemistry**, [*s. l.*], v. 82, n. 1, p. 61–71, 2003. Disponível em: https://linkinghub.elsevier.com/retrieve/pii/S0308814602005344.

MCMINN, W. A. M.; AL-MUHTASEB, A. H.; MAGEE, T. R. A. Enthalpy-entropy compensation in sorption phenomena of starch materials. **Food Research International**, [*s. l.*], v. 38, n. 5, p. 505–510, 2005.

MICHAILIDIS, P. A.; KROKIDA, M. K. Drying and Dehydration Processes in Food Preservation and Processing. *In*: CONVENTIONAL AND ADVANCED FOOD PROCESSING TECHNOLOGIES. Chichester, UK: John Wiley & Sons, Ltd, 2014. p. 1–32. Disponível em: https://onlinelibrary.wiley.com/doi/10.1002/9781118406281.ch1.

NIP, W. K. Manufacture of fermented product. **Handbook of Food Science, Technology, and Engineering - 4 Volume Set**, [*s. l.*], p. 3131–3154, 2005.

OECD, O. para la C. y el D. E.; FAO, F. and A. O. **OECD-FAO Agricultural Outlook 2021–2030**. [*S. l.: s. n.*], 2020. Disponível em: https://www.fao.org/publications/card/es/c/CB5339ES. Acesso em: 26 fev. 2024.

OKOS, M. R.; NARSIMHAN, G.; SINGH, R. K.; WEITNAUER, A. C. Food dehydration. *In*: HELDMAN, R.; LUND, D. B. (org.). **Handbook of Food Engineering**. New York: Marcel Dekker Inc., 1992. p. 437.

PANCHARIYA, P. C.; POPOVIC, D.; SHARMA, A. L. Thin-layer modelling of black tea drying process. **Journal of Food Engineering**, [*s. l.*], v. 52, n. 4, p. 349–357, 2002. Disponível em: https://linkinghub.elsevier.com/retrieve/pii/S0260877401001261.

PASCHOAL, V.; BATTISTELLA, A. B.; SANTOS SOUZA, N. **Nutrição funcional e sustentabilidade: alimentando um mundo saudável**. São Paulo: VP Editora, 2015. 2015.

PELEG, M. ASSESSMENT of A SEMI-EMPIRICAL FOUR PARAMETER GENERAL MODEL FOR SIGMOID MOISTURE SORPTION ISOTHERMS. **Journal of Food Process Engineering**, [*s. l.*], v. 16, n. 1, p. 21–37, 1993. Disponível em: https://onlinelibrary.wiley.com/doi/10.1111/j.1745-4530.1993.tb00160.x.

PENSSAN. **National Survey of Food Insecurity in the Context of the Covid-19 Pandemic in Brazil.** [*S. l.: s. n.*], 2021.

PINTO, N. A. V. D.; FERNANDES, S. M.; THÉ, P. M. P.; CARVALHO, V. D. Variabilidade da composição centesimal, vitamina C, ferro e cálcio de parte da folha de taioba (Xanthosoma sagittifolium Schott). **Revista Brasileira de Agrociência**, [*s. l.*], v. 7, n. 3, p. 205–208, 2001.

QUEIROZ, C. R. A. dos A.; FERREIRA, L.; GOMES, L. B. de P.; MELO, C. M. T.; DE ANDRADE, R. R. Ora-pro-nóbis em uso alimentar humano: percepção sensorial. **Revista Verde de Agroecologia e Desenvolvimento Sustentável**, [*s. l.*], v. 10, n. 3, p. 01, 2015. Disponível em: http://www.gvaa.com.br/revista/index.php/RVADS/article/view/3393.

RAHMAN, M. S. **Handbook of Food Preservation**. New York: CRC Press, 2007. 2007.

RAO, M. A.; RIZVI, S. S. H.; ASHIM, K. D.; AHMED, J. **Engineering Properties of Foods**. Boca Raton: CRC Press, 2014. 2014.

REID, D. S. Water Activity. *In*: BARBOSA-CÁNOVAS, Gustavo V.; FONTANA JR., Anthony J.; SCHMIDT, Shelly J.; LABUZA, Theodore P. (org.). **Water Activity in Foods**. 2nd. ed. Chicago: John Wiley & Sons, 2020. p. 13–26. Disponível em: https://onlinelibrary.wiley.com/doi/abs/10.1002/9781118765982.ch2.

RIBEIRO, C. S. C.; CARVALHO, S. I. C.; LANA, M. M. **Pimenta jalapeño|Para molho e muito mais**. [*S. l.: s. n.*], 2021. Disponível em: https://www.embrapa.br/hortalica-nao-e-so-salada/pimenta-jalapeno. Acesso em: 26 fev. 2024.

RIBEIRO, E. P.; SERAVALLI, E. A. G. **Química de Alimentos**. 2. ed. São Paulo: Blucher, 2007. 2007.

RIZVI, S. S. H. Thermodynamic properties of foods in dehydration. *In*: RAO, M. A.; RIZVI, S. S. H.; DATTA, A. K. (org.). **Engineering properties of foods**. 4th. ed. Boca Raton: CRC Press, 2014. p. 359–436.

RODRIGUES, I. R.; RAMOS, R. O.; QUEIROZ, C. R. A. A. Ora-pro-nóbis na mesa-aspecto agronômico. **Boletim Técnico IFTM**, [*s. l.*], v. 4, n. 3, p. 40–43, 2019.

SÁ, A. G. A.; MORENO, Y. M. F.; CARCIOFI, B. A. M. Plant proteins as high-quality nutritional source for human diet. **Trends in Food Science & Technology**, [*s. l.*], v. 97, p. 170–184, 2020. Disponível em: https://linkinghub.elsevier.com/retrieve/pii/S0924224419308994.

SAATH, K. C. de O.; FACHINELLO, A. L. Crescimento da Demanda Mundial de Alimentos e Restrições do Fator Terra no Brasil. **Revista de Economia e Sociologia Rural**, [*s. l.*], v. 56, n. 2, p. 195–212, 2018.

SANDOVAL-CASTRO, C. J.; VALDEZ-MORALES, M.; OOMAH, B. D.; GUTIÉRREZ-DORADO, R.; MEDINA-GODOY, S.; ESPINOSA-ALONSO, L. G. Bioactive compounds and antioxidant activity in scalded Jalapeño pepper industrial byproduct (Capsicum annuum). **Journal of Food Science and Technology**, [*s. l.*], v. 54, n. 7, p. 1999–2010, 2017.

SANDOVAL-CASTRO, C. J.; VALDEZ-MORALES, M.; PEREA-DOMÍNGUEZ, X. P.; MEDINA-GODOY, S.; ESPINOSA-ALONSO, L. G. Antioxidant activity of processed and raw seed byproduct from Jalapeño pepper. J Chem Biol Phys Sci Spec, (4), 5. **Journal of Chemical Biological and Physical Science**, [*s. l.*], v. 4, n. 5, 2014.

SARAVACOS, G.; KOSTAROPOULOS, A. E. **Handbook of Food Processing Equipment**. Cham: Springer International Publishing, 2016. 2016.(Food Engineering Series). Disponível em: http://link.springer.com/10.1007/978-3-319-25020-5.

SARTORI, V. C.; THEODORO, H.; MINELLO, L. V.; PANSERA, M. R.; BASSO, A.; SCUR, L. **Plantas Alimentícias Não Convencionais – PANC : resgatando a soberania alimentar e nutricional**. Caxias do Sul: Educs, 2020. 2020.

SHARIF, K. M.; RAHMAN, M. M.; ZAIDUL, I. S. M.; JANNATUL, A.; AKANDA, M. J. H.; MOHAMED, A.; SHAMSUDIN, S. H. Pharmacological Relevance of Primitive Leafy Cactuses Pereskia. **Research Journal of Biotechnology**, [*s. l.*], v. 8, n. 12, p. 134–142, 2013.

SOUSA, F. C. de; ROCHA, A. P. T.; GOMES, J. P.; MARTINS, J. J. A.; MARTINS, J. N. Isotermas de dessorção de folhas in natura de juazeiro e mororó. **Pesquisa Agropecuária Tropical**, [*s. l.*], v. 44, n. 3, p. 304–310, 2014. Disponível em: http://www.scielo.br/scielo.php?script=sci_arttext&pid=S1983-40632014000300009&lng=pt&tlng=pt.

SOUZA, L.; CAPUTO, L.; INCHAUSTI DE BARROS, I.; FRATIANNI, F.; NAZZARO, F.; DE FEO, V. Pereskia aculeata Muller (Cactaceae) Leaves: Chemical Composition and Biological Activities. **International Journal of Molecular Sciences**, [*s. l.*], v. 17, n. 9, p. 1478,

2016. Disponível em: http://www.mdpi.com/1422-0067/17/9/1478.

TAKEITI, C. Y.; ANTONIO, G. C.; MOTTA, E. M. P.; COLLARES-QUEIROZ, F. P.; PARK, K. J. Nutritive evaluation of a non-conventional leafy vegetable (Pereskia aculeata Miller). **International Journal of Food Sciences and Nutrition**, [*s. l.*], v. 60, n. SUPPL. 1, p. 148–160, 2009.

TELIS, V. R. N.; MAURO, M. A. Desidratação. *In*: TADINI, Carmen Cecília; TELIS, Vânia Regina Nicoletti; MEIRELLES, Antonio José de Almeida; PESSOA FILHO, Pedro de Alcântara (org.). **Operações Unitárias na Indústria de Alimentos**. 1 ediçãoed. Rio de Janeiro: LTC, 2016. p. 77–148.

TONON, R. V.; BARONI, A. F.; BRABET, C.; GIBERT, O.; PALLET, D.; HUBINGER, M. D. Water sorption and glass transition temperature of spray dried açai (Euterpe oleracea Mart.) juice. **Journal of Food Engineering**, [*s. l.*], v. 94, n. 3–4, p. 215–221, 2009. Disponível em: https://linkinghub.elsevier.com/retrieve/pii/S0260877409001344.

VALDEZ-MORALES, M.; SANDOVAL-CASTRO, C. J.; GUTIÉRREZ-DORADO, R.; MENDOZA-ESPINOZA, J. A.; MEDINA-GODOY, S.; ESPINOSA-ALONSO, L. G. Oil Recovery from Jalapeño Pepper By-Products and Analysis of the Industrial Scalding Process on Its Nutraceutical Potential. **Waste and Biomass Valorization**, [*s. l.*], v. 12, n. 8, p. 4475–4487, 2021.

VAN DER BERG, C. Description of water activity of foods for engineering purposes by means of the GAB model of sorption. *In*: MCKENNA, B. M. (org.). **Engineering and Food**. London: Elsevier Applied Science, 1984. p. 311–321.

XU, L.; ZHANG, Y.; WANG, L. Structure characteristics of a water-soluble polysaccharide purified from dragon fruit (Hylocereus undatus) pulp. **Carbohydrate Polymers**, [*s. l.*], v. 146, p. 224–230, 2016. Disponível em: https://linkinghub.elsevier.com/retrieve/pii/S0144861716302892.

2 CAPÍTULO 2 - Water desorption isotherms and thermodynamic properties of Ora-pro-nóbis (*Pereskia aculeata* Miller)

Published in LWT – Food Science and Technology (Print ISSN: 0023-6438):

https://doi.org/10.1016/j.lwt.2024.115749

André Luiz Borges-Machado[a,b]*, Marcio Augusto Ribeiro Sanches[a], Maria Júlia Neves Martins[a], Priscila Alonso dos Santos[b], Guadalupe Luna-Solano[c], Javier Telis-Romero[a].

[a]Food Engineering and Technology Department, State University of São Paulo, São José do Rio Preto, São Paulo, 15054-000, Brazil.

[b]Department of Food Engineering, Instituto Federal Goiano - Campus Rio Verde, Rio Verde, Goiás, 75901-970, Brazil.

[c]División de Estudios de Posgrado e Investigación, Instituto Tecnológico de Orizaba, Orizaba, Veracruz, 94300, Mexico.

ABSTRACT

Desorption isotherms of ora-pro-nóbis leaves were determined at storage (5 ºC, 10 ºC, 20 ºC, 30 ºC, and 40 ºC) and drying (40 ºC, 50 ºC, 60 ºC, 70 ºC, and 80 ºC) temperatures by the gravimetric static method using saturated saline solutions to obtain relative humidities ranging from 5.20% to 98.48%. The net isosteric heat of desorption and thermodynamic properties such as differential enthalpy, differential entropy, and Gibbs free energy were also estimated. The GAB model presented the best parameters of fitting and the lowest Akaike and Bayesian information criteria values. The desorption isotherm patterns presented a sigmoid shape and were categorized as BET Type II sigmoid shape. The monolayer moisture content was estimated in 0.06 kg of water/kg of dry matter using the GAB model, and it remained constant at all temperatures. The leaves presented an optimal water activity equal to 0.35 at storage temperatures. The net isosteric heat of desorption decreased with increasing X_{eq}, and differential entropy increased with rising equilibrium moisture content ($X_{eq} > 0.07$). The

enthalpy-entropy compensation was evaluated, and the desorption process is revealed to be entropy-driven and non-spontaneous.

Keywords: GAB model, Non-conventional edible plant, Barbados gooseberry, storage, drying.

2.1 INTRODUCTION

Many people believe that a typical cactus is a green succulent plant with no leaves and many spines, but, *Pereskia* Miller is a genus consisting of broad-leaved trees and shrubs found throughout Central and South America (Butterworth & Wallace, 2005). The leaves of ora-pro-nóbis (*Pereskia aculeata*), also known as Barbados gooseberry, present high mucilage content, a carbohydrate complex with a high water absorption capacity that has significant potential for usage as a hydrocolloid in processed foods (Martin et al., 2017) and pharmaceutical industries due to its emollient properties (Duarte & Hayashi, 2005). The high amount of protein in the leaves led to the plant being called "poor's meat" (Hoff et al., 2022). Some studies reported some chemical compounds associated with wound healing, antiulcer (Pinto et al., 2016), and analgesic properties (Pinto et al., 2015).

The production and consumption of ora-pro-nóbis leaves are extremely important due to their potential as a sustainable source of nutraceuticals and ingredients, favoring foods to enhance nutritional quality (Garcia et al., 2019), and being a good ally in guaranteeing food security once the prevalence of malnutrition remained constant for five years and increased with the COVID-19 pandemic, indicating that the problem of food insecurity was not going towards a solution until 2030 (FAO et al., 2021). In this way, providing data concerning the water desorption isotherms and thermodynamic properties of ora-pro-nóbis leaves is of great importance due to its applicability in shelf-life estimation, storage conditions, and drying process design.

Moisture sorption isotherms are a handy tool for food scientists since they permit predicting which chemical reactions would reduce stability at a particular moisture level, enable ingredient selection to adjust the water activity, improve stability, and estimate moisture gain or loss in a package with known water vapor permeability (Labuza & Altunakar, 2020). Further investigations into the sorption phenomenon can be conducted using thermodynamic properties such as differential enthalpy and entropy, which are variables that provide information about the material microstructure as well as theoretical interpretations for matrix-water interactions (Rizvi, 2014). The enthalpy-entropy compensation theory states that compensation happens when the behavior of the solvent-solute interaction changes and that there is a linear relationship between reaction enthalpy and entropy, with the associated slope representing the isokinetic temperature, which is the temperature at which all subsequent reactions proceed at the same rate (Moreira et al., 2008; Polachini et al., 2016). The evaluation of this theory also allows the estimation of Gibb's free energy at isokinetic temperature. According to Rizvi, (2014), Gibbs's free energy is indicative of the water-absorbent affinity, providing knowledge on the spontaneity of the sorption phenomenon.

Thus, this study aimed to (i) determine the water desorption isotherms of *Pereskia aculeata* Miller at storage and drying temperatures, (ii) estimate the thermodynamic parameters (net isosteric heat of desorption, differential enthalpy, differential entropy, and Gibbs free energy), and (iii) evaluate the enthalpy-entropy compensation theory.

2.2 MATERIAL AND METHODS

2.2.1 Raw material

Ora-pró-nobis leaves were cultivated and harvested at UNESP (Campus São José do Rio Preto) and conducted to the Laboratory of Physical Measurements of the Department of Engineering and Food Technology. After 20 minutes of sanitizing with a chlorinated solution (100 ppm), they were dried with absorbent paper and stored under refrigeration (4 ± 2 ºC). The saturated saline solutions utilized to simulate environments with relative humidity ($RH=100\cdot a_w$) ranging from 7.43% to 98.48% were prepared with distilled water and salts from Sigma-Aldrich

(St. Louis, MO, USA). Lithium iodide (LiI), ammonium sulfate ($(NH_4)_2SO_4$), sodium bromide (NaBr), lithium bromide (LiBr), sodium iodide (NaI), magnesium chloride ($MgCl_2$), lithium chloride (LiCl), potassium iodide (KI), potassium carbonate (K_2CO_3), potassium chloride (KCl), magnesium nitrate ($Mg(NO_3)_2$), potassium sulfate (K_2SO_4), sodium chloride (NaCl), and potassium nitrate (KNO_3) were used in this work.

2.2.2 Proximate composition

Lipid content was determined according to the Ai 3-75 procedure by the Soxhlet method using petroleum ether (AOCS, 2009). Moisture, ash, protein, and total fiber contents were determined following the *Association of Official Analytical Chemistry's* procedures (Horwitz et al., 2007). The moisture content was measured in an oven at 105 ºC for 24 hours (method 950.46), and the ash content was measured in a muffle at 550 ºC until white or slightly grey ashes were obtained (method 923.03). Micro-Kjeldahl was used to determine total nitrogen, and the protein amount was converted using 6.25 as the conversion factor (method 981.10). The total fiber content was determined using the enzymatic gravimetric approach, which used thermostable α-amylase, glucoamylase, and protease to break down proteins and starches. The insoluble and soluble fractions of the fibers were subsequently separated using a centrifuge (method 991.43). Carbohydrates were calculated by difference. The water activity (a_w) was measured using a digital hygrometer (Aqualab Model Series 3, Decagon Devices Inc., Pullman, USA).

2.2.3 Determination of the desorption isotherms

Desorption isotherms were assessed at nine temperatures: storage (5 ºC, 10 ºC, 20 ºC, 30 ºC, and 40 ºC) and drying (40 ºC, 50 ºC, 60 ºC, 70 ºC, and 80 ºC). The studies were carried out in a chamber-type BOD (MA415, Marconi, Piracicaba, Brazil) to obtain storage temperatures, and the drying temperatures experiments were carried out in an oven (MA030, Marconi, Piracicaba, Brazil). The static gravimetric method proposed by Spiess & Wolf, (1983) was used to determine the desorption isotherms of ora-pro-nóbis leaves, which consists of putting saturated saline solutions into desiccators to keep constant water activity (a_w) at each sample value while the equilibrium between the atmosphere and food sample was reached. The leaves were cut into a square shape with sides equal to 1 cm and allocated in small containers inside the desiccators. At the beginning of the experiment, which was conducted in triplicate, the moisture content and mass of the samples were determined using an analytical balance (AUW220D, Shimadzu, Japan), and the samples were weighted until they attained constant mass. Aiming to avoid microbial spoilage, a beaker containing toluene was put inside the desiccators where relative humidity was higher than 60% ($a_w > 0.6$). The experiments lasted six weeks and were based on a weight difference expressed on a dry basis that did not exceed 0.001 g/g dry solids. The salt solutions used to create atmospheres with different relative humidities (Table S1) were made according to Labuza, (1963) and Martins et al., (2023).

2.2.4 Modelling of desorption isotherms

The theoretical (GAB), empirical (Peleg and Oswin), and semi-empirical (Halsey and Henderson) sorption isotherm models typically used to describe the water sorption process in foodstuffs are shown in Table 1. The values of X_{eq} were plotted against a_w using the Origin 2023 program (OriginLab Corporation, Northampton, MA), and nonlinear regression was performed.

Table 1 - Mathematical models for adjusting the isotherms of ora-pro-nóbis leaves

Model	Equation	
GAB	$X_{eq} = \frac{X_m C k a_w}{(1 - k a_w)(1 + (C-1) k a_w)}$	(1)
Peleg	$X_{eq} = k_1 a_w^{n_1} + k_2 a_w^{n_2}$	(2)
Oswin	$X_{eq} = M \left(\frac{a_w}{1 - a_w}\right)^N$	(3)
Halsey	$X_{eq} = (-h_1 \, ln(a_w))^{-\frac{1}{h_2}}$	(4)
Henderson	$X_{eq} = \left(-\frac{1}{H_1} ln(1 - a_w)\right)^{\frac{1}{H_2}}$	(5)

C, k, k_1, n_1, k_2, n_2, M, N, h_1, h_2 H_1, and H_2 are constants of the models, X_m represents the monolayer moisture content (kg of water/kg dry matter), X_{eq} is the equilibrium moisture content, and a_w is the water activity.

The adjusted coefficient of determination (R^2_{adj}) and residual analysis of reduced chi-square (χ^2) and root mean square error (RMSE) were used to assess the quality of the nonlinear fit of the water desorption models to the experimental data. Furthermore, using Equations (6) and (7), Akaike (AIC) and Bayesian (BIC) information criteria were calculated to identify the optimum model for ora-pro-nóbis leaves water desorption by comparing the fitting results of the five models shown in Table 1 (Akaike, 1974; Stone, 1979). AIC and BIC are composed of a goodness-of-fit term and a penalty to prevent overfitting and they provide a standardized method for balancing sensitivity and specificity. The better the model, the lower the AIC and BIC (Wolfinger, 1993).

$$AIC = -2\log\mathcal{L}(\hat{\theta}) + 2p \quad (6)$$

$$BIC = -2\log\mathcal{L}(\hat{\theta}) + p\ln(n) \quad (7)$$

where n is the total number of observations, p is the total number of estimated parameters, and $\mathcal{L}(\hat{\theta})$ is the value of the likelihood function regarding the parameters of the model.

2.2.5 Optimal water activity

The experimental desorption points at storage temperatures were plotted on the same graph. A polynomial equation of the third degree was used to model the sorption isotherm. This calculating procedure entails doing a polynomial decomposition of the X_{eq} based on the a_w, allowing us to compute the "inflection point" of the second derivative of X_{eq} (Lahnine et al., 2016).

2.2.6 Thermodynamic properties

The isosteric heat of sorption informs about the energy required for drying and the design of drying equipment. It is defined as the smallest quantity of energy needed for eliminating water in the desorption or adding water in the adsorption of a hygroscopic material (Jhider & Bagané, 2019). The net isosteric heat of desorption (q_{st}) was calculated using the Clausius-Clapeyron equation (Equation 8) at different X_{eq} (Rizvi, 2014).

$$\left.\frac{\partial(\ln a_w)}{\partial(1/T)}\right|_{X_{eq}} = -\frac{Q_{st}-\lambda}{R} = -\frac{q_{st}}{R} \tag{8}$$

in which Q_{st} is the integral heat of sorption, λ is the latent heat of pure water vaporization and R is universal gas constant (8.314 $J \cdot mol^{-1} \cdot K^{-1}$). Assuming q_{st} constant over the temperature range investigated, linear regression was used to obtain the slope of each isostere of ln a_w versus 1/T, and hence, the net isosteric heat of desorption.

Differential enthalpy (ΔH) and differential entropy (ΔS) were calculated using the same approach as q_{st} but with Equation 9, derived from the Gibbs-Helmholtz equation (Rizvi, 2014).

$$\ln a_w = \left(\frac{\Delta H}{R}\right)\frac{1}{T} - \frac{\Delta S}{R} \tag{9}$$

The enthalpy-entropy mechanism could be verified by plotting q_{st}, which is equal to the negative of enthalpy, against entropy in the expectation of a linear correlation. Using Equation 10, the figure was also used to compute Gibbs' free energy (G_B) and the isokinetic temperature (T_B).

$$q_{st} = T_B(\Delta S) + \Delta G_B \tag{10}$$

Krug's statistical method was used to validate the enthalpy-entropy compensation theory (Krug et al., 1976a, 1976b). The procedure involved comparing the harmonic mean temperature (Equation 11) to the isokinetic temperature.

$$T_{hm} = \frac{n}{\sum_{i=1}^{n}\left(\frac{1}{T}\right)} \tag{11}$$

in which n is the number of sorption patterns. An interval of confidence for T_B close to (1-α) 100% was estimated by Equation 12.

$$T_B = T_B \pm t_{m-2,\alpha/2}\sqrt{Var(T_B)} \quad (12)$$

where,

$$T_B = \frac{\sum(\Delta H - \overline{\Delta H})(\Delta S - \overline{\Delta S})}{\sum(\Delta S - \overline{\Delta S})^2} \quad (13)$$

$$Var(T_B) = \frac{(\Delta H - \overline{\Delta G_B} - T_B \Delta S)^2}{(m-2)\sum(\Delta S - \overline{\Delta S})^2} \quad (14)$$

in which, $\overline{\Delta H}$ is the average enthalpy (kJ mol^{-1}), m is the number of data pairs (ΔH, ΔS), $\overline{\Delta S}$ is the average entropy (kJ/kg·K^{-1}).

2.3 RESULTS AND DISCUSSION

2.3.1 Proximate composition

The proximate composition findings are shown as the media ± standard deviation of three repetitions. The ora-pro-nóbis leaves presented, in wet basis,: 88.20±0.36 g of water/100 g; 4.99±0.02 g of total fibers/100 g; 3.10± 0.10 g of proteins /100 g; 1.78±0.50 g of carbohydrates/100 g; 1.64±0.01 g of ashes /100 g; 0.30±0.01g of lipids/100 g. Analogous results were found by Takeiti et al., (2009) and Botrel et al., (2020). The leaves presented a_w = 0.991 ± 0.02, suggesting that ora-pro-nóbis leaves are a highly perishable vegetable.

2.3.2 Desorption isotherms

The desorption isotherms were obtained for a relative humidity range of 5.80% to 98.48% at storage temperatures and 5.20% to 96.41% under drying temperatures (Figure 1, Table S2). At storage and drying temperatures, the a_w increased with increasing temperature for a constant X_{eq}. In contrast, the X_{eq} diminished with rising temperature at constant a_w, showing that the leaves became less hygroscopic. This behavior could be attributed to a decrease in the number of active sites for water binding caused by physical and chemical modifications in the leaves due to temperature (Hidar et al., 2018). Furthermore, as the temperature rises, the sorbed water molecules gain a high degree of freedom and kinetic energy allowing them to escape from the surface of the sorbent, and the volume of sorbed water reduces (Ojike et al., 2022), and consequently, the moisture content.

At storage temperatures, when 0.15<a_w<0.60 (Figure 1a), the X_{eq} increases linearly with increasing a_w. During storage, oxidative and biological reactions are favored when a_w is greater than 0.6, reducing the shelf life of food products and influencing the incidence of microorganisms (Pitt & Hocking, 2009). Therefore, leaves must be dried until 0.1058, 0.1032, 0.1003, 0.0960 kg of water/kg of dry matter to achieve a_w = 0.6 and prevent microbial spoilage when stored at 5ºC, 10 ºC, 20ºC, 30 ºC and 40 ºC, respectively. As stated by Brunauer-Emmett-Teller classification (Brunauer et al., 1938), the desorption isotherm patterns presented a typical sigmoidal shape and hence classified as BET type II, which is typical of a lot of foodstuffs (Hassini et al., 2015) such as black and green tea (Ocieczek et al., 2023), leaves and stems of lemon balm (Argyropoulos et al., 2012), papaya seeds (Rosa et al., 2021), *Cucumis melo* L. seeds (Mallek-Ayadi et al., 2020), and tiger nuts (Zhang et al., 2022).

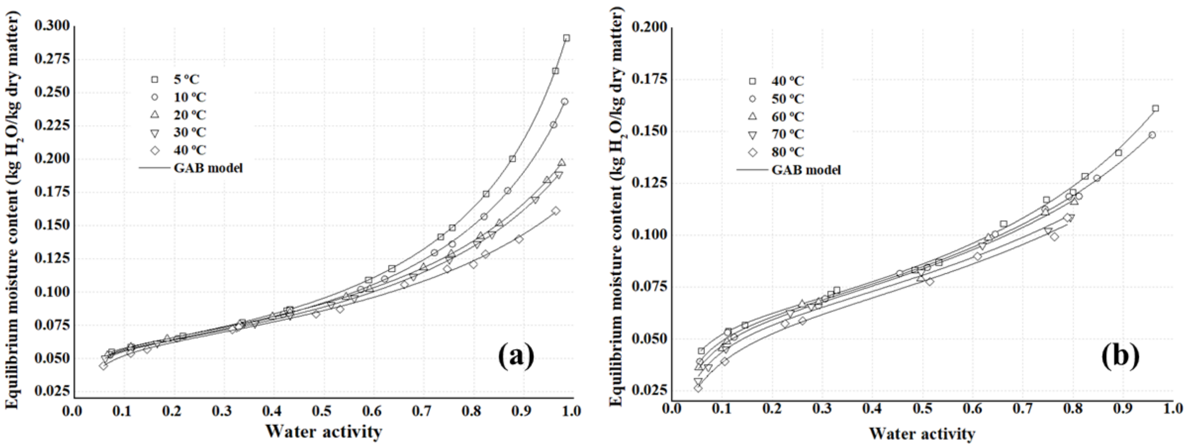

Figure 1 - Desorption isotherms of ora-pro-nóbis leaves at storage (a) and drying (b) temperatures.

Table 2 presents the estimated constants and fitting parameters of the evaluated models. Halsey's model showed the lowest values of coefficients of determination (R^2_{adj}) and the highest values of reduced chi-square (χ^2) and square root mean error (RMSE), followed by Oswin and Henderson models, respectively. In contrast, the GAB and Peleg models showed R^2_{adj} close to one and low calculated values of χ^2 and RMSE at all studied temperatures.

Comparing AIC and BIC values (Table 2) for the GAB and Peleg models, the first presented the lowest values; thus, the GAB model was selected to describe the desorption patterns of ora-pro-nóbis leaves at all temperatures. Moreover, the three constants of the GAB model pursue physical meaning (Labuza & Altunakar, 2020).

Table 2 - Constants and fitting parameters of the sorption equations for ora-pro-nóbis leaves

Model		Temperature (ºC)								
		5	10	20	30	40	50	60	70	80
GAB	X_m	0.057	0.057	0.056	0.061	0.060	0.061	0.062	0.062	0.062
	C	147.143	118.313	100.299	100.583	62.535	44.872	37.770	32.389	24.062
	k	0.817	0.781	0.715	0.715	0.653	0.619	0.604	0.573	0.558
	R^2_{aj}	0.999	0.999	0.998	0.996	0.998	0.998	0.993	0.991	0.992
	$\chi^2 \cdot 10^5$	0.001	0.099	0.001	0.001	0.309	0.248	0.634	0.729	0.692
	RSME	0.001	0.001	0.001	0.001	0.002	0.002	0.003	0.001	0.003
	AIC	-293.008	-184.536	-280.860	-279.649	-155.337	-158.204	-93.370	-105.033	-78.079
	BIC	-294.897	-186.425	-282.748	-281.537	-158.078	-160.944	-102.581	-114.244	-91.095
Peleg	k_1	0.107	0.103	0.097	0.094	0.096	0.097	0.101	0.115	0.110
	n_1	0.278	0.272	0.235	0.234	0.271	0.301	0.342	0.439	0.467
	k_2	0.196	0.151	0.109	0.105	0.074	0.060	0.052	15.204	770.415
	n_2	5.025	4.629	3.767	3.742	3.597	3.259	3.670	35.525	47.6563
	R^2_{aj}	0.999	0.999	0.999	0.999	0.997	0.997	0.990	0.996	0.993
	$\chi^2 \cdot 10^5$	0.828	0.441	0.084	0.071	0.371	0.307	0.836	0.365	0.599
	RSME	0.003	0.002	0.001	0.001	0.002	0.002	0.003	0.002	0.003
	AIC	-151.039	-159.868	-183.137	-185.383	-148.774	-151.229	-80.515	-87.986	-61.743
	BIC	-155.344	-164.173	-187.441	-189.688	-154.520	-156.98	-99.529	-106.999	-91.346
Oswin	M	0.106	0.099	0.096	0.092	0.087	0.084	0.083	0.079	0.075
	N	0.262	0.243	0.215	0.224	0.207	0.207	0.259	0.261	0.280
	R^2_{aj}	0.966	0.970	0.970	0.974	0.972	0.961	0.989	0.971	0.975
	$\chi^2 \cdot 10^5$	19.311	11.186	6.329	4.712	3.725	4.438	0.939	2.448	2.113
	RSME	0.014	0.011	0.008	0.007	0.006	0.007	0.003	0.005	0.005
	AIC	-113.489	-121.133	-129.108	-133.237	-126.076	-123.8	-95.647	-87.021	-76.419
	BIC	-113.972	-121.616	-129.591	-133.720	-127.048	-124.772	-99.855	-91.229	-82.181
Halsey	$H_1 \cdot 10^5$	32.206	15.747	5.651	8.343	3.866	3.755	94.678	91.980	114.000
	H_2	3.392	3.602	3.966	3.746	3.966	3.918	2.593	2.553	2.43
	R^2_{aj}	0.939	0.939	0.932	0.939	0.920	0.895	0.959	0.915	0.928
	$\chi^2 \cdot 10^5$	34.689	22.340	14.168	11.229	10.524	11.944	3.490	7.199	6.095
	RSME	0.019	0.015	0.012	0.011	0.010	0.011	0.006	0.009	0.008

	AIC	-105.289	-111.45	-117.825	-121.080	-112.576	-110.93	-83.8292	-77.3122	-67.9448
	BIC	-105.772	-111.933	-118.308	-121.563	-113.547	-111.902	-88.0375	-81.5205	-73.7065
Henderson	H_1	36.048	67.394	203.312	220.339	600.772	799.359	892.730	952.788	610.703
	H_2	1.744	1.9870	2.448	2.454	2.823	2.901	2.921	2.894	2.662
	R_{aj}^2	0.974	0.975	0.973	0.974	0.987	0.993	0.990	0.991	0.989
	$\chi^2 \cdot 10^5$	15.012	9.335	4.884	4.831	1.726	0.788	0.869	0.731	0.926
	RSME	0.012	0.010	0.007	0.007	0.004	0.003	0.003	0.003	0.003
	AIC	-117.015	-123.666	-132.736	-132.888	-136.077	-146.271	-96.342	-97.896	-83.018
	BIC	-117.498	-124.149	-133.219	-133.371	-137.049	-147.243	-100.550	-102.104	-88.780

The monolayer moisture content (X_m) provides information regarding the volume of water strongly attached to the polar sites of the food matrix, and it is a relevant value in ensuring food stability during storage (Kurozawa et al., 2015). The X_m values were around 0.06 kg of water kg^{-1} dry matter at all the temperatures studied (Table 2). However, it was observed that there was a discreet increase in the X_m values as the temperature rose, which can be associated with the fitting of the GAB model to the data. During desorption, the water binding sites at the monolayer are initially fully satisfied, so an increase in temperature is expected to have a reduced impact on the sorption surface area (Yogendrarajah et al., 2015). Above the monolayer, chemical reactions which require a water phase start, while above and below the region, the rate of oxidation of lipids increases compromising shelf-life (Labuza & Altunakar, 2020). In this way, after reducing the moisture content until X_m, the leaves maintain their stability when stored under 13%–15% relative humidity (RH=100·a_w) in a temperature range of 5 ºC–30 ºC.

The constant 'C' determines the force of water molecule interaction with the main binding sites on the product surface (Muzaffar & Kumar, 2016) while the constant K is an estimation of the interactions between the food matrix and molecules in multilayers (Velázquez-Gutiérrez et al., 2015). In this study, both constants C and k diminished with rising temperature, indicating a decrease in the binding energies associated with the dry matter and the monolayer water, related to the constant C, while a lower value of K implies that the sorbate is in a significantly less structured state in the layer succeeding the monolayer, which is the sorbate's pure liquid state (Ojike et al., 2022).

2.3.3 Optimal storage conditions

The second derivative of the third-degree polynomial equation indicated that the optimal water activity for preserving the ora-pro-nóbis leaves is 0.35, corresponding to 0.08 kg of water/kg dry matter (Figure 2). Knowledge and determination of the optimal water activity are necessary during the drying process because they ensure the best drying and processing conditions for hygroscopic materials (Manga Bengono et al., 2023). Peppermint (Machhour et al., 2012) and stevia leaf powder (Hidar et al., 2018) presented the same optimal a_w.

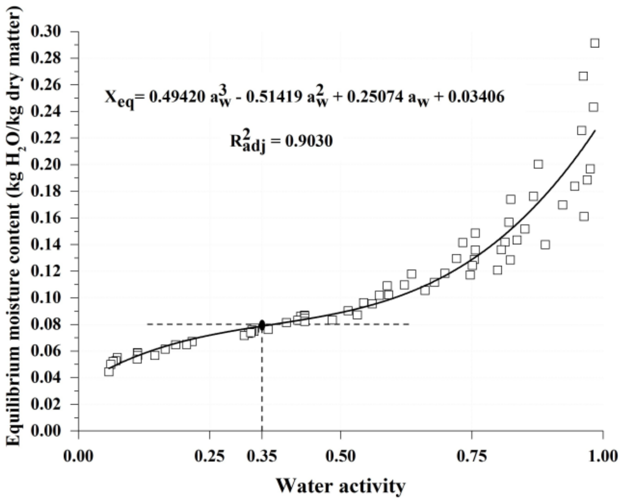

Figure 2 - Determination of the optimal water activity for preservation of ora-pro-nóbis leaves.

2.3.4 Thermodynamic properties

The isosteric heat of desorption is a measure of the energy necessary to break the intermolecular interactions between the bound water and the food matrix in the hygroscopic zone. The heat required to remove water molecules in the hygroscopic domain is the sum of the heat necessary for the liquid-vapor phase change and the desorption isosteric heat (Ouertani et al., 2014). The GAB model was used to calculate the values of a_w and hence, the q_{st} which were plotted against the $X_{eq.}$ The q_{st} decreased abruptly from 7059.25 J/mol to 1342.13 J/mol at the lowest moisture contents. The highest value of q_{st} is the highest binding energy for water removal, and it is also indicative of the strongest water-solid interaction once the water occupies the most active accessible sites (Khiari et al., 2020). Then, q_{st} slightly increased up to 1782.06 J/mol at 0.13 kg of water/kg of dry matter and thereafter remained approximately constant. The hydrophilic sites became scarcer as the moisture content increased, resulting in decreased coverage of active sorption sites and the creation of a multilayer. This may need less binding energy for water removal and, as a result, less heat (Ojike et al., 2022). A similar trend was observed in another leaves (Argyropoulos et al., 2012; Dalgıç et al., 2012; Moussaoui et al., 2019).

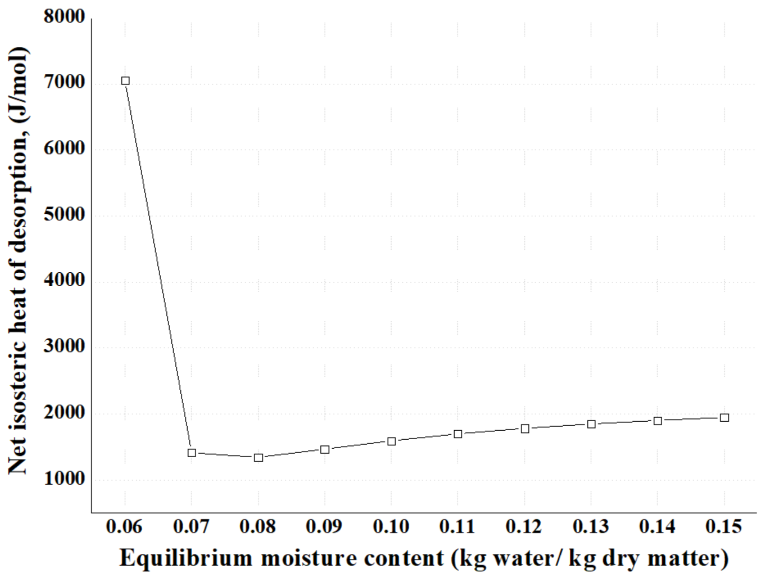

Figure 3 - Calculated net isosteric heat of desorption of ora-pro-nóbis leaves as function of the equilibrium moisture content.

Similar to q_{st}, the differential enthalpy (ΔH) of sorption measures the water binding strength, which is critical for designing efficient dehydration process equipment and understanding qualitatively the status of water on the food surface (Tagnamas et al., 2021). Generally, differential enthalpy is a positive quantity when heat is evolved during adsorption and negative when heat is absorbed during desorption (Al-Muhtaseb et al., 2002). Figure 4 shows that the ΔH increased as the X_{eq} decreased, indicating the occupation of highly accessible sites (Velázquez-Gutiérrez et al., 2015); thus, more energy is required to remove water as the X_{eq} reduces from 0.15 to 0.06 kg of water/kg of dry matter once the water binding strength is higher. Differential entropy was calculated as the intercept of the line ln(aw) vs. 1/T using Equation (9), and it showed a considerable dependence on moisture content. The change in differential entropy (ΔS) is proportional to the number of available sorption sites associated with a certain energy level and is related to the degree of disorder or randomness (spatial arrangement) in the water-sorbent system (Khiari et al., 2020). In Figure 4, it is shown that the ΔS presented its biggest value, 8.36 J/(mol·K), at X_m. The highest water mobility is shown by the biggest entropy value, which may be explained by the strongest interactions between water molecules and the adsorbent surface that has the most active sorption sites (Mbarek & Mihoubi, 2019). As the moisture content increased, ΔS achieved its minimum value of -5.72 J/(mol·K), then increased until 5.18 J/(mol·K). This is indicative of some mobility and vibrational/rotational freedom at low moisture coverage, followed by a decrease in entropy due to localization as the first layer builds up. Finally, the entropy of sorbed water increases with the higher mobility associated with the buildup of layers further removed from the food surface (Rizvi, 2014). Other vegetables, such as apple (Moraes et al., 2008), sugar beet (de Oliveira et al., 2017) and tiger nut (Zhang et al., 2022) presented the same behavior.

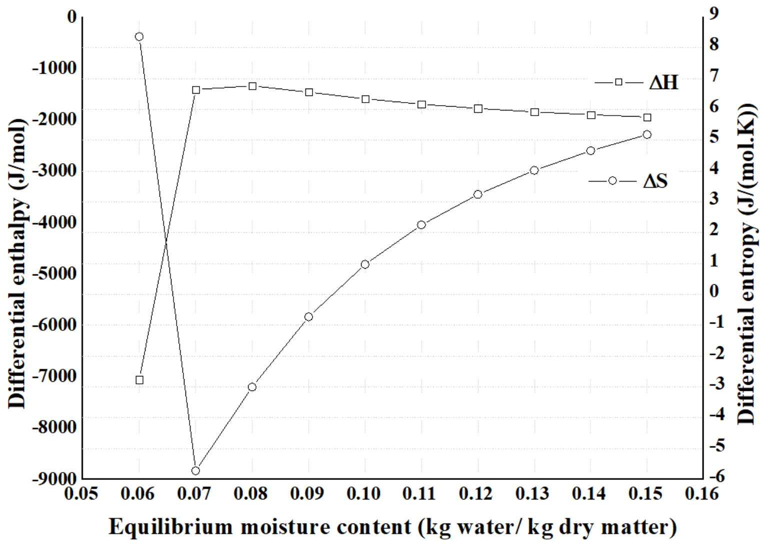

Figure 4 - Calculated differential enthalpy and differential entropy of ora-pro-nóbis leaves as function of the equilibrium moisture content.

The first condition to ensure enthalpy-entropy compensation is a strong linear correlation between enthalpy and entropy (Sanches et al., 2023), and the second is concerning the isokinetic temperature (T_B), in which T_B must be statistically different from the harmonic mean temperature (T_{hm}) (Krug et al., 1976a, 1976b). In Figure 5, it is shown the linear relationship (R^2_{adj} = 0.9924) between q_{st} and entropy, confirming the existence of a compensation mechanism. In this study, T_B = 75.72 ± 6.11 K was significantly ($p<0.05$) different from the T_{hm} = 311.72 K, corroborating the enthalpy-entropy compensation theory. Moreover, the desorption process is entropy-driven because $T_B < T_{hm}$ (Leffler, 1955). When the sorption process is entropy-driven, the barriers that confine the water molecules inside the microstructure of the food matrix are more relevant than energy interactions regarding the chemical composition of food (Spada et al., 2013). Gibb's free energy was equal to +1540.92 J/mol, thus, the desorption process is non-spontaneous. A positive value for Gibbs free energy is characteristic of an endothermic reaction, meaning that the reaction is not spontaneous and needs energy from the surroundings to proceed (de Oliveira et al., 2017).

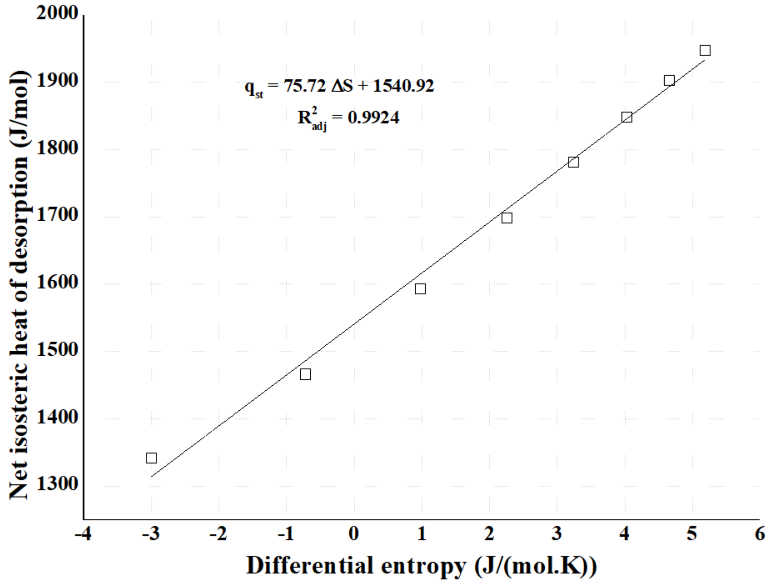

Figure 5 - Linear relationship between net isosteric heat of desorption and entropy.

2.4 CONCLUSION

The reduction in temperature and increase in relative humidity resulted in increase of equilibrium moisture content. The desorption isotherm patterns present a sigmoid shape, which were classified as BET Type II, best described by the GAB model due to its good fitting parameter and lowest AIC and BIC values. Ora-pro-nóbis leaves must contain about 0.1 kg of water/kg dry matter when stored at temperatures between 5 and 40 ºC to guarantee microbiological safety ($a_w \leq 0.6$), in addition, the optimal water activity is 0.35 in the same range of temperature. The X_m indicated that ora-pro-nóbis leaves maintain their stability when stored under 13%–15% relative humidity (RH=100·aw) in a temperature range of 5 ºC–30 ºC. The net isosteric heat of desorption decreased with rising Xeq, and differential entropy increased directly when Xeq > 0.07. The enthalpy-entropy compensation theory was confirmed, and desorption was entropy-driven ($T_B < T_{hm}$), endothermic, and non-spontaneous ($\Delta G_B > 0$).

ACKNOWLEDGMENTS

The authors thank the Coordenação de Aperfeiçoamento de Pessoal de Nível Superior - Brasil (CAPES) - Finance Code 001 and the Conselho Nacional de Desenvolvimento Científico e Tecnológico (CNPq) - Award Number: 314459/2021-9.

2.5 REFERENCES

Akaike, H. (1974). A new look at the statistical model identification. *IEEE Transactions on Automatic Control*, *19*(6), 716–723. https://doi.org/10.1109/TAC.1974.1100705

Al-Muhtaseb, A. H., McMinn, W. A. M., & Magee, T. R. A. (2002). Moisture sorption isotherm characteristics of food products: A review. *Food and Bioproducts Processing: Transactions of the Institution of of Chemical Engineers, Part C*, *80*(2), 118–128. https://doi.org/10.1205/09603080252938753

AOCS. (2009). *Official methods and recommended practices of the American oil chemists' society* (V. C. Mehlenbacher & I. L. Urbana (eds.); 6th ed.). American oil chemists' society.

Argyropoulos, D., Alex, R., Kohler, R., & Müller, J. (2012). Moisture sorption isotherms and isosteric heat of sorption of leaves and stems of lemon balm (Melissa officinalis L.) established by dynamic vapor sorption. *LWT - Food Science and Technology*, *47*(2), 324–331. https://doi.org/10.1016/j.lwt.2012.01.026

Botrel, N., Freitas, S., de Oliveira Fonseca, M. J., de Castro e Melo, R. A., & Madeira, N. (2020). Nutritional value of unconventional leafy vegetables grown in the Cerrado Biome/Brazil. *Brazilian Journal of Food Technology*, *23*, 1–8. https://doi.org/10.1590/1981-6723.17418

Brunauer, S., Emmett, P. H., & Teller, E. (1938). Adsorption of Gases in Multimolecular Layers. *Journal of the American Chemical Society*, *60*(2), 309–319. https://doi.org/10.1021/ja01269a023

Butterworth, C. A., & Wallace, R. S. (2005). Molecular Phylogenetics of the Leafy Cactus

Genus Pereskia (Cactaceae). *Systematic Botany*, *30*(4), 800–808. https://doi.org/https://www.jstor.org/stable/25064111

Dalgıç, A. C., Pekmez, H., & Belibağlı, K. B. (2012). Effect of drying methods on the moisture sorption isotherms and thermodynamic properties of mint leaves. *Journal of Food Science and Technology*, *49*(4), 439–449. https://doi.org/10.1007/s13197-011-0302-7

de Oliveira, G. H. H., Corrêa, P. C., de Oliveira, A. P. L. R., Reis, R. C. dos, & Devilla, I. A. (2017). Application of GAB Model for Water Desorption Isotherms and Thermodynamic Analysis of Sugar Beet Seeds. *Journal of Food Process Engineering*, *40*(1). https://doi.org/10.1111/jfpe.12278

Duarte, M. R., & Hayashi, S. S. (2005). Estudo anatômico de folha e caule de Pereskia aculeata Mill. (Cactaceae). *Revista Brasileira de Farmacognosia*, *15*(2), 103–109. https://doi.org/10.1590/s0102-695x2005000200006

FAO, IFAD, UNICEF, WFP, & WHO. (2021). *In brief to The state of food security and nutrition in the world. Transforming food systems for food security, improved nutrition and affordable healthy diets for all*. https://doi.org/10.4060/cb5409en

Garcia, J. A. A., Corrêa, R. C. G., Barros, L., Pereira, C., Abreu, R. M. V., Alves, M. J., Calhelha, R. C., Bracht, A., Peralta, R. M., & Ferreira, I. C. F. R. (2019). Phytochemical profile and biological activities of “Ora-pro-nobis” leaves (Pereskia aculeata Miller), an underexploited superfood from the Brazilian Atlantic Forest. *Food Chemistry*, *294*(May), 302–308. https://doi.org/10.1016/j.foodchem.2019.05.074

Hassini, L., Bettaieb, E., Desmorieux, H., Torres, S. S., & Touil, A. (2015). Desorption isotherms and thermodynamic properties of prickly pear seeds. *Industrial Crops and Products*, *67*, 457–465. https://doi.org/10.1016/j.indcrop.2015.01.078

Hidar, N., Ouhammou, M., Idlimam, A., Jaouad, A., Bouchdoug, M., Lamharrar, A., Kouhila, M., & Mahrouz, M. (2018). Investigation of water adsorption and thermodynamic properties of stevia powder. *Journal of Food Measurement and Characterization*, *12*(4), 2615–2625. https://doi.org/10.1007/s11694-018-9879-0

Hoff, R., Daguer, H., Deolindo, C. T. P., de Melo, A. P. Z., & Durigon, J. (2022). Phenolic compounds profile and main nutrients parameters of two underestimated non-conventional edible plants: Pereskia aculeata Mill. (ora-pro-nóbis) and Vitex megapotamica (Spreng.) Moldenke (tarumã) fruits. *Food Research International*, *162*(PA), 112042. https://doi.org/10.1016/j.foodres.2022.112042

Horwitz, W., Latimer, G. W., & Association of Official Analytical Chemistry, A. (2007). *Official Methods of Analysis* (18th ed.). AOAC International.

Jhider, N., & Bagané, M. (2019). Moisture sorption isotherms and isosteric heat of sorption of Tunisian clay product. *Heat and Mass Transfer/Waerme- Und Stoffuebertragung*, *55*(2), 571–579. https://doi.org/10.1007/s00231-018-2428-x

Khiari, R., Zemni, H., Maury, C., & Mihoubi, D. (2020). Modeling desorption isotherms and thermodynamic properties of Italia grapes. *Journal of Food Processing and Preservation*, *44*(10), 1–13. https://doi.org/10.1111/jfpp.14731

Krug, R. R., Hunter, W. G., & Grieger, R. A. (1976a). Enthalpy-entropy compensation. 1. Some fundamental statistical problems associated with the analysis of van't hoff and arrhenius data. *Journal of Physical Chemistry*, *80*(21), 2335–2341. https://doi.org/10.1021/j100562a006

Krug, R. R., Hunter, W. G., & Grieger, R. A. (1976b). Enthalpy-entropy compensation. 2. Separation of the chemical from the statistical effect. *Journal of Physical Chemistry*, *80*(21), 2341–2351. https://doi.org/10.1021/j100562a007

Kurozawa, L. E., de Oliveira, R. A., Hubinger, M. D., & Park, K. J. (2015). Thermodynamic Properties of Water Desorption of Papaya. *Journal of Food Processing and Preservation*, *39*(6), 2412–2420. https://doi.org/10.1111/jfpp.12491

Labuza, T. (1963). Creation of moisture sorption isotherms for hygroscopic materials. Sorption isotherm methods. In *International symposium on humidity and moisture., May 20-23*. Washington: American Society of Heating, Refrigerating and Air Conditioning Engineers.

Labuza, T. P., & Altunakar, B. (2020). Water Activity Prediction and Moisture Sorption Isotherms. In G. V. Barbosa-Cánovas, A. J. Fontana Jr., S. J. Schmidt, & T. P. Labuza (Eds.), *Water Activity in Foods* (2nd ed., pp. 161–205). John Wiley & Sons. https://doi.org/10.1002/9781118765982.ch7

Lahnine, L., Idlimam, A., Mahrouz, M., Jada, A., Hanine, H., Mouhib, M., Zantar, S., & Kouhila, M. (2016). Adsorption measurements and modeling of thyme treated with gamma irradiation and thermal-biochemical treatment. *Industrial Crops and Products*, *88*, 36–43. https://doi.org/10.1016/j.indcrop.2016.02.049

Leffler, J. E. (1955). The enthalpy-entropy relationshipg and its implications for organic chemistry. *The Journal of Organic Chemistry, 20,* 1202–1231.

Machhour, H., Idlimam, A., Mahrouz, M., El Hadrami, I., & Kouhila, M. (2012). Sorption isotherms and thermodynamic properties of peppermint tea (Mentha piperita) after thermal and biochemical treatment. *Journal of Materials and Environmental Science*, *3*(2), 232–247.

Mallek-Ayadi, S., Bahloul, N., & Kechaou, N. (2020). Mathematical modelling of water sorption isotherms and thermodynamic properties of Cucumis melo L. seeds. *Lwt*, *131*(June), 109727. https://doi.org/10.1016/j.lwt.2020.109727

Manga Bengono, D. M., Tamba, J. G., Zobo Mfomo, J., Fopah-Lele, A., Diboma, B. S., Banyuy, F. G., & Biwolé, A. B. (2023). Influence of the anatomical structure on the moisture sorption and thermodynamic properties of the African tropical woods. *Heat and Mass Transfer/Waerme- Und Stoffuebertragung*, *59*(1), 113–130. https://doi.org/10.1007/s00231-022-03242-x

Martin, A. A., de Freitas, R. A., Sassaki, G. L., Evangelista, P. H. L., & Sierakowski, M. R. (2017). Chemical structure and physical-chemical properties of mucilage from the leaves of Pereskia aculeata. *Food Hydrocolloids, 70*, 20–28. https://doi.org/10.1016/j.foodhyd.2017.03.020

Martins, M. J. N., Sanches, M. A. R., Polachini, T. C., Oliveira, E. B., Coimbra, J. S. R., & Telis-Romero, J. (2023). Solubility of different salts used in the control of the water activity of foods. *Science and Agrotechnology*, *47*, e018722. https://doi.org/10.1590/1413-7054202347018722

Mbarek, R., & Mihoubi, D. (2019). Thermodynamic properties and water desorption isotherms of Golden Delicious apples. *Heat and Mass Transfer/Waerme- Und Stoffuebertragung*, *55*(5), 1405–1418. https://doi.org/10.1007/s00231-018-2527-8

Moraes, M. A., Rosa, G. S., & Pinto, L. A. A. (2008). Moisture sorption isotherms and thermodynamic properties of apple Fuji and garlic. *International Journal of Food Science and Technology*, *43*(10), 1824–1831. https://doi.org/10.1111/j.1365-2621.2008.01716.x

Moreira, R., Chenlo, F., Torres, M. D., & Vallejo, N. (2008). Thermodynamic analysis of experimental sorption isotherms of loquat and quince fruits. *Journal of Food Engineering*, *88*(4), 514–521. https://doi.org/10.1016/j.jfoodeng.2008.03.011

Moussaoui, H., Bahammou, Y., Idlimam, A., Lamharrar, A., & Abdenouri, N. (2019). Investigation of hygroscopic equilibrium and modeling sorption isotherms of the argan products: A comparative study of leaves, pulps, and fruits. *Food and Bioproducts Processing*, *114*, 12–22. https://doi.org/10.1016/j.fbp.2018.11.002

Muzaffar, K., & Kumar, P. (2016). Moisture sorption isotherms and storage study of spray dried tamarind pulp powder. *Powder Technology*, *291*, 322–327. https://doi.org/10.1016/j.powtec.2015.12.046

Ocieczek, A., Pukszta, T., Żyłka, K., & Kirieieva, N. (2023). The influence of storage conditions on the stability of selected health-promoting properties of tea. *LWT*, 115029. https://doi.org/10.1016/j.lwt.2023.115029

Ojike, O., Uzodinma, E. O., Ali, E. O., Nweze, B. C., Okoyeuzu, C. F., & Eze, C. R. (2022). Moisture Adsorption potentials and energy models of Gongronema latifolium leaves dried in separate environments. *Food Science and Nutrition*, *10*(2), 388–401. https://doi.org/10.1002/fsn3.2616

Ouertani, S., Azzouz, S., Hassini, L., Koubaa, A., & Belghith, A. (2014). Moisture sorption isotherms and thermodynamic properties of Jack pine and palm wood: Comparative study. *Industrial Crops and Products*, *56*, 200–210. https://doi.org/10.1016/j.indcrop.2014.03.004

Pinto, N. C. C., Duque, A. P. N., Pacheco, N. R., Mendes, R. F., Motta, E. V. S., Bellozi, P. M. Q., Ribeiro, A., Salvador, M. J., & Scio, E. (2015). Pereskia aculeata: A plant food with antinociceptive activity. *Pharmaceutical Biology*, *53*(12), 1780–1785. https://doi.org/10.3109/13880209.2015.1008144

Pinto, N. de C. C., Cassini-Vieira, P., Souza-Fagundes, E. M. de, Barcelos, L. S., Castañon, M. C. M. N., & Scio, E. (2016). Pereskia aculeata Miller leaves accelerate excisional wound healing in mice. *Journal of Ethnopharmacology*, *194*, 131–136. https://doi.org/10.1016/j.jep.2016.09.005

Pitt, J. I., & Hocking, A. D. (2009). *Fungi and Food Spoilage* (3rd ed.). Springer New York.

Polachini, T. C., Betiol, L. F. L., Lopes-Filho, J. F., & Telis-Romero, J. (2016). Water adsorption isotherms and thermodynamic properties of cassava bagasse. *Thermochimica Acta*, *632*, 79–85. https://doi.org/10.1016/j.tca.2016.03.032

Rizvi, S. S. H. (2014). Thermodynamic properties of foods in dehydration. In M. A. Rao, S. S. H. Rizvi, & A. K. Datta (Eds.), *Engineering properties of foods* (4th ed., pp. 359–436). CRC Press.

Rosa, D. P., Evangelista, R. R., Borges Machado, A. L., Sanches, M. A. R., & Telis-Romero, J. (2021). Water sorption properties of papaya seeds (Carica papaya L.) formosa variety: An assessment under storage and drying conditions. *Lwt*, *138*(June 2020). https://doi.org/10.1016/j.lwt.2020.110458

Sanches, M. A. R., Augusto, P. E. D., Polachini, T. C., & Telis-Romero, J. (2023). Water sorption properties of brewer's spent grain: A study aimed at its stabilization for further conversion into value-added products. *Biomass and Bioenergy*, *170*(December 2022), 106718. https://doi.org/10.1016/j.biombioe.2023.106718

Spada, J. C., Noreña, C. P. Z., Marczak, L. D. F., & Tessaro, I. C. (2013). Water adsorption isotherms of microcapsules with hydrolyzed pinhão (Araucaria angustifolia seeds) starch as wall material. *Journal of Food Engineering*, *114*(1), 64–69. https://doi.org/10.1016/j.jfoodeng.2012.07.019

Spiess, W. E. L., & Wolf, W. F. (1983). The results of the COST 90 project on water activity. In R. Jowitt (Ed.), *Physical Properties of Foods* (pp. 65–91). Applied Science Publishers.

Stone, M. (1979). Comments on Model Selection Criteria of Akaike and Schwarz. *Journal of the Royal Statistical Society. Series B (Methodological)*, *41*(2), 276–278. https://www.jstor.org/stable/2985044

Tagnamas, Z., Bahammou, Y., Moussaoui, H., Kouhila, M., Lamsyehe, H., Idlimam, A., & Lamharrar, A. (2021). Exploring the sorption and thermodynamic proprieties of white truffle (Terfezia boudieri). *Journal of Food Process Engineering*, *44*(12), 1–11. https://doi.org/10.1111/jfpe.13888

Takeiti, C. Y., Antonio, G. C., Motta, E. M. P., Collares-Queiroz, F. P., & Park, K. J. (2009). Nutritive evaluation of a non-conventional leafy vegetable (Pereskia aculeata Miller). *International Journal of Food Sciences and Nutrition*, *60*(SUPPL. 1), 148–160. https://doi.org/10.1080/09637480802534509

Velázquez-Gutiérrez, S. K., Figueira, A. C., Rodríguez-Huezo, M. E., Román-Guerrero, A., Carrillo-Navas, H., & Pérez-Alonso, C. (2015). Sorption isotherms, thermodynamic properties and glass transition temperature of mucilage extracted from chia seeds (Salvia hispanica L.). *Carbohydrate Polymers*, *121*, 411–419. https://doi.org/10.1016/j.carbpol.2014.11.068

Wolfinger, R. (1993). Covariance structure selection in general mixed models. *Communications in Statistics - Simulation and Computation*, *22*(4), 1079–1106. https://doi.org/10.1080/03610919308813143

Yogendrarajah, P., Samapundo, S., Devlieghere, F., De Saeger, S., & De Meulenaer, B. (2015). Moisture sorption isotherms and thermodynamic properties of whole black peppercorns (Piper nigrum L.). *Lwt*, *64*(1), 177–188. https://doi.org/10.1016/j.lwt.2015.05.045

Zhang, Z. shan, Li, X. dan, Jia, H. jie, & Liu, Y. lan. (2022). Moisture sorption isotherms and thermodynamic properties of tiger nuts: An oil-rich tuber. Lwt, 167(100), 113866. https://doi.org/10.1016/j.lwt.2022.113866

2.6 SUPPLEMENTARY TABLES

Table S1 - Water activity of saturated salt solutions at different temperatures.

Salt	Water activity								
	Storage temperatures				Storage/Drying	Drying temperatures			
	5 ºC	10 ºC	20 ºC	30 ºC	40 ºC	50 ºC	60 ºC	70 ºC	80 ºC
LiBr	0.0743	0.0714	0.0661	0.0616	0.0580	0.0553	0.0533	0.0523	0.0520
LiCl	0.1126	0.1129	0.1131	0.1128	0.1121	0.1110	0.1095	0.1075	0.1051
LiI	0.2168	0.2061	0.1856	0.1657	0.1455	0.1238	0.0998	0.0723	-
$MgCl_2$	0.3366	0.3347	0.3307	0.3244	0.3160	0.3054	0.2926	0.2777	0.2605
NaI	0.4242	0.4183	0.3965	0.3615	0.3288	0.2921	0.2595	0.2357	0.2252
K_2CO_3	0.4313	0.4314	0.4315	0.4317	-	-	-	-	-
$Mg(NO_3)_2$	0.5886	0.5736	0.5438	0.5140	0.4842	0.4544	-	-	-
NaBr	0.6351	0.6215	0.5914	0.5603	0.5317	0.5093	0.4966	0.4970	0.5033
KI	0.7330	0.7211	0.6990	0.6789	0.6609	0.6449	0.6311	0.6193	0.6097
NaCl	0.7565	0.7567	0.7547	0.7509	0.7468	0.7443	0.7450	0.7506	0.7629
$(NH_4)_2SO_4$	0.8242	0.8206	0.8134	0.8063	0.7991	0.7920	-	-	-
KCl	0.8767	0.8677	0.8511	0.8362	0.8232	0.8120	0.8025	0.7949	0.7890
KNO_3	0.9627	0.9596	0.9462	0.9231	0.8903	0.8478	-	-	-
K_2SO_4	0.9848	0.9818	0.9759	0.9700	0.9641	0.9582	-	-	-

Table S2 - Ora-pro-nobis experimental data of equilibrium moisture content versus water activity at storage and drying temperatures.

Temperature (Celsius)									
5		10		20		30		40	
a_w	X_{eq}	a_w	X_{eq}	a_w	X_{eq}	a_w	X_{eq}	a_w	X_{eq}
0.074	0.054±0.002	0.071	0.053±0.001	0.066	0.052±0.004	0.062	0.050±0.001	0.058	0.044±0.001
0.113	0.059±0.002	0.113	0.057±0.001	0.113	0.058±0.002	0.113	0.057±0.038	0.112	0.054±0.001
0.217	0.067±0.003	0.206	0.065±0.001	0.186	0.065±0.003	0.166	0.061±0.041	0.146	0.057±0.003
0.336	0.077±0.003	0.335	0.075±0.001	0.331	0.077±0.003	0.324	0.073±0.05	0.316	0.072±0.001
0.424	0.086±0.002	0.418	0.083±0.002	0.397	0.081±0.003	0.362	0.076±0.053	0.329	0.074±0.001
0.431	0.086±0.001	0.431	0.086±0.001	0.432	0.085±0.003	0.432	0.082±0.056	0.484	0.083±0.004
0.589	0.109±0.001	0.574	0.102±0.002	0.544	0.096±0.002	0.514	0.090±0.066	0.532	0.087±0.001
0.635	0.117±0.005	0.622	0.110±0.003	0.591	0.102±0.004	0.560	0.095±0.068	0.661	0.106±0.006
0.733	0.141±0.003	0.721	0.129±0.003	0.699	0.118±0.002	0.679	0.112±0.081	0.747	0.117±0.006
0.757	0.149±0.006	0.757	0.136±0.003	0.755	0.129±0.003	0.751	0.124 ±0.09	0.799	0.121±0.008
0.824	0.174±0.005	0.821	0.157±0.002	0.813	0.142±0.004	0.806	0.136 ±0.095	0.823	0.128±0.007
0.877	0.200±0.004	0.868	0.176±0.002	0.851	0.152±0.007	0.836	0.143±0.100	0.890	0.140±0.003
0.963	0.267±0.009	0.960	0.226±0.005	0.946	0.184±0.004	0.923	0.170±0.132	0.964	0.161±0.008
0.985	0.291±0.004	0.982	0.243±0.001	0.976	0.197±0.007	0.970	0.188±0.141		
50		60		70		80			
a_w	X_{eq}	a_w	X_{eq}	a_w	X_{eq}	a_w	X_{eq}		
0.055	0.039±0.001	0.053	0.036±0.001	0.052	0.03±0.001	0.052	0.026±0.001		
0.111	0.053±0.001	0.110	0.049±0.001	0.108	0.045±0.001	0.105	0.039±0.001		
0.124	0.051±0.002	0.100	0.045±0.001	0.072	0.036±0.001	0.261	0.059±0.001		
0.305	0.069±0.001	0.293	0.068±0.001	0.278	0.066±0.001	0.225	0.057±0.001		
0.292	0.066±0.002	0.260	0.067±0.001	0.236	0.062±0.002	0.514	0.077±0.004		
0.454	0.082±0.003	0.497	0.079±0.002	0.497	0.082±0.004	0.610	0.090±0.002		
0.509	0.084±0.004	0.631	0.099±0.005	0.619	0.095±0.006	0.763	0.099±0.005		
0.645	0.100±0.005	0.745	0.111±0.008	0.751	0.102±0.005	0.789	0.108±0.002		
0.744	0.112±0.003	0.803	0.116±0.002	0.795	0.109±0.005				
0.792	0.118±0.003								
0.812	0.119±0.008								
0.848	0.127±0.003								
0.958	0.148±0.006								

3 Capítulo 3 - Thin layer convective drying kinetics of ora-pro-nóbis (*Pereskia aculeata* Miller) leaves.

André Luiz Borges-Machado[a,b]*, Marcio Augusto Ribeiro Sanches[a], Maria Júlia Neves Martins[a] Priscila Alonso dos Santos[b], Guadalupe Luna-Solano[c], Javier Telis-Romero[a].

[a] Food Engineering and Technology Department, State University of São Paulo, São José do Rio Preto, São Paulo, 15054-000, Brazil

[b] Department of Food Engineering, Institute Federal Goiano Campus Rio Verde, Rod. Sul Goiana, 75901-970 Rio Verde, Goiás, Brazil

[c] Instituto Tecnologico de Orizaba - Division de Estudios de Posgrado e Investigación - Orizaba – México.

ABSTRACT

Ora-pro-nóbis is a cactus whose leaves are source of fibers, proteins, minerals, and vitamins and its flour has been added to many food products such as cereal bars, ice cream, cheese and pasta aiming at nutritional enhancing. It this way, this study aimed to determine and model the ora-pro-nóbis leaves drying curves at 50-80 ºC as well as to determine the effective diffusion coefficient, activation energy, enthalpy, entropy, and Gibbs free energy. The leaves presented 0.868 kg water/kg w.b. of initial moisture content. The drying assays were conducted in an oven and the leaves were dried until they achieved the equilibrium moisture content. Among the five models fitted to the drying data, the Weibull model is the one the best described the drying curves of ora-pro-nóbis leaves from 50 ºC to 80 ºC. The effective diffusion coefficient increased with temperature and ranged from $2.64 \cdot 10^{-12}$ to $2.02 \cdot 10^{-11}$ m^2/s. The activation energy was equal to 65.81 kJ/mol. The enthalpy and entropy decreased while the Gibbs free energy increased.

Keywords: AIC, BIC, Weibull model, cactus, Barbados gooseberry

3.1 INTRODUCTION

Originating from tropical dry forests, *Pereskia aculeata*, commonly known as ora-pro-nóbis in Brazil, is a *Cactaceae* plant with succulent and edible leaves which are rich in protein, minerals, vitamins, and fiber (Silva et al., 2018). From the southern to the northeastern regions of Brazil, ora-pro-nóbis leaves find application in traditional cuisine, serving as a key ingredient in a variety of sweet and savory dishes (Garcia et al., 2019). Recently, some researchers have been investigating the addition of ora-pro-nóbis in different types of foods such as cereal bars (da Cruz et al., 2024), ice cream (Santos et al., 2022), petit Suisse cheese (Silva et al., 2021), and pasta (Sato et al., 2019) aiming to enhance their nutritional quality. In addition, ora-pro-nóbis is commonly employed for pharmacological purposes in Brazilian folk medicine, a usage attributed to its bioactive molecules known for their metabolic, anti-inflammatory, antioxidant, and antimicrobial properties (Nogueira Silva et al., 2023). Fresh leaves utilized for both culinary and medicinal purposes are inherently highly perishable. Frequently, post-harvest losses occur and a noticeable decline in quality ensues due to increased enzymatic and microbial activity resulting from moisture, climate changes, inadequate handling, delayed transportation, improper storage, and delayed sales (Babu et al., 2018).

Drying processes play a crucial role in lowering the moisture content of food materials, preventing microbial growth, and deterioration. This contributes to extending shelf life, reducing packaging requirements, and enhancing storage conditions for convenient transportation (Inyang et al., 2018). Researches indicate that relying solely on experimental drying methods without incorporating mathematical considerations of drying kinetics can substantially impact dryer efficiency, elevate production costs, and compromise the quality of the dried product (Onwude et al., 2016). Therefore, the utilization of mathematical models for estimating drying kinetics, energy requirements in the drying process together with mass transfer parameters, and thermodynamic properties of agricultural and food products becomes imperative.

Various internal transport mechanisms such as pure diffusion, surface diffusion, Knudsen diffusion, capillary flow, evaporation, and condensation are involved in a drying process, with moisture diffusivity (Vasi et al., 2012). Among the mass transfer parameters, the effective diffusion coefficient and the activation energy are fundamental in the design of drying systems. Effective moisture diffusivity characterizes the pace of moisture migration, serving as a valuable metric for designing efficient dryers in terms of both drying duration and energy expenditure, while activation energy plays a crucial role in elucidating the responsiveness of effective moisture diffusivity to temperature changes (Delfiya et al., 2022).

Therefore, the aims of this work are: (i) to determine the ora-pro-nóbis leaves drying curves at 50-80 ºC, (ii) to model the drying process, (iii) to estimate the effective diffusion coefficient and activation energy, and (iv) calculate the enthalpy, entropy, and Gibbs free energy.

3.2 MATERIAL AND METHODS

3.2.1 Raw material

Ora-pro-nóbis leaves were cultivated at Instituto Federal Goiano – Campus Rio Verde. They were harvested in the morning and transported to the Laboratory of Food Analysis of the same institute. The leaves were washed with tap water and sanitized with a chlorinated solution (100 ppm/20 min). Then, they were carefully dried with paper towels.

3.2.2 Drying experiments

Drying experiments were performed in a forced air circulation oven (TH.510, Thoth Equipamentos, Piracicaba, Brazil) at temperatures of 50, 60, 70, and 80 ºC. The samples were placed into the oven after the desired condition had been maintained for at least 1 hour. Approximately 25 grams of ora-pro-nóbis leaves were used in each repetition, which were performed in quadruplicate using stainless steel sieved bowls to allow air flux through all the leaf surfaces. The drying air temperatures and room temperature were monitored using thermohygrometers inside and outside the dryer. The relative humidity inside the oven was estimated using psychrometry concepts with the support of the software GRAPSI. The sample weight was continuously recorded every five minutes during the first 30 minutes, and then, the interval between weight measurements was gradually increased but did not exceed 30 minutes between each measurement. This procedure allowed us to calculate the moisture content by mass difference at each drying time. The drying process was considered complete when three consecutive measurements of the sample weight showed no significant change, thus indicating equilibrium moisture content (X_{eq}).

3.2.3 Drying kinetics and modelling

The initial moisture content of ora-pro-nóbis leaves were determined by AOAC, (2007) gravimetric method nº 950.46 and the leaves presented 88.20±0.36 g of water/100 g. The moisture ratio of each repetition at each time and temperature were calculating using Equation 1.

$$MR = \frac{X_t - X_{eq}}{X_0 - X_{eq}} \tag{1}$$

in which, X_{eq}, X_t and X_0 are the equilibrium moisture content, moisture content at time t and the initial moisture content, respectively. The moisture ratio (MR) values were plotted against time and Newton, Page, Henderson and Pabis, Logarithm and Weibull models (Equations 2-6) were fitted to the data using non-linear regression by the Levenberg–Marquardt method with the aid of Origin 2022 (OriginLab Corporation, Northampton, MA).

$$MR = exp(-kt) \tag{2}$$
$$MR = exp(-kt^n) \tag{3}$$
$$MR = a \cdot exp(-kt) \tag{4}$$
$$MR = a \cdot exp(-kt) + c \tag{5}$$
$$MR = exp\left[-\left(\frac{t}{\alpha}\right)^{\beta}\right] \tag{6}$$

in which: a, c, n: model coefficients; k: drying constant; α: scale parameter (min); β: shape parameter; t: drying time (min).

3.2.4 Effective diffusion coefficient (D_{eff}) and activation energy (E_a)

The effective diffusion coefficients at different temperatures were calculated by non-linear regression using the solutions of Fick's second law purposed by Crank, (1975) truncated in the twelfth term. The D_{eff} of ora-pro-nóbis leaves was calculated through Equation 8 for flat slab geometry.

$$MR = \frac{8}{\pi^2}\sum_{n=0}^{\infty}\frac{1}{(2n+1)^2} exp\left[\frac{-(2n+1)^2\,\pi^2 \cdot D_{eff} \cdot t}{4}\left(\frac{A}{V}\right)^2\right] \tag{8}$$

where n is the number of terms, A is the medium area of 15 leaves surface and V is the volume of the leaf.

The area of each leaf was determined by integrating the digital image of leaves using the software ImageJ and the volume of the leaf were determined by Equation 9.

$$V = A \cdot d \tag{9}$$

where d is the leaf thickness.

The Arrhenius model (Equation 10) was used to evaluate the dependence of D_{eff} to the temperature and to calculate the activation energy (E_a) in J/mol through the linearized form of Equation 13.

$$D_{eff} = D_0 \; exp\left[\frac{E_a}{RT}\right] \tag{10}$$

where D_0 is the pre-exponential factor of the Arrhenius equation (m^2/s); T is the absolute air temperature (K) and R is the universal gas constant (8.314 J/mol/K).

3.2.5 Enthalpy (ΔH), entropy (ΔS) and Gibbs free energy (ΔG)

The drying thermodynamic properties were calculated following the mathematical procedure described by Jideani and Mpotokwana (2009) and presented by Corrêa et al. (2012). The ΔH, ΔS and ΔG in J/mol were calculated using Equations 11, 12 and 13.

$$H = E_a - R \cdot T_{abs} \tag{11}$$

$$S = R\left[\ln D_0 - \ln\left(\frac{k_B}{h_P}\right) - \ln T_{abs}\right] \tag{12}$$

$$G = H - T_{abs} \cdot S \tag{13}$$

in which k_B is the Boltzmann constant, 1.38 x 10^{-23} J/K and h_P is the Planck constant, 6.626 x 10^{-34} J/s.

3.2.6 Statistical analysis

The quality of the fitting of the drying models to moisture ratio data were evaluated based on the adjusted coefficient of determination (R^2_{adj}) and reduced chi-square (χ^2). An excellent fit is obtained when R^2_{adj} is equal one and χ^2 is low (Inyang et al., 2018). The Akaike information criterion (AIC) and Bayesian-Schwarz information criterion (BIC) were applied as decisive criteria in selecting the model that best suited the experimental data among those that were adequate in terms of parameters R^2_{adj} and χ^2. The AIC and SIC values were calculated according to Equations 14 and 15 (Akaike, 1974; Schwarz, 1978). Lower values of these parameters reflect best fit.

$$AIC = -2\log\mathcal{L}(\hat{\theta}) + 2p \tag{14}$$

$$BIC = -2\log\mathcal{L}(\hat{\theta}) + p\ln(n) \tag{15}$$

in which, n is the number of experimental points, p is the number of parameters of the model, and $\mathcal{L}(\hat{\theta})$ is the value of the likelihood function considering the parameters of the obtained model.

3.3 RESULTS AND DISCUSSION

Aiming to normalize the curves, the weight loss data were converted to moisture ratios and plotted against drying time. Table 1 presents the estimated coefficients, adjusted coefficients of determination, reduced chi-square, AIC, and BIC. The five drying models showed a good fit to the drying data as they presented R^2_{adj}>0.97 and χ^2 close to zero. Newton model presented the lowest R^2_{adj} and the highest χ^2 among the models evaluated while Logarithmic and Weibull models the highest R^2_{adj} and lowest χ^2 at the four temperatures studied. In this way, the models were ranked using the AIC and BIC values, in which the higher the value, the worse the model (Wolfinger, 1993). The Newton model presented the highest values for both criteria at all temperatures, being the least suitable among the models. The Logarithmic model presented the lowest AIC and BIC values at 50 ºC and 60 ºC, and the third lowest values at 70 ºC and 80 ºC. On the other hand, the Weibull model was more suitable at 70 ºC and 80 ºC and is the second most suitable model at 60 ºC. Thus, the Weibull model was selected to describe the drying process of ora-pro-nóbis leaves. Additionally, the Logarithmic model is mathematically more complex than the Weibull model due to having more coefficients. This model was also appropriate for describing the drying curves of other leaves, such as bollén (*Kageneckia oblonga*) leaves (Zambra et al., 2021) and stevia (*Rebaudiana Bertoni*) leaves (Castillo Téllez et al., 2018).

Table 1 - Estimated coefficients and fitting parameters of the models selected to represent the drying curves at different temperatures of ora-pro-nóbis (Pereskia aculeata Miller) leaves

Model	Parameters	Temperature (ºC)			
		50	**60**	**70**	**80**
Newton	$k \cdot 10^3$	1.900	4.480	9.970	12.690
	R^2_{aj}	0.9827	0.9869	0.9802	0.9752
	$\chi^2 \cdot 10^5$	126	158	253	310
	AIC	-223.704	-248.331	-145.983	-123.480
	BIC	-221.039	-245.337	-144.091	-121.930
Page	$k \cdot 10^3$	3.360	1.470	2.300	2.740
	n	0.905	1.206	1.321	1.351
	R^2_{aj}	0.9858	0.9969	0.9991	0.9970
	$\chi^2 \cdot 10^5$	103	37.479	11.568	37.755
	AIC	-228.957	-303.046	-221.560	-168.164
	BIC	-225.178	-298.741	-219.047	-166.224
Henderson and Pabis	a	0.965	1.050	1.077	1.069
	$k \cdot 10^3$	1.780	4.760	10.920	13.720
	R^2_{aj}	0.9879	0.9908	0.9882	0.9811

	$\chi^2 \cdot 10^5$	87.970	111	151	236
	AIC	-234.483	-260.735	-157.372	-127.876
	BIC	-230.704	-256.430	-154.858	-125.936
Logarithmic	a	1.106	1.193	1.174	1.198
	$k \cdot 10^3$	1.380	3.360	8.470	10.010
	c	-0.153	-0.176	-0.125	-0.162
	R^2_{aj}	0.9919	0.9995	0.9964	0.9935
	$\chi^2 \cdot 10^5$	59.107	6.278	46.371	81.325
	AIC	-246.503	-371.305	-185.102	-149.391
	BIC	-241.777	-365.828	-182.227	-147.380
Weibull	α	541.890	224.076	99.425	78.792
	β	0.907	1.211	1.323	1.353
	R^2_{aj}	0.9858	0.9969	0.9991	0.9970
	$\chi^2 \cdot 10^5$	103.000	37.395	11.560	37.750
	AIC	-228.961	-303.131	-221.576	-168.166
	BIC	-225.182	-298.826	-219.062	-166.227

The α and β coefficients of Weibull model are known as scale and shape parameters, respectively. The scale parameter, which is the time required to execute approximately 63% of the process (Corzo et al., 2008), reduced from 541.89 min at 50 ºC to 78.79 min at 80 ºC. The shape parameter is related to the mass transfer speed, in which different values of this parameter result in distinct curves that can describe different mechanisms such as relaxation, convection, and diffusion (Corzo et al., 2008). In this study, β increased with temperature from 0.907 to 1.353. When the shape parameter is equal to one, the model predicts a practically first-order drying time. Furthermore, when $\beta > 1$, a lag phase is likely to happen during the early stage (Ju et al., 2016), and the drying process is controlled by both internal and external water diffusion (Huang et al., 2021).

Despite the Weibull model being chosen to describe the drying curves, the good fit of the other models allowed us to make some considerations regarding their constants. The k constant of Newton, Page, Henderson and Pabis, and Logarithmic models, also known as the drying constant, is related to the effect of external drying conditions such as air velocity, temperature, and humidity (Goneli et al., 2009; Inyang et al., 2018). Table 3 shows that the drying constant increased directly with temperature, except in the Page model where a clear tendency was not observed. These findings can be associated with the effective diffusivity of drying in the falling-rate period and might provide useful information to understand the behavior of the drying air temperature (Siqueira et al., 2020).

Figure 1 presents the experimental and calculated moisture content ratios of ora-pro-nóbis as a function of drying time at temperatures ranging from 50 ºC to 80 ºC. The leaves initially had a moisture content of 0.868 kg water/kg w.b. and took 1230 min (50 ºC), 600 min (60 ºC), 300 min (70 ºC), and 230 min (80 ºC) to reach equilibrium moisture contents of 0.056, 0.046, 0.034, and 0.026 kg water/kg w.b., respectively. The increase in temperature caused a decrease in vapor pressure, which facilitated water removal, consequently reducing drying time. According to Babu et al. (2018), the quality of leaves heavily depends on drying time, emphasizing the need for a rapid completion of the process to reach critical humidity levels to inhibit mold growth. Prolonged drying to final moisture levels leads to significant declines in color, nutritional content, and structural integrity.

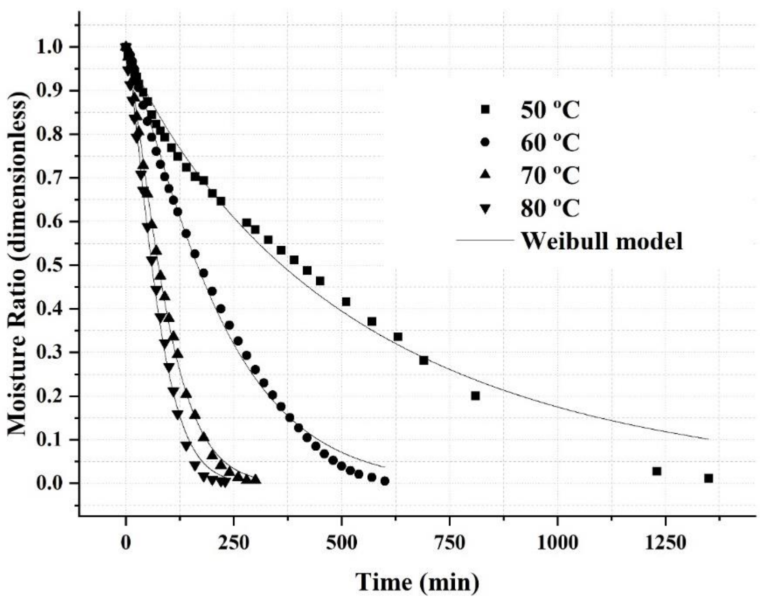

Figure 1 – Experimental and estimated values by the Weibull model for the drying of ora-pro-nóbis (*Pereskia aculeata* Miller) leaves at temperatures of 50, 60, 70, and 80 ºC

Figure 2 shows the values of effective diffusion coefficient plotted against temperature, which increased from $2.64 \cdot 10^{-12}$ to $2.02 \cdot 10^{-11}$ m^2/s directly to temperature. This could be attributed to the higher temperature, which boosts heating energy and consequently elevates the activity of water molecules, resulting in a higher effective moisture diffusivity. Comparable results were reported for *Allium roseum* leaves (Ben Haj Said et al., 2015), rosemary leaves (Mghazli et al., 2017), sadabahar (*Catharanthus roseus*) leaves (Kasara et al., 2021), scent, and lemon basil leaves (Mbegbu et al., 2021). The dependence of the effective diffusion coefficient on temperature ranged from 50 ºC to 80 ºC and was represented by an Arrhenius-type function (Figure 3). The estimated pre-exponential factor D_0 was equal to 7.58 m^2/s, and the activation energy for liquid diffusion in the drying process of ora-pro-nóbis leaves was 65.81 kJ/mol for a temperature range between 50 and 80 °C. According to Zogzas et al., (1996), the activation energy of food materials ranges between 12.7–110 kJ/mol, which is in agreement with our result.

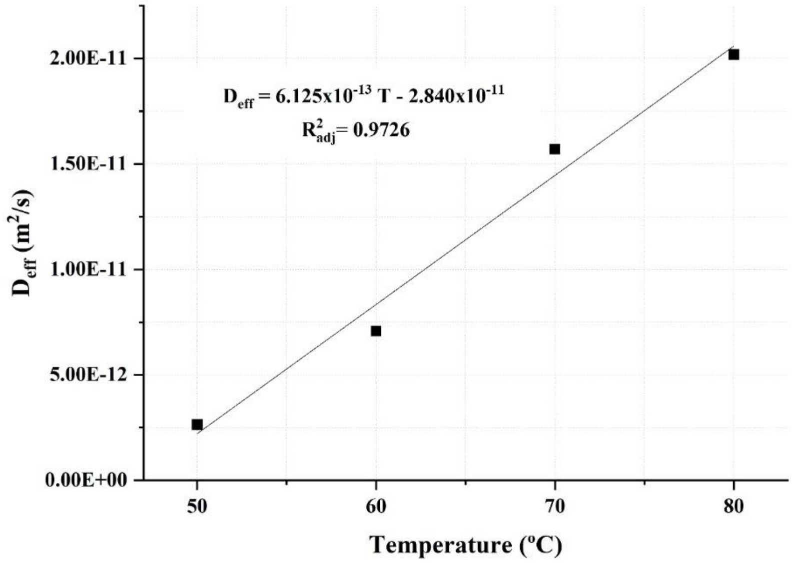

Figure 2 - Effective diffusion coefficient of ora-pro-nóbis drying plotted as function temperatures of 50, 60, 70, and 80 ºC.

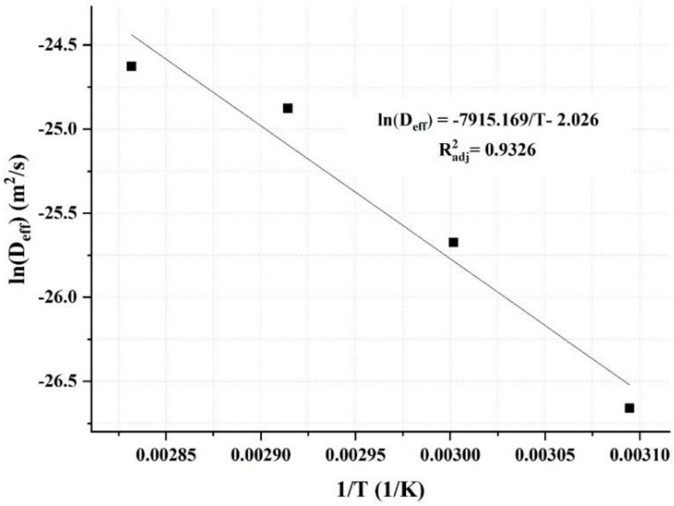

Figure 3 – Linearized Arrhenius plot of the effective diffusion coefficient at 50, 60, 70, and 80 ºC for ora-pro-nóbis (Pereskia aculeata Miller) leaves.

Enthalpy is associated with the energy required to remove water from a food matrix (Rizvi, 2014), i.e. the energy required to dry a product such as ora-pro-nóbis leaves. On the other hand, entropy is a measure of the degree of disorder between the water and the product and corresponds to the energy that is not available to complete a particular operation such as drying (McMinn et al., 2005; Sanches et al., 2023). In Table 2, the enthalpy, entropy, and Gibbs free energy of the ora-pro-nóbis leaves at temperatures ranging from 50-80 ºC are presented. It was noted that the enthalpy decreased from 63.124 to 62.874 kJ/mol as temperature increased; thus, the energy requirement reduces with the increase of drying air temperature. In contrast, the entropy behaved inversely, increasing directly with air temperature, in absolute values, from 0.22948 to 0.22874 kJ/mol/K (Table 2). This occurs because an increase in temperature causes more agitation in water molecules, leading to an increase in the disorder of the water–ora-pro-nóbis leaves system. Gibbs free energy is indicative of the spontaneity of a water vapor desorption process (Collazos-Escobar et al., 2022), showing positive values for non-spontaneous processes and negative values for spontaneous processes. Additionally, ΔG can be calculated as the difference between the total available energy (enthalpy) and the unavailable energy (entropy) (Rizvi, 2014). The Gibbs free energy rose directly with temperature from +0.137 to +0.144 kJ/mol, showing positive values, which indicates that drying is an endergonic process, requiring an energy supply to occur. The thermodynamic behavior presented above is consistent with the results presented for other leafy vegetables such as jambu (*Acmella oleracea*) leaves (Gomes et al., 2022), bitter melon (*Momordica charantia* L.) leaves (Silva et al., 2020), boldo leaves (*Plectranthus barbatus* Andrews) (Silva et al., 2019), and pata-de-vaca (*Bauhinia forficata* Link) leaves (Silva et al., 2017).

Table 2 - Values of enthalpy (H), entropy (S) and Gibbs free energy (G) for different drying air temperatures of ora-pro-nóbis (Pereskia aculeata Miller) leaves.

Temperature (ºC)	**Thermodynamic properties**		
	H (kJ/mol)	**S (kJ/mol/K)**	**G (kJ/mol)**
50	63.124	-0.22874	0.137
60	63.041	-0.22900	0.139
70	62.958	-0.22924	0.142
80	62.874	-0.22948	0.144
Equation	$-8.3 \cdot 10^{-3} \cdot T + 63.54$	$-2 \cdot 10^{-5} \cdot T - 0.228$	$2 \cdot 10^{-4} \cdot T + 0.126$
R^2_{adj}	0.999	0.999	0.999

3.4 CONCLUSION

The Weibull model best describes the drying curves of ora-pro-nóbis leaves at 50, 60, 70, and 80 ºC. Based on the shape parameter, 63% of the drying process is achieved after 541.89 min at 50 ºC and 78.79 min at 80 ºC. The drying time required for ora-pro-nóbis leaves to reach equilibrium moisture content ranges from 1230 (50 ºC) to 230 minutes (80 ºC). The effective diffusion coefficient increases directly with temperature, and the energy required to initiate the drying process is equal to 65.81 kJ/mol. The enthalpy and entropy decrease, while the Gibbs free energy increases.

3.5 REFERENCES

Akaike, H., 1974. A new look at the statistical model identification, in: IEEE Transactions on Automatic Control. pp. 716–723. https://doi.org/10.1109/TAC.1974.1100705

AOAC, 2007. Association of Official Analytical Chemistry, 18th ed, In: Official methods of analysis to AOAC International. Gaithersburg.

Babu, A.K., Kumaresan, G., Raj, V.A.A., Velraj, R., 2018. Review of leaf drying: Mechanism and influencing parameters, drying methods, nutrient preservation, and mathematical models. Renew. Sustain. Energy Rev. 90, 536–556. https://doi.org/10.1016/j.rser.2018.04.002

Ben Haj Said, L., Najjaa, H., Farhat, A., Neffati, M., Bellagha, S., 2015. Thin layer convective air drying of wild edible plant (Allium roseum) leaves: experimental kinetics, modeling and quality. J. Food Sci. Technol. 52, 3739–3749. https://doi.org/10.1007/s13197-014-1435-2

Castillo Téllez, M., Pilatowsky Figueroa, I., Castillo Téllez, B., López Vidaña, E.C., López Ortiz, A., 2018. Solar drying of Stevia (Rebaudiana Bertoni) leaves using direct and indirect technologies. Sol. Energy 159, 898–907.

https://doi.org/10.1016/j.solener.2017.11.031

Collazos-Escobar, G.A., Gutiérrez-Guzmán, N., Váquiro-Herrera, H.A., Bon, J., Garcia-Perez, J. V., 2022. Thermodynamic analysis and modeling of water vapor adsorption isotherms of roasted specialty coffee (Coffee arabica L. cv. Colombia). Lwt 160. https://doi.org/10.1016/j.lwt.2022.113335

Corrêa, P.C., Oliveira, G.H.H., Santos, E.S., 2012. Thermodynamic Properties of Agricultural Products Processes, in: Arana, I. (Ed.), Physical Properties of Foods Novel Measurement Techniques and Applications. CRC Press, Boca Raton, pp. 131–141.

Corzo, O., Bracho, N., Pereira, A., Vásquez, A., 2008. Weibull distribution for modeling air drying of coroba slices. Lwt 41, 2023–2028. https://doi.org/10.1016/j.lwt.2008.01.002

Crank, J., 1975. The Mathematics of Diffusion, 2nd ed, Journal of the American Chemical Society. Clarendon Press, Oxford, UK. https://doi.org/10.1021/ja01562a072

da Cruz, G.S., da Silva, C.N.P., Gomes-Junior, E.A., de Souza, T.L., Latif, A.L.O., Maciel, L.F., Santos, L.F.P., Linde, G.A., Colauto, N.B., Menezes-Filho, J.A., de Jesus Benevides, C.M., Pinto, L.C., 2024. Cereal bar enriched with ora-pro-nóbis (Pereskia aculeata Miller): physicochemical and sensory characterization. J. Food Sci. Technol. https://doi.org/10.1007/s13197-024-05924-2

Delfiya, D.S.A., Prashob, K., Murali, S., Alfiya, P. V., Samuel, M.P., Pandiselvam, R., 2022. Drying kinetics of food materials in infrared radiation drying: A review. J. Food Process Eng. 45, 1–19. https://doi.org/10.1111/jfpe.13810

Garcia, J.A.A., Corrêa, R.C.G., Barros, L., Pereira, C., Abreu, R.M.V., Alves, M.J., Calhelha, R.C., Bracht, A., Peralta, R.M., Ferreira, I.C.F.R., 2019. Phytochemical profile and biological activities of “Ora-pro-nobis” leaves (Pereskia aculeata Miller), an underexploited superfood from the Brazilian Atlantic Forest. Food Chem. 294, 302–308. https://doi.org/10.1016/j.foodchem.2019.05.074

Gomes, F.P., Resende, O., Sousa, E.P. de, Célia, J.A., de Oliveira, K.B., 2022. Application of Mathematical Models and Thermodynamic Properties in the Drying of Jambu Leaves. Agriculture 12, 1252. https://doi.org/10.3390/agriculture12081252

Goneli, A.L.D., Corrêa, P.C., Afonso Júnior, P.C., Oliveira, G.H.H. de., 2009. Cinética de secagem dos grãos de café descascados em camada delgada. Rev. Bras. Armazenamento 11, 64–73.

Huang, X., Li, W., Wang, Y., Wan, F., 2021. Drying characteristics and quality of Stevia rebaudiana leaves by far-infrared radiation. LWT 140, 110638. https://doi.org/10.1016/j.lwt.2020.110638

Inyang, U.E., Oboh, I.O., Etuk, B.R., 2018. Kinetic Models for Drying Techniques—Food Materials. Adv. Chem. Eng. Sci. 08, 27–48. https://doi.org/10.4236/aces.2018.82003

Jideani, V.A., Mpotokwana, S.M., 2009. Modeling of water absorption of Botswana bambara varieties using Peleg's equation. J. Food Eng. 92, 182–188. https://doi.org/10.1016/j.jfoodeng.2008.10.040

Ju, H.Y., Zhang, Q., Mujumdar, A.S., Fang, X.M., Xiao, H.W., Gao, Z.J., 2016. Hot-air Drying Kinetics of Yam Slices under Step Change in Relative Humidity. Int. J. Food Eng. 12, 783–792. https://doi.org/10.1515/ijfe-2015-0340

Kasara, A., Babar, O.A., Tarafdar, A., Senthilkumar, T., Sirohi, R., Arora, V.K., 2021. Thin-layer drying of sadabahar (Catharanthus roseus) leaves using different drying techniques and fate of bioactive compounds. J. Food Process. Preserv. 45, 1–12. https://doi.org/10.1111/jfpp.15140

Mbegbu, N.N., Nwajinka, C.O., Amaefule, D.O., 2021. Thin layer drying models and characteristics of scent leaves (Ocimum gratissimum) and lemon basil leaves (Ocimum africanum). Heliyon 7, e05945. https://doi.org/10.1016/j.heliyon.2021.e05945

McMinn, W.A.M., Al-Muhtaseb, A.H., Magee, T.R.A., 2005. Enthalpy-entropy compensation in sorption phenomena of starch materials. Food Res. Int. 38, 505–510. https://doi.org/10.1016/j.foodres.2004.11.004

Mghazli, S., Ouhammou, M., Hidar, N., Lahnine, L., Idlimam, A., Mahrouz, M., 2017. Drying characteristics and kinetics solar drying of Moroccan rosemary leaves. Renew. Energy 108, 303–310. https://doi.org/10.1016/j.renene.2017.02.022

Nogueira Silva, N.F., Silva, S.H., Baron, D., Oliveira Neves, I.C., Casanova, F., 2023. Pereskia aculeata Miller as a Novel Food Source: A Review. Foods 12, 1–12. https://doi.org/10.3390/foods12112092

Onwude, D.I., Hashim, N., Janius, R.B., Nawi, N.M., Abdan, K., 2016. Modeling the Thin-Layer Drying of Fruits and Vegetables: A Review. Compr. Rev. Food Sci. Food Saf. 15, 599–618. https://doi.org/10.1111/1541-4337.12196

Rizvi, S.S.H., 2014. Thermodynamic properties of foods in dehydration, in: Rao, M.A., Rizvi, S.S.H., Datta, A.K. (Eds.), Engineering Properties of Foods. CRC Press, Boca Raton, pp. 359–436.

Sanches, M.A.R., Augusto, P.E.D., Polachini, T.C., Telis-Romero, J., 2023. Water sorption properties of brewer’s spent grain: A study aimed at its stabilization for further conversion into value-added products. Biomass and Bioenergy 170, 106718. https://doi.org/10.1016/j.biombioe.2023.106718

Santos, P.P.A. dos, Ferrari, G. da S., Rosa, M. da S., Almeida, K., Araújo, L. de A. de, Pereira, M.H.C., Wanderley, M.E.F., Morato, P.N., 2022. Desenvolvimento e caracterização de sorvete funcional de alto teor proteico com ora-pro-nóbis (Pereskia aculeata Miller) e inulina. Brazilian J. Food Technol. 25, 1–13. https://doi.org/10.1590/1981-6723.12920

Sato, R., Cilli, L.P.L., Oliveira, B.E., Maciel, V.B.B., Venturini, A.C., Yoshida, C.M.P., 2019. Nutritional improvement of pasta with Pereskia aculeata Miller: a non-conventional edible vegetable. Food Sci. Technol. 39, 28–34. https://doi.org/10.1590/fst.35617

Schwarz, G., 1978. Estimating the Dimension of a Model. Ann. Stat. 6, 461–464. https://doi.org/10.1214/aos/1176344136

Silva, D.O., Seifert, M., Schiedeck, G., Dode, J.S., Nora, L., 2018. Phenological and physicochemical properties of pereskia aculeata during cultivation in south brazil. Hortic. Bras. 36, 325–329. https://doi.org/10.1590/s0102-053620180307

Silva, D.P. da, Santos, S.G.F. dos, Silva, I.L., Silva, H.W. da, Rodovalho, R.S., 2020. Drying kinetics and thermodynamic properties of bitter melon (Momordica charantia L.) leaves. Rev. Bras. Eng. Agrícola e Ambient. 24, 707–712. https://doi.org/10.1590/1807-1929/agriambi.v24n10p707-712

Silva, F.P. da, Siqueira, V.C., Martins, E.A.S., Miranda, F.M.N., Melo, R.M., 2017. Thermodynamic properties and drying kinetics of Bauhinia forficata Link leaves. Rev. Bras. Eng. Agrícola e Ambient. 21, 61–67. https://doi.org/10.1590/1807-1929/agriambi.v21n1p61-67

Silva, N.C.B., dos Santos, S.G., da Silva, D.P., Silva, I.L., Rodovalho, R.S., 2019. Drying kinetics and thermodynamic properties of boldo (Plectranthus barbatus Andrews) leaves. Científica 47, 1–7. https://doi.org/https://doi.org/10.15361/1984-5529.2019v47n1p1-7

Silva, S.H., Neves, I.C.O., Meira, A.C.F. de O., Alexandre, A.C.S., Oliveira, N.L., Resende, J.V. de, 2021. Freeze-dried Petit Suisse cheese produced with ora-pro-nóbis (Pereskia aculeata Miller) biopolymer and carrageenan mix. LWT 149, 111764. https://doi.org/10.1016/j.lwt.2021.111764

Siqueira, V.C., Leite, R.A., Mabasso, G.A., Martins, E.A.S., Quequeto, W.D., Isquierdo, E.P., 2020. Drying kinetics and effective diffusion of buckwheat grains. Cienc. e Agrotecnologia 44, 1–10. https://doi.org/10.1590/1413-7054202044011320

Vasi, M., Grbavi, E., Radojevi, Z., 2012. Methods of Determination for Effective Diffusion Coefficient During Convective Drying of Clay Products, in: Clay Minerals in Nature -

Their Characterization, Modification and Application. InTech. https://doi.org/10.5772/48217

Wolfinger, R., 1993. Covariance structure selection in general mixed models. Commun. Stat. - Simul. Comput. 22, 1079–1106. https://doi.org/10.1080/03610919308813143

Zambra, C., Hernández, D., Reyes, H., Riveros, N., Lemus-Mondaca, R., 2021. Kageneckia oblonga Leaves Subjected to Different Drying Methods: Drying Kinetics, Energy Consumption and Interesting Compounds. Front. Sustain. Food Syst. 5. https://doi.org/10.3389/fsufs.2021.641858

Zogzas, N.P., Maroulis, Z.B., Marinos-Kouris, D., 1996. Moisture Diffusivity Data Compilation in Foodstuffs. Dry. Technol. 14, 2225–2253. https://doi.org/10.1080/07373939608917205

4 Capítulo 4 - Desorption properties of taioba (*Xanthosoma taioba* E.G. Gonç.) leaves, stems, and tubers: A non-conventional edible plant

André Luiz Borges-Machado[1]*, Marcio Augusto Ribeiro-Sanches[1], Maria Júlia Neves Martins[2], Priscila Alonso dos Santos[3], Silvio José Ferreira de Souza[1], Javier Telis-Romero[1]

[1]Food Engineering and Technology Department, State University of São Paulo, São José do Rio Preto, São Paulo, 15.054-000, Brazil.
[2]Instituo Federal de São Paulo – Câmpus Sertãozinho
[3]Department of Food Engineering, Institute Federal Goiano Campus Rio Verde, Rod. Sul Goiana, 75901-970 Rio Verde, Goiás, Brazil

ABSTRACT

The gravimetric-static method was employed to obtain desorption isotherms data for taioba leaves, stems, and tubers at nine temperatures (5-80 ºC), simulating storage and drying conditions. The proximate composition of taioba leaves, stems, and tubers was also determined. The equilibrium moisture content (EMC) decreased with rising temperature and increased directly with water activity (a_w). Five sorption models were fitted to desorption data, and the relationship between EMC and a_w for the three parts of taioba was best described by the GAB model for the entire range of aw and temperatures. The highest monolayer moisture contents found for taioba leaves, stems, and tubers were 0.070, 0.126, and 0.163 kg water/kg dry matter, respectively. The desorption curves presented a sigmoid shape, classified as BET Type II. The net isosteric heat of desorption and entropy of sorption were calculated and decreased as the moisture content increased for all parts of taioba. The linear relationship between them supported the enthalpy-entropy compensation theory, where $T_B > T_{hm}$, indicating an enthalpy-driven process. The free Gibbs energy was higher than zero, indicating that water desorption was non-spontaneous.

Keywords: Cocoyam, sorption isotherms, GAB model, enthalpy-entropy theory, thermodynamic properties.

4.1 INTRODUCTION

In 2020, due to the pandemic and the impact of the spread of COVID-19, the number of people worldwide affected by hunger continued to increase. From 2014 to 2019, malnutrition, which remained almost unchanged at 8.4%, rose to approximately 9.9% in 2020, going in the opposite direction of efforts to reach the zero hunger target by 2030 (FAO et al., 2021). The existing food insecurity is justified by the inability of the poorest classes to obtain the necessary food for a healthy and balanced diet. Projections of population growth, the expansion of cities, the increase in per capita consumption, and restrictions on land use in the coming decades make the debate about the inability to meet human needs for food more relevant (Saath & Fachinello, 2018). One of the alternatives to solving food insecurity is research on plants with food potential, however, little consumed.

Many plants are called "weeds" or "invasive" and even harmful, only because they develop amid traditional cultures or in places where people believe they cannot or should not occur. However, many of these species have great food importance (Kinupp & Lorenzi, 2014). Non-conventional edible plants (NCEP) are those present in certain locations or regions, exerting influence on the food of a traditional population; however, they are not organized as a production chain itself (Brasil, 2010; Gomes de Souza et al., 2023).

Taioba (*Xanthosoma taioba* E.G. Gonç.) is a tuberous, stem-height herb, with a height varying between 50-90 cm, native to Minas Gerais, and has membranous leaves measuring between 20-35 cm in length and an erect and spongy petiole of length between 30 -50 cm. For a long time, it was believed that this plant belonged to the *Xanthosoma sagittifolium* (L.) Schott species, originally from Central America until a more detailed study showed that the Brazilian taioba is a new species (Kinupp & Lorenzi, 2014).

Taioba leaves are a source of proteins, showing their potential as an edible plant, following global trends in food science and technology for the use of vegetable proteins as a high-quality nutritional source for the human diet (Sá et al., 2020; Sim et al., 2021). Fibers are present in the leaves, being mainly constituted by insoluble dietary fibers (Jackix et al., 2013b), which are little fermented by the human gut microbiota and not digested by the enzymes in the human gastrointestinal tract, resulting in positive physiological effects (Cantu-Jungles et al., 2021; Jackix et al., 2013a). The cholesterol-reducing and bile-acid binding properties of taioba leaves (*Xanthosoma sagittifolium*) in rats fed with a diet rich in saturated fat were studied by Jackix et al., (2013a). Their study suggests that the consumption of taioba leaves resulted in an increased excretion of primary acids in the feces. Thus, they showed the potential of being a dietary aid to reduce blood cholesterol and the risk of bowel cancer. Caxito et al. (2015) reported antitumor activities of hydroethanolic extract of *Xanthosoma sagittifolium* leaves, including Fe^{2+} chelation, inhibition of NO production, and inhibition of leukemia cell proliferation. The compound apigenin glycoside in HEXs-L is responsible for the antitumor properties.

The leaves, stems, and tubers can be used in human food if they are well-sautéed to eliminate the calcium oxalate present. Tubers, flours, and starches could be investigated in the snack and complementary food industries using their unusual processing properties, ease of crop production and storability, as well as their nutritional value. In Ghana, indigenous peoples use *X. sagittifolium* leaves to prepare palava sauce, Abunuabunu, which is used as a thickening agent in dish preparations, and Kontomire abomuu, which is a puree with the addition of pepper, onion, and fermented fish, generally served with ampesi made of taioba cormels. Food technologists must pay special attention to the leaves to make them available and usable throughout the year (Boakye et al., 2018).

The quality of biological material can be preserved by studying parameters such as drying and storage. Information on the equilibrium moisture content of these materials is essential, as it defines the appropriate conditions for the storage of fruits and vegetables (Sousa et al., 2014). Thus, moisture sorption isotherm is useful to predict food stability, allowing knowing which reactions might decrease its stability at a given moisture, assist the selection of ingredients for a product to change its water activity, in addition to being able to estimate the moisture loss or gain of a packaged product, knowing the permeability of this package (Bell & Labuza, 2000). Additionally, the drying kinetics of foods also depend on their sorption properties, which can change the diffusion coefficient and boundary used conditions (Viollaz & Rovedo, 1999). Sorption isotherms also allow the estimation of thermodynamic properties such as sorption heat, sorption enthalpy, and differential entropy.

The isosteric heat of sorption is an essential parameter in the food storage and drying processes, being used to quantify the energy required to break the intermolecular forces between the adsorbent surface and the water vapor molecules (Rizvi, 2014). The binding force between water and food compounds is related to differential enthalpy, and the number of available sorption sites at a specific energy level is represented by differential entropy (Moreira et al., 2008). These two properties are correlated through the Gibbs free energy, representing the useful energy of the system that is used to do the work (Rizvi, 2014).

Considering the lack of data providing information about storage and drying conditions for taioba, the aims of this work are: (i) to determine the desorption isotherms of taioba leaves, stems, and tubers under storage and drying conditions; (ii) to model the desorption isotherms using sorption models; (iii) to evaluate the thermodynamic properties and the theory of enthalpy–entropy compensation to expound on the water sorption phenomena.

4.2 MATERIAL AND METHODS

4.2.1 Raw material

Taioba plants were harvested at the Institute of Biosciences, Humanities, and Exact Sciences and transported to the Laboratory of Physical Measures (UNESP – São José do Rio Preto), where they were divided into three parts: leaves, stems, and tubers. They were washed with tap water and sanitized with a chlorinated solution at 100 ppm for 20 minutes. The leaves were cut into square shapes of 1 cm, the stems were cut into cylindrical shapes of 0.5 cm in height, and the tubers were sliced into 0.5 cm thick slices.

Saturated salt solutions were prepared with distilled water and salts from Sigma-Aldrich (St. Louis, MO, USA). The salts used were lithium bromide (LiBr), lithium chloride (LiCl), lithium iodide (LiI), magnesium chloride ($MgCl_2$), sodium iodide (NaI), potassium carbonate (K_2CO_3), magnesium nitrate ($Mg(NO_3)_2$), sodium bromide (NaBr), potassium iodide (KI), sodium chloride (NaCl), ammonium sulfate ($(NH_4)_2SO_4$), potassium chloride (KCl), potassium nitrate (KNO_3) and potassium sulfate (K_2SO_4). These saline solutions promoted environments where a_w ranged from 0.0743 to 0.9848.

4.2.2 Proximate composition of taioba leaves, stems, and tubers

All methods attended AOAC protocols (AOAC, 2007). Dry matter and moisture content (method 950.46) were determined in a conventional oven at 105 ºC until reach constant weight, ash (method 923.03) in a muffle furnace at 550 ºC until white ash was obtained, lipids by Soxhlet method, proteins by micro-Kjeldahl (method 981.10) using 6.25 as a conversion factor, and carbohydrates by difference.

4.2.3 Desorption isotherms

Using static gravimetric method (Spiess & Wolf, 1983), the water desorption isotherms of each taioba part were determined at 5 ºC, 10 ºC, 20 ºC, 30 ºC, 40 ºC, 50 ºC, 70 ºC, and 80 ºC. LiBr, LiCl, LiI, $MgCl_2$, NaI, K_2CO_3, $Mg(NO_3)_2$, NaBr, KI, NaCl, $(NH_4)_2SO_4$, KCl, KNO_3, and K_2SO_4 saturated salt solutions were put in a glass desiccator to achieve different relative humidity (RH = a_w x 100). Simulating storage conditions (5 ºC, 10 ºC, 20 ºC, 30 ºC, 40 ºC), the desiccators were stored in the BOD chamber (MA415, Marconi, Piracicaba, Brazil) with monitored temperatures, and for drying conditions (40 ºC,50 ºC, 70 ºC, and 80 ºC), using an oven (MA030, Marconi, Piracicaba, Brazil). Table S1 shows the values of a_w for saturated saline solutions at each temperature studied (Labuza, 1963). In triplicate, two grams of each taioba part were loaded in containers using an analytical balance (AUW220D, Shimadzu, Japan) and put in the desiccator. A beaker containing toluene was placed in the desiccators with $a_w > 0.6$ aiming to prevent microbiological deterioration (Wolf et al., 1985). First, the moisture content and the mass were determined. The samples were weighted every five days until they reached constant mass. The experiment lasted 4 to 5 weeks based on the alterations in weight expressed on a dry basis, not exceeding 0.1% (0.001 g/g dry solids). The equilibrium moisture content (EMC) was determined by gravimetric method using the difference of weight for each temperature.

4.2.4 Modelling of desorption isotherms

The models GAB, Peleg, Oswin, Henderson and Halsey are theoretical, empirical, and semi-empirical models and commonly used to represent food sorption isotherms (Table 1). The models were fitted to desorption data by nonlinear regression with the aid of the software OriginPro 2022 (OriginLab Corporation, Northampton, MA) which was also used to calculate the adjusted coefficient of determination (R^2_{adj}) and reduced chi-square (χ^2). These parameters were used to evaluate the fitting quality that is considered acceptable when R^2_{adj} value is close to the unity and reduced χ^2 is close to zero.

Table 1 - Mathematical models for adjusting the desorption isotherms of taioba parts.

Model	Equation	
GAB	$EMC = \frac{X_m C k a_w}{(1 - k a_w)(1 + (C-1) k a_w)}$	(1)
Peleg	$EMC = k_1 a_w^{n_1} + k_2 a_w^{n_2}$	(2)
Oswin	$EMC = M \left(\frac{a_w}{1 - a_w}\right)^N$	(3)
Halsey	$EMC = (-h_1 \, ln(a_w))^{-\frac{1}{h_2}}$	(4)
Henderson	$EMC = \left(-\frac{1}{H_1} ln(1 - a_w)\right)^{\frac{1}{H_2}}$	(5)

C, *k*, k_1, n_1, k_2, n_2, *M*, *N*, h_1, h_2 H_1, and H_2 are constants of the models, X_m represents the monolayer moisture content (kg of water/kg dry matter), X_{eq} is the equilibrium moisture content, and a_w is the water activity.

The Akaike, (1974) and Schwarz, (1978) information criteria (AIC and BIC) were used to select the best model among those that presented good fit to the desorption data. AIC estimates predictive accuracy based on out-of-sample deviation while BIC is associated to the logarithm of the average likelihood of a linear models and preventing overfitting (McElreath, 2016). The AIC and BIC were obtained by Equations 6 and 7, in which, the lower the AIC and SIC, the better the model.

$$AIC = -2\log\mathcal{L}(\hat{\theta}) + 2c \tag{6}$$

$$BIC = -2\log\mathcal{L}(\hat{\theta}) + c\ln(n) \tag{7}$$

where n is the total number of observations, c is the total number of estimated coefficients, and $\mathcal{L}(\hat{\theta})$ is the value of the likelihood function concerning the coefficients of the model.

4.2.5 Thermodynamic approach

4.2.5.1 Net isosteric heat of desorption and entropy of desorption

At a given hydration level of the food matrix, there is an energy responsible for the binding of water molecules with the matrix called net isosteric heat of desorption (q_{st}) (Polachini et al., 2016) or differential enthalpy (ΔH). The values of q_{st} can be obtained through the difference between the integral heat of desorption (Q_{st}) and the heat of water vaporization (λ). By plotting the ln (a_w) versus (1/T) at a fixed moisture content, the slope of Clausius Clapeyron equation (8) was used to estimate q_{st}. (Rizvi, 2014). The equilibrium moisture content was calculated using the model that best fitted the desorption data.

$$\left.\frac{\partial(\ln a_w)}{\partial(1/T)}\right|_{EMC} = -\frac{Q_{st}-\lambda}{R} = -\frac{q_{st}}{R} \tag{8}$$

where Q_{st} is the integral heat of desorption, λ is the latent heat of pure water vaporization and R is universal gas constant (8.314 $J.mol^{-1}.K^{-1}$). After calculating the q_{st} values at specific equilibrium moisture, it was used Riedel's model to evaluate de relationship between these parameters (Equation 9)

$$q_{st} = C_r \exp(-B_r\ EMC) \tag{9}$$

where C_r is the isosteric heat of desorption at the first water molecule, EMC is the equilibrium moisture content (dry basis) and B_r is the model's constant.

Thermodynamic properties can be used to express water desorption behavior, thus, the water behavior in taioba parts was studied using quantitative theoretical models. For food energy evaluation, the variation of entropy is an important parameter. According to Koua et al., (2014), when Equation (10) is fitted to equilibrium moisture is possible to calculate the differential entropy or desorption entropy (ΔS) using the same method applied to calculate the values of net isosteric heat of desorption.

$$\ln a_w = -\frac{\Delta H}{RT} + \frac{\Delta S}{R} \tag{10}$$

4.2.5.2 Enthalpy-entropy compensation mechanism

Using equation (11), if entropy and enthalpy present a linear correlation, enthalpy-entropy compensation can be confirmed (Polachini et al., 2016).

$$q_{st} = T_B(\Delta S) + \Delta G_B \tag{11}$$

where T_B is the isokinetic temperature, which the rate of all desorption phenomena is equal, ΔG_B is the free Gibbs energy at isokinetic temperature and it is related to the desorption water process, being a spontaneous process ($-\Delta G_B$) or not ($+\Delta G_B$).

Krug et al., (1976 a,b) purposed the validation of this theory applying a statistical method, which consists in comparing the harmonic mean temperature (T_{hm}) (Equation 10) to the isokinetic temperature, where n is the number of isotherms.

$$T_{hm} = \frac{n}{\sum_{i=1}^{n}\left(\frac{1}{T}\right)} \tag{12}$$

Equation (11) was used to determine an interval of confidence of (1-α) 100%:

$$T_B = T_B \pm t_{m-2,\frac{\alpha}{2}}\sqrt{Var(T_B)}$$

(13)

where

$$T_B = \frac{\sum(\Delta H - \overline{\Delta H})(\Delta S - \overline{\Delta S})}{\sum(\Delta S - \overline{\Delta S})^2}$$

(14)

$$Var(T_B) = \frac{\sum(\Delta H - \overline{\Delta G_B} - T_B\Delta S)^2}{(m-2)\sum(\Delta S - \overline{\Delta S})^2} \quad (15)$$

and $\overline{\Delta H}$ is the average enthalpy, $\overline{\Delta S}$ is the average entropy, and m is the number of (ΔH, ΔS) data pairs.

4.3 RESULTS AND DISCUSSION

4.3.1 Proximate composition of taioba leaves, stems, and tubers.

The following results of the triplicate of the proximate composition of taioba parts are presented as mean values ± standard deviation of three replicates. The leaves presented 89.10 ± 0.28 g of moisture/100 g, 5.32 ± 0.28 g of carbohydrates/100 g, 3.33 ± 0.02 g of proteins/100 g, 1.51 ± 0.05 g of ashes/100 g, and 0.74 ± 0.01 g of lipids/100g. The stems showed 93.46 ± 0.26 g of moisture/100 g, 4.36 ± 0.18 g of carbohydrates/100 g, 0.80 ± 0.04 g of proteins/100 g, 1.38 ± 0.06 g of ashes/100 g, and 0.18 ± 0.03 g of lipids/100g. The tubers presented 79.52 ± 0.08 g of moisture/100 g, 18.20 ± 0.10 g of carbohydrates/100 g, 1.49 ± 0.06 g of proteins/100 g, 0.79 ± 0.01 g of ashes/100 g, and 0.30 ± 0.04 g of lipids/100g.

4.3.2 Desorption isotherms modeling

In this study, water activity values for storage temperatures ranged from 0.0580 to 0.9848, and for drying temperatures, they ranged from 0.0520 to 0.9641. Figures 1, 2, and 3 present the experimental data of the equilibrium desorption isotherm for taioba leaves, stems, and tubers at storage and drying temperatures, respectively. At a constant temperature, the EMC showed a decreasing tendency as the water activity decreased. This behavior is prevalent among many food materials (Borges-Machado et al., 2024; Rosa et al., 2021; Sanches et al., 2023) and suggests that taioba parts would lose more water at lower relative humidity environments.

In Figures 1, 2, and 3, it is observed that for $0.3 > a_w > 0.7$, a small decrease in a_w resulted in a greater volume of desorbed water, being more pronounced in the leaves and stems. At low water activities, physical sorption occurs on substrates with strongly active binding sites, like the -OH groups (Ojike et al., 2022) found on insoluble dietary fibers (Jackix et al., 2013b) composed by cellulose and lignin (Jiménez-Escrig & Sánchez-Muniz, 2000) that are present in the leaves and stems, and carbohydrate molecules such as starch present in the tubers. Furthermore, the proteins, also present in the food matrix, have the ability to prevent the release or ejection of water from their three-dimensional structure (Haque et al., 2016). Hence, the taioba parts lost lower quantities of water at low moisture contents.

On the other hand, for a fixed water activity, the equilibrium moisture content of taioba leaves, stems, and tubers showed a decreasing tendency with the rise of the temperature. This phenomenon is probably connected to the increase in the kinetic energy and agitation state of the water molecules due to the elevation in temperature, which might diminish the attractive forces between the water molecules and the solid matrix's binding sites (Sanches et al., 2023), lowering their stability and breaking them away from the water-binding site of the food matrix, hence, diminishing the moisture content. In addition, the effect of the temperature on EMC is more pronounced in tubers than in the leaves and stems once the gaps between each tuber desorption pattern are larger than the gaps in the patterns of the leaves and stems. This fact is due to the different composition of each taioba part, mainly due to the large amount of starch present in the tuber (Farias et al., 2020), reinforcing the relevance of obtaining the sorption isotherms of each food.

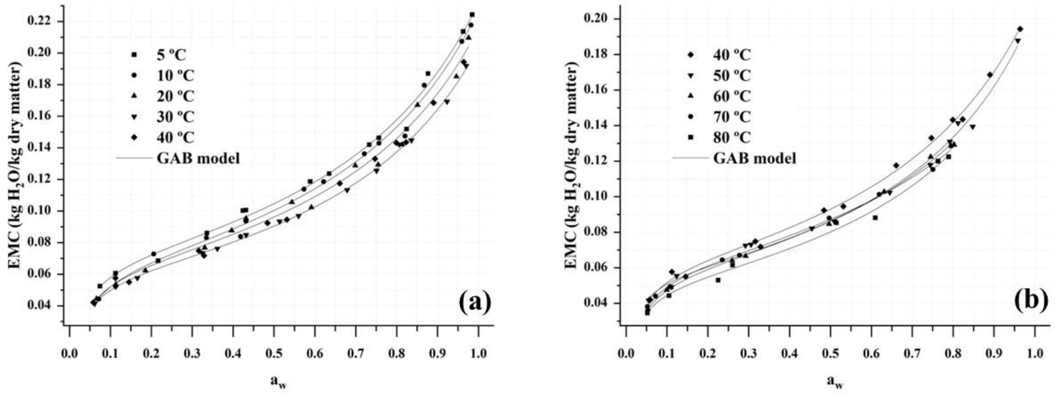

Figure 4 – Water desorption isotherms of taioba leaves adjusted to the GAB model under storage (a) and drying (b) conditions.

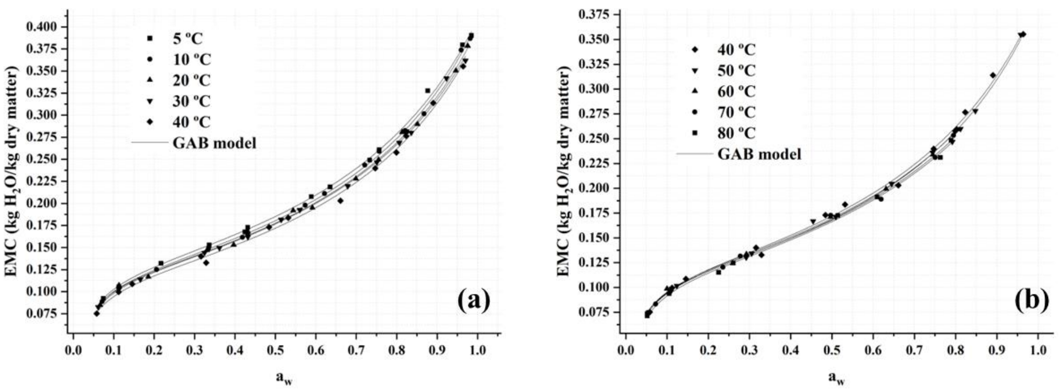

Figure 5 – Water desorption isotherms of taioba stems adjusted to the GAB model under storage (a) and drying (b) conditions.

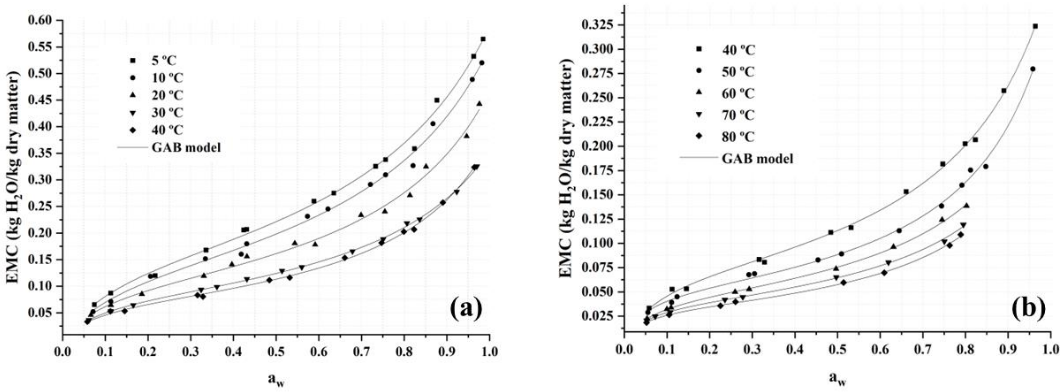

Figure 6 – Water desorption isotherms of taioba tubers adjusted to the GAB model under storage (a) and drying (b) conditions.

The fitting parameters of the non-linear regression and estimated coefficients for each model fitted to the EMC data of the leaves, stems, and tubers are presented in Tables S2, S3, and S4, respectively. In general, the GAB and Peleg models presented the highest R^2_{adj} (> 0.99) and the lowest values of reduced χ^2 among the models evaluated at all temperatures for all taioba parts. Thus, AIC and BIC were used to choose one model that best describes the desorption patterns at both storage and drying temperatures. As shown in Tables S2, S3, and S4, the GAB model presented the lowest AIC and BIC values when compared to the other models at storage temperatures (5 - 40 ºC) for the leaves, stems, and tubers (except at 5 ºC). Regarding the drying temperatures, the GAB model also presented the lowest AIC and BIC values at 50 ºC for the stems and tubers, at 60 ºC for the leaves and stems, at 70 ºC for the tubers, and at 80 ºC for the stems and tubers. The AIC and BIC values showed that at some temperatures, such as at 50 ºC for the leaves and at 5 ºC and at 60 ºC for the tubers, the Peleg model was more adequate. The Oswin model presented the lowest values of AIC and BIC for the leaves at 70 ºC and 80 ºC and for the stems at 70 ºC. When ranking the GAB, Peleg, and Oswin models based on the AIC and BIC values, the GAB model presented the second lowest values when the Peleg or Oswin model appeared to be more suitable. In this way, the GAB model was chosen to describe the desorption isotherms of taioba leaves, stems, and tubers at storage and drying temperatures due to its excellent fitting quality and lowest AIC and BIC values. The estimated coefficients and fitting parameters of the non-linear regression for the GAB model fitted to the EMC data of the leaves, stems, and tubers are presented in Table 2.

Table 2 - Coefficients predicted by the GAB model fitted to the desorption data and fitting parameters of taioba leaves, stems, and tubers at storage and drying conditions.

Taioba part		Temperature (ºC)								
		5	10	20	30	40	50	60	70	80
Leaves	X_m	0.070	0.069	0.066	0.061	0.061	0.058	0.058	0.058	0.052
	C	64.235	44.950	43.040	41.540	41.540	40.930	40.722	40.245	40.000
	k	0.703	0.700	0.669	0.702	0.709	0.715	0.706	0.681	0.738

	R_{aj}^2	0.992	0.992	0.987	0.999	0.996	0.992	0.998	0.997	0.987
	$\chi^2 \cdot 10^5$	2.491	2.494	3.126	0.296	0.860	1.480	0.236	0.320	1.383
	AIC	-139.336	-139.317	-136.156	-169.178	-169.178	-134.986	-102.270	-99.525	-71.936
	BIC	-141.225	-141.206	-138.044	-171.066	-171.066	-137.726	-111.481	-108.736	-84.951
Stems	X_m	0.126	0.122	0.120	0.120	0.115	0.115	0.115	0.114	0.102
	C	55.868	45.471	44.728	43.337	42.594	42.594	42.027	41.167	40.777
	k	0.694	0.701	0.701	0.697	0.707	0.708	0.702	0.693	0.775
	R_{aj}^2	0.9978	0.9992	0.9982	0.9984	0.9939	0.9986	0.9986	0.9966	0.9948
	$\chi^2 \cdot 10^5$	2.00	0.736	1.48	1.25	4.56	1.00	0.587	1.45	2.53
	AIC	-142.415	-156.405	-146.610	-149.028	-120.347	-140.032	-94.054	-85.945	-67.111
	BIC	-144.304	-158.293	-148.499	-150.916	-123.087	-142.773	-103.266	-95.156	-80.127
Tubers	X_m	0.163	0.146	0.113	0.086	0.075	0.054	0.047	0.040	0.034
	C	10.776	9.883	12.323	13.902	14.719	23.202	17.586	21.101	23.088
	k	0.732	0.744	0.765	0.764	0.803	0.843	0.836	0.840	0.870
	R_{aj}^2	0.9948	0.9948	0.9922	0.9991	0.9984	0.9968	0.9988	0.9980	0.9982
	$\chi^2 \cdot 10^5$	12.777	10.994	10.933	0.687	1.267	1.652	0.218	0.249	0,198
	AIC	-116.446	-118.549	-118.628	-157.365	-136.999	-133.551	-102.984	-101.778	-87.504
	BIC	-118.334	-120.438	-120.516	-159.253	-139.739	-136.291	-112.195	-110.989	-100.519

One advantage of the GAB model is the physical meaning of its constants, such as the monolayer moisture content, X_m, which is fundamental for storage studies because it represents the last layer of water in the food matrix (Freitas et al., 2016). Under storage conditions (5 - 40 °C), tubers (0.163 - 0.075 kg water/kg d.m.) showed higher X_m values, followed by stems (0.126 - 0.115 kg water/kg d.m.) and leaves (0.070 - 0.061 kg water/kg d.m.). This difference in X_m values between different parts of the taioba can be attributed to the intrinsic characteristics of each component of the taioba such as its chemical composition and physical structure. In the case of tubers, which showed the highest X_m values during storage, this may be related to their high concentration of starch and other molecules that retain water, providing greater moisture for the monolayer. Furthermore, the dense structure of the tuber may contribute to less desorption during storage, resulting in higher X_m values. On the other hand, during drying, the stems showed higher X_m values. This may be due to the presence of carbohydrates, fibers, and other molecules capable of contributing to water retention in the stems, making them more likely to retain moisture under drying conditions. Furthermore, prolonged exposure to heat during drying can also lead to the denaturation of proteins present in the leaves (Erbaş et al., 2016) or the loosening of the structure and/or gelatinization of starch in the tubers (Singh et al., 2003) facilitating the release of water and reducing the value of X_m.

In addition to the variations between the parts of the taioba, it was observed that the X_m values decreased for all of them with the increase in temperature, reflecting a decrease in the number of active sites caused by physico-chemical changes induced by temperature on the product (Sharma et al., 2009). The same trend was also observed for other agricultural products (Koua et al., 2014; Rosa et al., 2021; Sanches et al., 2023; Tunç & Duman, 2007). The monolayer moisture content values also indicated the first region of the desorption isotherms, $a_w<0.20$ for the leaves and stems, and $a_w<0.34$ for the tubers, suggesting that taioba leaves and stems are more stable when stored under RH < 20% and the tubers in RH < 34%. This is because the probability of microbial growth is minimum, and chemical and enzymatic reactions should only happen at a very slow rate, supporting storage stability (Vega-Gálvez et al., 2007) after a drying process. In addition to these chemical and enzymatic reactions, it is important to highlight the need for more research on the glass transition, especially to identify the glassy to gummy phase transitions that can cause significant changes in the molecular mobility of food polymers. These changes can result in loss of stability for low-moisture amorphous foods, highlighting the importance of better understanding these processes to ensure food quality and safety.

The constant C, related to the heat of sorption in the region of the monolayer, while the constant k is related to the heat of sorption in the multilayers, ranges from zero to one (Blahovec, 2004; Lewicki, 2008). In this study, the values of constant C varied from 40 to 64.235 for the leaves and from 40.777 to 55.868 for the stems, tending to decrease directly with temperature. The higher the C values, the stronger the water bounds (Silva et al., 2021). Concerning the tubers, the constant C ranged from 9.883 to 23.202; however, a clear tendency in the values was not observed. Analyzing the constant k of the three taioba parts, it was observed that k ranged from 0.669 to 0.870, tending to increase directly with temperature. When k is equal to 1, the water in the multilayers pursues the properties of liquid water (Pérez-Alonso et al., 2006). In this sense, as the temperatures rose, the water bound between the monolayer and multilayers weakened, hence, releasing the water molecules.

The desorption isotherm curves of the leaves, stems, and tubers (Figure 1, 2, and 3) for both storage and drying conditions presented a sigmoid shape, classified as Type II (Brunauer et al., 1940), a common shape for foodstuff, also observed in other plants such as ora-pro-nóbis leaves (Borges-Machado et al., 2024), rosemary leaves (Bensebia & Allia, 2016), elephant foot yam (Sangeeta & Hathan, 2017), rice flour (Torres & Seijo, 2016), and lemon balm leaves (Argyropoulos et al., 2012). Type II isotherms have three different regions: the region where $a_w<0.3$ corresponds to the water in the monolayer, which is strongly linked to the food matrix; the region with aw between 0.3 and 0.7 is related to the water of the following layers, showing a behavior similar to a linear one; the region with $a_w \geq 0.7$ corresponds to water molecules that are weakly bound to the food matrix, being available for chemical and microbiological reactions (Polachini et al., 2016).

4.3.3 Thermodynamic approach

4.3.3.1 Net isosteric heat of desorption and entropy of desorption

Isosteric heat of desorption shows the effect of temperature on foods and provides important information about the state of water in foods and the amount of energy required to disrupt the intermolecular connections between bound water and the food matrix in the hygroscopic zone (Ouertani et al., 2014). The GAB model was used to calculate the water activities at different temperatures and for a specific equilibrium moisture content. This procedure allowed us to estimate the net isosteric heat of desorption (q_{st}) using Equation (8), which was plotted against equilibrium moisture content and fitted to the Riedel model (Equation

9). Table 3 presents the estimated coefficients of the Riedel model fitted to calculated heat data and the adjusted coefficient of determination. In Figure 4, it is shown that qst decreased with increasing moisture content for taioba leaves, stems, and tubers. The highest value of qst indicates the existence of active polar sites on the product surface which are enclosed with water molecules forming the monolayer molecules (Tagnamas et al., 2021). For an EMC equal to 0.11 kg water/kg d.m., the qst of the tubers, stems, and leaves were 17712.98 J/mol, 5656.63 J/mol, and 3058.11 J/mol, respectively. Thus, the tubers presented the highest energy requirement to remove water, followed by the stems and leaves.

Table 3 - Estimated coefficients of Riedel model and adjusted coefficient of determination.

Taioba part	**C_r (J/mol)**	**B_r**	R^2_{adj}
Leaves	30427.153	19.761	0.96201
Stems	25820.268	13.803	0.98916
Tubers	38102.609	7.366	0.99417

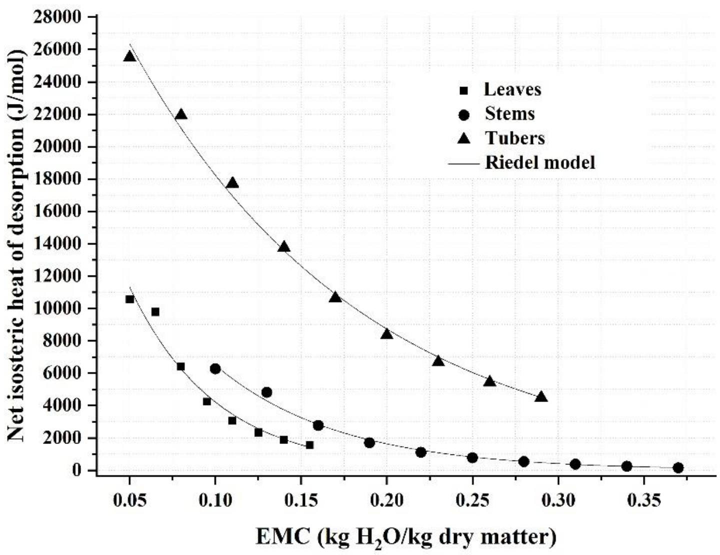

Figure 7 – Net isosteric heat of desorption of taioba leaves, stems, and tubers as a function of the equilibrium moisture content.

The relationship between the heat of desorption of taioba leaves, stems and tubers may be related to their chemical compositions and physical structures, as water molecules are linked to the polar sites of food components, such as starch and proteins, via bonding hydrogen (Erbaş et al., 2016).

The leaves have a finer structure and are characterized by a smaller amount of carbohydrates and a greater amount of proteins, when compared to the stem and tuber. Although water can bind to polar amino groups of proteins present in the leaf via hydrogen bonding, the finer structure of the leaves, with a larger contact surface, can facilitate water sorption during the drying process, resulting in lower desorption heat, especially in comparison with the tubers. The taioba stem stands out for its composition with a relatively greater amount of carbohydrates compared to the leaves. This higher carbohydrate content may establish more polar sites to bond with water molecules, requiring greater heat of desorption to break these bonds, although not as high as in tubers. Furthermore, the structure of the stem tends to be more rigid when compared to the thinner structure of the leaves. This rigidity can make it difficult for water to escape during the drying process, compared to leaves. On the other hand, the taioba tuber, known for its high concentration of carbohydrates, especially starch (Farias et al., 2020), is probably capable of establishing many polar sites to bind with water molecules, which is why which tuber requires the highest heat of sorption among the three parts evaluated. The dense structure of the tuber can also contribute to greater internal resistance to water outflow, thus requiring a significantly greater amount of energy to remove water during the drying process.

Entropy (ΔS) indicates both the level of order or disorder of the water-absorbing system, contributing to the configuration of spatial arrangements at the water and sorbent interface and the lack of energy needed to complete a particular process (Apostolopoulos & Gilbert, 1990; McMinn et al., 2005), such as drying. Similar to q_{st}, the entropy showed a strong dependence on EMC, increasing with decreasing EMC for taioba leaves, stems, and tubers (Figure 5). This trend was expected since the rise of entropy is governed by the heat transfer between two systems, and its size is always proportional to the heat transmitted at a given temperature (de

Oliveira et al., 2017). In addition, an increase in ΔS signifies the buildup of water layers on the product surface, which will be subsequently eliminated. The tubers presented the highest values of entropy (70.86 - 13.40 J/mol/K) while the stems showed the lowest (4.22-0.23 J/mol/K), with these changes in ΔS values being more pronounced when the EMC was in the range of X_m. These changes are more pronounced in regions where the moisture content is lower than 0.15 kg water/kg of d.m., indicating that more energy is required to remove water molecules in these situations. It is also noteworthy that the maximum entropy values were reached at a moisture level that is very similar to the monolayer moisture values determined by the GAB model. This happens because the food matrix monolayer has highly active polar sites that can bind water and incorporate moisture. (Al-Mahasneh et al., 2012).

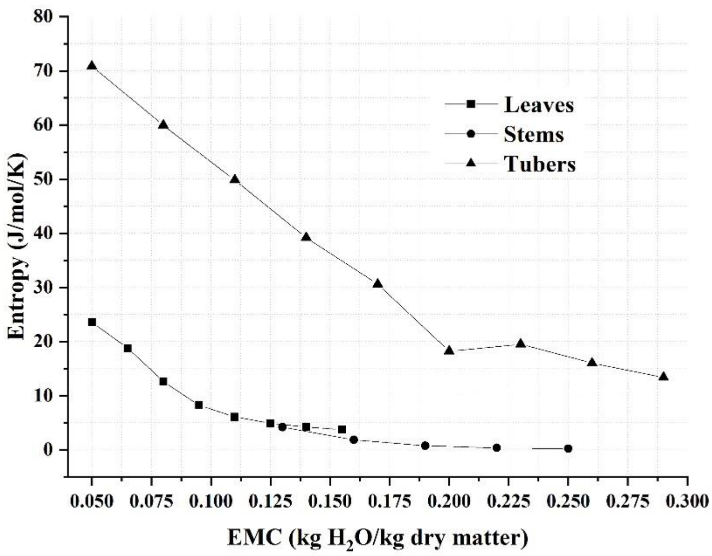

Figure 8 - Entropy of taioba leaves, stems, and tubers as function of the equilibrium moisture content.

4.3.3.2 Enthalpy-entropy compensation theory

Sorption reactions can be evaluated by the compensation theory. In Figure 4, the linear relationship between the net isosteric heat of desorption and entropy confirmed the theory of compensation in the studied moisture range, with $R_{adj}^2 > 0.99$ for the three taioba parts. According to Polachini et al., (2016), this linear tendency means that if the enthalpy changes, both entropy and Gibbs free energy change simultaneously. In a thermodynamic approach, the free energy change indicates the water-absorbent affinity and provides knowledge about the water sorption process, being spontaneous if $\Delta G_B < 0$ or non-spontaneous if $\Delta G_B > 0$ (McMinn et al., 2005). Gibb's free energy (ΔG_B) and isokinetic temperature (T_B) were calculated using linear regression and Equation (11). The ΔG_B values of the leaves, stems, and tubers were positive and equal to, in J/mol, 71.53, 761.63, and 61.38, respectively. Thus, desorption was reinforced to be a non-spontaneous process. Regarding the isokinetic temperatures, the T_B of the leaves, stems and tubers and their interval of confidence were 477.25 ± 84.45 K, 981.22 ± 181.39 K, and 358.60 ± 30.11 K, respectively. The T_B values were higher than the harmonic mean temperature (T_{hm}), 311.72 K, and were out of the calculated interval of confidence, so, they were significantly different from each other. This fact fulfilled the second requirement to corroborate the linear chemical compensation which is evidenced by the difference between T_B and T_{hm} (Krug et al., 1976 a,b). Furthermore, water desorption can be classified as enthalpy-driven for the leaves, stems, and tubers because $T_B > T_{hm}$ (Leffler, 1955).

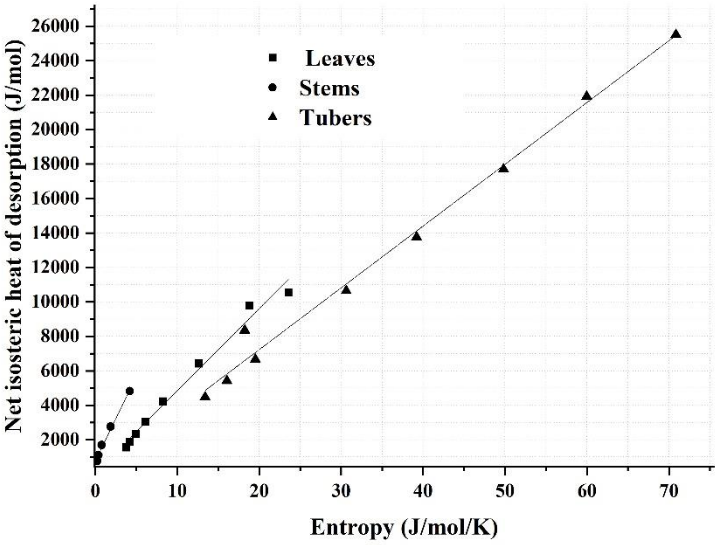

Figure 9 - Net isosteric heat of desorption of taioba leaves, stems, and tubers as function of the entropy.

4.4 CONCLUSION

The equilibrium moisture of taioba leaves, stems, and tubers increased as relative moisture raised and reduced with temperature. The GAB model fitted with good accuracy the experimental data of taioba leaves, stems, and tubers over the range of temperatures simulating storage and drying conditions, and the desorption isotherms presented a sigmoid shape, classified as BET Type II. The X_m decreased with increasing temperature and indicated that taioba leaves and stems are less susceptible to deteriorate if stored under a relative humidity lower than 20% at storage conditions. For taioba tubers, the relative humidity should be lower than 34%. However, further research on glass transition is required aiming to identify the vitreous to gummy phase transitions that cause significant changes in the food polymers' molecular mobility and may result in a loss of stability for amorphous foods with low moisture. Taioba leaves presented the lowest energy requirements, followed by the stems, while the tubers presented the highest, and these differences are directly related to their different chemical compositions. Net isosteric heat of desorption and entropy of desorption reduced with the rise of equilibrium moisture content. The linear relationship observed when enthalpy was plotted versus entropy confirmed the compensation theory; hence, the desorption mechanisms of taioba leaves, stems, and tubers were non-spontaneous and enthalpy-driven.

4.5 REFERENCES

Akaike, H. (1974). A new look at the statistical model identification. *IEEE Transactions on Automatic Control*, *19*(6), 716–723. https://doi.org/10.1109/TAC.1974.1100705

Al-Mahasneh, M. A., Bani Amer, M. M., & Rababah, T. M. (2012). Modeling moisture sorption isotherms in roasted green wheat using least square regression and neural-fuzzy techniques. *Food and Bioproducts Processing*, *90*(2), 165–170. https://doi.org/10.1016/j.fbp.2011.02.007

Apostolopoulos, D., & Gilbert, S. G. (1990). Water Sorption of Coffee Solubles by Frontal Inverse Gas Chromatography: Thermodynamic Considerations. *Journal of Food Science*, *55*(2), 475–487. https://doi.org/10.1111/j.1365-2621.1990.tb06790.x

Argyropoulos, D., Alex, R., Kohler, R., & Müller, J. (2012). Moisture sorption isotherms and isosteric heat of sorption of leaves and stems of lemon balm (Melissa officinalis L.) established by dynamic vapor sorption. *LWT - Food Science and Technology*, *47*(2), 324–331. https://doi.org/10.1016/j.lwt.2012.01.026

Bell, L. N., & Labuza, T. P. (2000). *Moisture Sorption: Practical Aspects of Isotherms Measurements and Use*. AACC International Publishing.

Bensebia, O., & Allia, K. (2016). Analysis of adsorption–desorption moisture isotherms of rosemary leaves. *Journal of Applied Research on Medicinal and Aromatic Plants*, *3*(3), 79–86. https://doi.org/10.1016/j.jarmap.2016.01.005

Blahovec, J. (2004). Sorption isotherms in materials of biological origin mathematical and physical approach. *Journal of Food Engineering*, *65*(4), 489–495. https://doi.org/10.1016/j.jfoodeng.2004.02.012

Boakye, A. A., Wireko-Manu, F. D., Oduro, I., Ellis, W. O., Gudjónsdóttir, M., & Chronakis, I. S. (2018). Utilizing cocoyam (Xanthosoma sagittifolium) for food and nutrition security: A review. *Food Science and Nutrition*, *6*(4), 703–713. https://doi.org/10.1002/fsn3.602

Borges-Machado, A. L., Ribeiro-Sanches, M. A., Neves-Martins, M. J., dos Santos, P. A., Luna-Solano, G., & Telis-Romero, J. (2024). Water desorption isotherms and thermodynamic properties of Ora-pro-nóbis (Pereskia aculeata Miller). *LWT - Food Science and Technology*, *193*(January). https://doi.org/10.1016/j.lwt.2024.115749

BRASIL, Ministério da Agricultura, P. e A. (2010). *Hortaliças não-convencionais: (tradicionais)*. MAPA/ACS. https://www.abcsem.com.br/docs/cartilha_hortalicas.pdf

Brunauer, S., Deming, L. S., Deming, W. E., & Teller, E. (1940). On the theory of the van der Waals adsorption of gases. *Journal of the American Chemical Society*, *62*(7), 1723–1732.

Cantu-Jungles, T. M., Zhang, X., Kazem, A. E., Iacomini, M., Hamaker, B. R., & Cordeiro, L. M. C. (2021). Microwave treatment enhances human gut microbiota fermentability of isolated insoluble dietary fibers. *Food Research International*, *143*(March), 110293. https://doi.org/10.1016/j.foodres.2021.110293

Caxito, M. L. C., Correia, R. R., Gomes, A. C. C., Justo, G., Coelho, M. G. P., Sakuragui, C. M., Kuster, R. M., & Sabino, K. C. C. (2015). In Vitro Antileukemic Activity of Xanthosoma sagittifolium (Taioba) Leaf Extract. *Evidence-Based Complementary and Alternative Medicine*, *2015*. https://doi.org/10.1155/2015/384267

de Oliveira, G. H. H., Corrêa, P. C., de Oliveira, A. P. L. R., Reis, R. C. dos, & Devilla, I. A. (2017). Application of GAB Model for Water Desorption Isotherms and Thermodynamic Analysis of Sugar Beet Seeds. *Journal of Food Process Engineering*, *40*(1). https://doi.org/10.1111/jfpe.12278

Erbaş, M., Aykın, E., Arslan, S., & Durak, A. N. (2016). Adsorption behaviour of bulgur. *Food Chemistry*, *195*, 87–90. https://doi.org/10.1016/j.foodchem.2015.06.050

FAO, IFAD, UNICEF, WFP, & WHO. (2021). *In brief to The state of food security and nutrition in the world. Transforming food systems for food security, improved nutrition and affordable healthy diets for all*. https://doi.org/10.4060/cb5409en

Farias, F. de A. C., Moretti, M. M. de S., Costa, M. S., BordignonJunior, S. E., Cavalcante, K. S. B., Boscolo, M., Gomes, E., Franco, C. M. L., & Silva, R. da. (2020). Structural and physicochemical characteristics of taioba starch in comparison with cassava starch and its potential for ethanol production. *Industrial Crops and Products*, *157*(July), 112825. https://doi.org/10.1016/j.indcrop.2020.112825

Freitas, M. L. F., Polachini, T. C., de Souza, A. C., & Telis-Romero, J. (2016). Sorption isotherms and thermodynamic properties of grated Parmesan cheese. *International Journal of Food Science and Technology*, *51*(1), 250–259. https://doi.org/10.1111/ijfs.12969

Gomes de Souza, P., Rosane P. Azeredo, D., da Silva, T. T. C., Carneiro, C. da S., Junger Teodoro, A., & Menezes Ayres, E. M. (2023). Food neophobia, risk perception and attitudes associations of Brazilian consumers towards non-conventional edible plants and research on sale promotional strategies. *Food Research International*, *167*(February). https://doi.org/10.1016/j.foodres.2023.112628

Haque, M. A., Timilsena, Y. P., & Adhikari, B. (2016). Food Proteins, Structure, and Function. In *Reference Module in Food Science*. Elsevier. https://doi.org/10.1016/b978-0-08-100596-5.03057-2

Horwitz, W., Latimer, G. W., & Association of Official Analytical Chemistry, A. (2007). *Official Methods of Analysis* (18th ed.). AOAC International.

Jackix, E. D. A., Monteiro, E. B., Raposo, H. F., Vanzela, E. C., & Amaya-Farfán, J. (2013a). Cholesterol reducing and bile-acid binding properties of taioba (Xanthosoma sagittifolium) leaf in rats fed a high-fat diet. *Food Research International*, *51*(2), 886–891.

https://doi.org/10.1016/j.foodres.2013.02.017

Jackix, E. D. A., Monteiro, E. B., Raposo, H. F., Vanzela, E. C., & Amaya-Farfán, J. (2013b). Taioba (xanthosoma sagittifolium) leaves: Nutrient composition and physiological effects on healthy rats. *Journal of Food Science*, *78*(12), 1929–1934. https://doi.org/10.1111/1750-3841.12301

Jiménez-Escrig, A., & Sánchez-Muniz, F. J. (2000). Dietary fibre from edible seaweeds: Chemical structure, physicochemical properties and effects on cholesterol metabolism. *Nutrition Research*, *20*(4), 585–598. https://doi.org/10.1016/S0271-5317(00)00149-4

Kinupp, V. F., & Lorenzi, H. (2014). *Plantas alimentícias não convencionais (PANC) no Brasil: guia de identificação, aspectos nutricionais e receitas ilustradas.* (1st ed.). Instituto Plantarum.

Koua, B. K., Koffi, P. M. E., Gbaha, P., & Toure, S. (2014). Thermodynamic analysis of sorption isotherms of cassava (Manihot esculenta). *Journal of Food Science and Technology*, *51*(9), 1711–1723. https://doi.org/10.1007/s13197-012-0687-y

Krug, R. R., Hunter, W. G., & Grieger, R. A. (1976a). Enthalpy-entropy compensation. 1. Some fundamental statistical problems associated with the analysis of van’t hoff and arrhenius data. *Journal of Physical Chemistry*, *80*(21), 2335–2341. https://doi.org/10.1021/j100562a006

Krug, R. R., Hunter, W. G., & Grieger, R. A. (1976b). Enthalpy-entropy compensation. 2. Separation of the chemical from the statistical effect. *Journal of Physical Chemistry*, *80*(21), 2341–2351. https://doi.org/10.1021/j100562a007

Labuza, T. (1963). Creation of moisture sorption isotherms for hygroscopic materials. Sorption isotherm methods. In *International symposium on humidity and moisture., May 20-23*. Washington: American Society of Heating, Refrigerating and Air Conditioning Engineers.

Leffler, J. E. (1955). The enthalpy-entropy relationshipg and its implications for organic chemistry. *The Journal of Organic Chemistry*, *20*, 1202–1231.

Lewicki, P. P. (2008). Data and Models of Water Activity. II: Solid Foods. In *Food Properties Handbook* (2nd ed.). Taylor & Francis Group.

McElreath, R. (2016). Overfitting, Regularization, and Information Criteria. In *Statistical Rethinking: A Bayesian Course with Examples in R and Stan* (1st ed., pp. 165–205). Chapman and Hall/CRC. https://doi.org/https://doi.org/10.1201/9781315372495

McMinn, W. A. M., Al-Muhtaseb, A. H., & Magee, T. R. A. (2005). Enthalpy-entropy compensation in sorption phenomena of starch materials. *Food Research International*, *38*(5), 505–510. https://doi.org/10.1016/j.foodres.2004.11.004

Moreira, R., Chenlo, F., Torres, M. D., & Vallejo, N. (2008). Thermodynamic analysis of experimental sorption isotherms of loquat and quince fruits. *Journal of Food Engineering*, *88*(4), 514–521. https://doi.org/10.1016/j.jfoodeng.2008.03.011

Ojike, O., Uzodinma, E. O., Ali, E. O., Nweze, B. C., Okoyeuzu, C. F., & Eze, C. R. (2022). Moisture Adsorption potentials and energy models of Gongronema latifolium leaves dried in separate environments. *Food Science and Nutrition*, *10*(2), 388–401. https://doi.org/10.1002/fsn3.2616

Ouertani, S., Azzouz, S., Hassini, L., Koubaa, A., & Belghith, A. (2014). Moisture sorption isotherms and thermodynamic properties of Jack pine and palm wood: Comparative study. *Industrial Crops and Products*, *56*, 200–210. https://doi.org/10.1016/j.indcrop.2014.03.004

Pérez-Alonso, C., Beristain, C. I., Lobato-Calleros, C., Rodríguez-Huezo, M. E., & Vernon-Carter, E. J. (2006). Thermodynamic analysis of the sorption isotherms of pure and blended carbohydrate polymers. *Journal of Food Engineering*, *77*(4), 753–760. https://doi.org/10.1016/j.jfoodeng.2005.08.002

Polachini, T. C., Betiol, L. F. L., Lopes-Filho, J. F., & Telis-Romero, J. (2016). Water adsorption isotherms and thermodynamic properties of cassava bagasse. *Thermochimica Acta*, *632*, 79–85. https://doi.org/10.1016/j.tca.2016.03.032

Rizvi, S. S. H. (2014). Thermodynamic properties of foods in dehydration. In M. A. Rao, S. S. H. Rizvi, & A. K. Datta (Eds.), *Engineering properties of foods* (4th ed., pp. 359–436). CRC Press.

Rosa, D. P., Evangelista, R. R., Borges Machado, A. L., Sanches, M. A. R., & Telis-Romero, J. (2021). Water sorption properties of papaya seeds (Carica papaya L.) formosa variety: An assessment under storage and drying conditions. *Lwt*, *138*(June 2020). https://doi.org/10.1016/j.lwt.2020.110458

Sá, A. G. A., Moreno, Y. M. F., & Carciofi, B. A. M. (2020). Plant proteins as high-quality nutritional source for human diet. *Trends in Food Science & Technology*, *97*, 170–184. https://doi.org/10.1016/J.TIFS.2020.01.011

Saath, K. C. de O., & Fachinello, A. L. (2018). Crescimento da Demanda Mundial de Alimentos e Restrições do Fator Terra no Brasil. *Revista de Economia e Sociologia Rural*, *56*(2), 195–212. https://doi.org/10.1590/1234-56781806-94790560201

Sanches, M. A. R., Augusto, P. E. D., Polachini, T. C., & Telis-Romero, J. (2023). Water sorption properties of brewer's spent grain: A study aimed at its stabilization for further conversion into value-added products. *Biomass and Bioenergy*, *170*(December 2022), 106718. https://doi.org/10.1016/j.biombioe.2023.106718

Sangeeta, & Hathan, B. S. (2017). Sorption behavior, thermodynamic properties and storage stability of ready-to-eat Elephant Foot Yam (Amorphophallus spp.) product: physic-chemical properties, minerals, total dietary fiber and phenolic content of stored product. *Journal of Food Measurement and Characterization*, *11*(2), 401–416. https://doi.org/10.1007/s11694-016-9408-y

Schwarz, G. (1978). Estimating the Dimension of a Model. *The Annals of Statistics*, *6*(2), 461–

464. https://doi.org/10.1214/aos/1176344136

Silva, K. S., Polachini, T. C., Luna-Flores, M., Luna-Solano, G., Resende, O., & Telis-Romero, J. (2021). Sorption isotherms and thermodynamic properties of wheat malt under storage conditions. *Journal of Food Process Engineering*, *44*(9), 1–12. https://doi.org/10.1111/jfpe.13784

Sim, S. Y. J., Srv, A., Chiang, J. H., & Henry, C. J. (2021). Plant Proteins for Future Foods: A Roadmap. *Foods 2021, Vol. 10, Page 1967*, *10*(8), 1967. https://doi.org/10.3390/FOODS10081967

Singh, N., Singh, J., Kaur, L., Singh Sodhi, N., & Singh Gill, B. (2003). Morphological, thermal and rheological properties of starches from different botanical sources. *Food Chemistry*, *81*(2), 219–231. https://doi.org/10.1016/S0308-8146(02)00416-8

Sousa, F. C., Rocha, A. P. T., Gomes, J. P., Martins, J. J. A., & Martins, J. N. (2014). Isotermas de dessorção de folhas in natura de juazeiro e mororó. *Pesquisa Agropecuária Tropical*, *44*(3), 304–310.

Spiess, W. E. L., & Wolf, W. F. (1983). The results of the COST 90 project on water activity. In R. Jowitt (Ed.), *Physical Properties of Foods* (pp. 65–91). Applied Science Publishers.

Tagnamas, Z., Bahammou, Y., Moussaoui, H., Kouhila, M., Lamsyehe, H., Idlimam, A., & Lamharrar, A. (2021). Exploring the sorption and thermodynamic proprieties of white truffle (Terfezia boudieri). *Journal of Food Process Engineering*, *44*(12), 1–11. https://doi.org/10.1111/jfpe.13888

Torres, M. D., & Seijo, J. (2016). Water sorption behaviour of by-products from the rice industry. *Industrial Crops and Products*, *86*, 273–278. https://doi.org/10.1016/j.indcrop.2016.04.014

Tunç, S., & Duman, O. (2007). Thermodynamic properties and moisture adsorption isotherms of cottonseed protein isolate and different forms of cottonseed samples. *Journal of Food*

Engineering, *81*(1), 133–143. https://doi.org/10.1016/j.jfoodeng.2006.10.015

Vega-Gálvez, A., Lemus-Mondaca, R., Fito, P., & Andrés, A. (2007). Note: Moisture sorption isotherms and isosteric heat of red bell pepper (var. Lamuyo). *Food Science and Technology International*, *13*(4), 309–316. https://doi.org/10.1177/1082013207082530

Viollaz, P. E., & Rovedo, C. O. (1999). Equilibrium sorption isotherms and thermodynamic properties of starch and gluten. *Journal of Food Engineering*, *40*(4), 287–292. https://doi.org/10.1016/S0260-8774(99)00066-7

Wolf, W., Spiess, W. E. L., & Jung, G. (1985). Standardization of Isotherm Measurements (Cost-Project 90 and 90 BIS). In *Properties of Water in Foods* (pp. 661–679). Springer Netherlands. https://doi.org/10.1007/978-94-009-5103-7_40

SUPPLEMENTARY TABLES

Table S1 - Water activity of saturated salt solutions at different temperatures (Labuza, 1963).

Salt	Water activity								
	Storage temperature				Storage/Drying	Drying temperature			
	5 ºC	10 ºC	20 ºC	30 ºC	40 ºC	50 ºC	60 ºC	70 ºC	80 ºC
LiBr	0.074	0.071	0.066	0.062	0.058	0.055	0.053	0.052	0.052
LiCl	0.113	0.113	0.113	0.113	0.112	0.111	0.110	0.108	0.105
LiI	0.217	0.206	0.186	0.166	0.146	0.124	0.100	0.072	-
$MgCl_2$	0.337	0.335	0.331	0.324	0.316	0.305	0.293	0.278	0.261
NaI	0.424	0.418	0.397	0.362	0.329	0.292	0.2600	0.236	0.225
K_2CO_3	0.431	0.431	0.432	0.432	-	-	-	-	-
$Mg(NO_3)_2$	0.589	0.574	0.544	0.514	0.484	0.454	-	-	-
NaBr	0.635	0.622	0.591	0.560	0.532	0.509	0.500	0.497	0.503
KI	0.733	0.721	0.699	0.679	0.661	0.645	0.631	0.619	0.610
NaCl	0.757	0.757	0.755	0.751	0.747	0.744	0.745	0.751	0.763
$(NH_4)_2SO_4$	0.824	0.821	0.813	0.806	0.799	0.792	-	-	-
KCl	0.877	0.868	0.851	0.836	0.823	0.812	0.803	0.795	0.789
KNO_3	0.963	0.960	0.946	0.923	0.890	0.848	-	-	-
K_2SO_4	0.985	0.982	0.976	0.970	0.964	0.958	-	-	-

Table S2- Parameters predicted by the models fitted to the desorption data of taioba leaves at storage and drying conditions.

Model		Temperature (ºC)								
		5	10	20	30	40	50	60	70	80
GAB	X_m	0.070	0.069	0.066	0.061	0.061	0.058	0.058	0.058	0.052
	C	64.235	44.950	43.040	41.540	41.540	40.930	40.722	40.245	40.000
	k	0.703	0.700	0.669	0.702	0.709	0.715	0.706	0.681	0.738
	R_{aj}^2	0.992	0.992	0.987	0.999	0.996	0.992	0.998	0.997	0.987
	$\chi^2 \cdot 10^5$	2.491	2.494	3.126	0.296	0.860	1.480	0.236	0.320	1.383
	AIC	-139.336	-139.317	-136.156	-169.178	-169.178	-134.986	-102.270	-99.525	-71.936
	SIC	-141.225	-141.206	-138.044	-171.066	-171.066	-137.726	-111.481	-108.736	-84.951
Peleg	k_1	0.133	0.126	0.124	0.108	0.102	0.104	0.095	0.104	0.096
	n_1	0.377	0.392	0.393	0.345	0.301	0.316	0.310	0.336	0.345
	k_2	0.099	0.100	0.093	0.094	0.105	0.105	0.082	0.073	0.107
	n_2	4.866	4.456	5.076	4.179	3.529	4.905	3.043	3.903	43697
	R_{aj}^2	0.991	0.991	0.987	0.998	0.995	0.994	0.997	0.996	0.985
	$\chi^2 \cdot 10^5$	2.527	2.787	3.139	0.380	1.027	1.082	0.293	0.384	1.692
	AIC	-135.412	-134.044	-132.382	-161.933	-161.933	-134.855	-89.963	-87.511	-53.443
	SIC	-139.717	-138.349	-136.687	-166.238	-166.238	-140.602	-108.977	-106.525	-83.046
Oswin	M	0.108	0.103	0.098	0.092	0.095	0.090	0.087	0.088	0.082
	N	0.198	0.212	0.222	0.232	0.240	0.248	0.291	0.273	0.301
	R_{aj}^2	0.938	0.938	0.960	0.970	0.966	0.985	0.997	0.998	0.988
	$\chi^2 \cdot 10^5$	18.351	18.168	9.921	6.256	7.580	2.834	0.389	0.246	1.347
	AIC	-114.204	-114.344	-122.814	-129.270	-129.270	-129.631	-103.583	-107.699	-80.025
	SIC	-114.686	-114.827	-123.297	-129.753	-129.753	-130.603	-107.791	-111.907	-85.786
Halsey	H_1	$3.41 \cdot 10^{-5}$	$5.53 \cdot 10^{-5}$	$8.24 \cdot 10^{-5}$	$1.07 \cdot 10^{-4}$	$1.81 \cdot 10^{-4}$	$2.24 \cdot 10^{-4}$	$2.14 \cdot 10^{-3}$	$1.68 \cdot 10^{-3}$	$2.25 \cdot 10^{-3}$
	H_2	4.425	4.114	3.854	3.641	3.461	3.283	2.315	2.417	2.243
	R_{aj}^2	0.882	0.882	0.910	0.921	0.917	0.949	0.982	0.978	0.981
	$\chi^2 \cdot 10^5$	34.753	34.563	22.117	16.223	18.677	9.533	2.041	2.326	2.028
	AIC	-105.263	-105.340	-111.590	-115.929	-115.929	-113.861	-88.658	-87.483	-76.748
	SIC	-105.746	-105.823	-112.073	-116.412	-116.412	-114.833	-92.867	-91.691	-82.510
Henderson	H_1	156.772	133.583	152.401	171.591	157.775	193.789	341.592	550.441	316.083
	H_2	2.459	2.335	2.352	2.345	2.346	2.379	2.588	2.791	2.495
	R_{aj}^2	0.986	0.986	0.985	0.991	0.985	0.972	0.986	0.991	0.971
	$\chi^2 \cdot 10^5$	4.031	4.093	3.627	1.959	3.363	5.176	1.545	0.963	3.144
	AIC	-135.421	-135.209	-136.900	-145.524	-145.524	-121.802	-91.162	-95.422	-73.242
	SIC	-135.904	-135.692	-137.383	-146.007	-146.007	-122.774	-95.370	-99.630	-79.003

Table S3 - Parameters predicted by the models fitted to the desorption data of taioba stems at storage and drying conditions.

Model		Temperature (ºC)								
		5	10	20	30	40	50	60	70	80
GAB	X_m	0.126	0.122	0.120	0.120	0.115	0.115	0.115	0.114	0.102
	C	55.868	45.471	44.728	43.337	42.594	42.594	42.027	41.167	40.777
	k	0.694	0.701	0.701	0.697	0.707	0.708	0.702	0.693	0.775
	R_{aj}^2	0.9978	0.9992	0.9982	0.9984	0.9939	0.9986	0.9986	0.9966	0.9948
	$\chi^2 \cdot 10^5$	2	0.736	1.48	1.25	4.56	1	0.587	1.45	2.53
	AIC	-142.415	-156.405	-146.610	-149.028	-120.347	-140.032	-94.054	-85.945	-67.111
	SIC	-144.304	-158.293	-148.499	-150.916	-123.087	-142.773	-103.266	-95.156	-80.127
Peleg	k_1	0.217	0.211	0.208	0.207	0.208	0.205	0.193	0.208	0.173
	n_1	0.330	0.329	0.325	0.328	0.355	0.346	0.312	0.352	0.282
	k_2	0.189	0.191	0.187	0.182	0.180	0.181	0.174	0.211	0.234
	n_2	4.010	3.995	4.036	3.960	4.485	4.335	3.672	5.430	3.691
	R_{aj}^2	0.9979	0.9986	0.9977	0.9983	0.9938	0.9979	0.9972	0.9970	0.994
	$\chi^2 \cdot 10^5$	1.96	1.22	1.48	1.27	4.66	1.46	1.16	1.24	2.89
	AIC	-138.955	-145.648	-139.632	-144.994	-115.868	-130.994	-77.548	-76.949	-49.154
	SIC	-143.260	-149.953	-143.937	-149.299	-121.615	-136.741	-96.562	-95.963	-78.757
Oswin	M	0.192	0.186	0.182	0.180	0.174	0.174	0.173	0.170	0.169
	N	0.197	0.207	0.219	0.227	0.240	0.247	0.283	0.283	0.311
	R_{aj}^2	0.9325	0.9496	0.96239	0.9613	0.9663	0.9799	0.9973	0.9974	0.9873
	$\chi^2 \cdot 10^5$	61.741	44.818	30.581	29.170	25.286	14.109	1.12	1.09	6.12
	AIC	-97.218	-101.703	-107.054	-107.715	-101.180	-108.765	-94.058	-94.313	-67.912
	SIC	-97.701	-102.185	-107.537	-108.198	-102.152	-109.737	-98.266	-98.521	-73.674
Halsey	$H_1 \cdot 10^4$	4.01	5.46	8.04	10.8	14.8	18.6	9.5	9.62	129
	H_2	4.464	4.202	3.915	3.713	3.456	3.315	2.368	2.337	2.169
	R_{aj}^2	0.8755	0.8971	0.9138	0.9109	0.9163	0.9310	0.9869	0.9840	0.9914
	$\chi^2 \cdot 10^5$	114	91.519	70.087	67.190	62.882	48.400	5.52	7.72	4.15
	AIC	-88.647	-91.707	-95.443	-96.034	-89.337	-92.740	-79.707	-77.936	-71.020
	SIC	-89.129	-92.190	-95.926	-96.517	-90.309	-93.711	-83.915	-82.144	-76.782
Henderson	H_1	39.360	37.381	37.885	38.573	38.368	39.722	67.306	73.480	45.500
	H_2	2.472	2.403	2.389	2.391	2.348	2.370	2.672	2.701	2.413
	R_{aj}^2	0.9867	0.9904	0.9888	0.9869	0.9836	0.9890	0.9832	0.9858	0.9629
	$\chi^2 \cdot 10^5$	1.22	8.51	9.14	9.86	1.23	7.72	7.04	5.98	17.87
	AIC	-119.951	-124.961	-123.955	-122.906	-110.525	-116.602	-77.508	-78.985	-65.100
	SIC	-120.434	-125.443	-124.438	-123.389	-111.497	-117.574	-81.717	-83.193	0.963

Table S4 - Parameters predicted by the models fitted to the desorption data of taioba tubers at storage and drying conditions.

Model		Temperature (ºC)								
		5	10	20	30	40	50	60	70	80
GAB	X_m	0.163	0.146	0.113	0.086	0.075	0.054	0.047	0.040	0.034
	C	10.776	9.883	12.323	13.902	14.719	23.202	17.586	21.101	23.088
	k	0.732	0.744	0.765	0.764	0.803	0.843	0.836	0.840	0.870
	R_{aj}^2	0.9948	0.9948	0.9922	0.9991	0.9984	0.9968	0.9988	0.9980	0.9982
	$\chi^2 \cdot 10^5$	12.777	10.994	10.933	0.687	1.267	1.652	0.218	0.249	0,198
	AIC	-116.446	-118.549	-118.628	-157.365	-136.999	-133.551	-102.984	-101.778	-87.504
	SIC	-118.334	-120.438	-120.516	-159.253	-139.739	-136.291	-112.195	-110.989	-100.519
Peleg	k_1	0.354	0.307	0.253	0.179	0.155	0.122	0.089	0.085	0.077
	n_1	0.664	0.655	0.638	0.570	0.538	0.496	0.451	0.481	0.488
	k_2	0.238	0.240	0.216	0.172	0.205	0.207	0.134	0.136	0.153
	n_2	6.233	5.518	6.285	5.332	5.184	6.127	3.757	5.149	5.744
	R_{aj}^2	0.9953	0.9942	0.9922	0.9987	0.9975	0.9968	0.9991	0.9974	0.9979
	$\chi^2 \cdot 10^5$	11.545	12.276	10.949	0.942	1.924	1.654	0.160	0.331	0.231
	AIC	-114.144	-177.589	-114.887	-153.537	-127.372	-129.332	-95.379	-88.861	-69.367
	SIC	-118.449	-113.285	-119.192	-149.232	-133.119	-135.079	-114.392	-107.874	-98.970
Oswin	M	0.230	0.205	0.166	0.127	0.118	0.094	0.077	0.067	0.060
	N	0.243	0.261	0.285	0.294	0.328	0.358	0.421	0.409	0.426
	R_{aj}^2	0.9177	0.9264	0.9545	0.9630	0.9714	0.9896	0.9979	0.9972	0.9947
	$\chi^2 \cdot 10^5$	201	157	64.104	27.500	22.016	5.356	0.364	0.345	0.583
	AIC	-80.6817	-84.186	-96.692	-108.540	-102.980	-121.357	-104.172	-104.652	-86.720
	SIC	-81.165	-84.669	-97.175	-109.023	-103.952	-122.329	-108.381	-108.860	-92.482
Halsey	$H_1 \cdot 10^3$	3.05	3.05	2.69	1.55	2.48	2.42	9.00	6.68	6.34
	H_2	3.646	3.384	3.056	2.921	2.602	2.363	1.649	1.688	1.630
	R_{aj}^2	0.8581	0.8700	0.9061	0.9140	0.9282	0.9610	0.9887	0.9907	0.9943
	$\chi^2 \cdot 10^5$	347	276	132	63.876	55.226	20.031	1.988	1.160	0.625
	AIC	-73.047	-76.233	-86.534	-96.742	-91.025	-104.209	-88.892	-93.745	-86.164
	SIC	-73.520	-76.715	-87.026	-97.225	-91.996	-105.180	-93.100	-97.953	-91.925
Henderson	H_1	11.368	12.097	15.207	24.511	19.853	22.276	51.907	83.069	75.160
	H_2	1.900	1.804	1.727	1.740	1.575	1.471	1.725	1.807	1.702
	R_{aj}^2	0.9902	0.9904	0.9931	0.9972	0.9932	0.9789	0.9859	0.9826	0.9759
	$\chi^2 \cdot 10^5$	23.89	20.49	9.710	2.089	5.273	10.811	2.476	2.174	2.664
	AIC	-110.509	-112.663	-123.116	-122.626	-121.559	-112.226	-86.919	-88.089	-74.564
	SIC	-110.991	-113.146	-123.599	-145.108	-122.531	-113.198	-91.127	-92.297	-80.325

5 Capítulo 5 - Drying kinetics and thermodynamic approach of taioba (*Xanthosoma taioba* E. C. Gonç.): leaves, stems, and tubers

André Luiz Borges-Machado[a,b]*, Marcio Augusto Ribeiro-Sanches[a], , Priscila Alonso dos Santos[b], Guadalupe Luna-Solano[c], Javier Telis-Romero[a].

[a] Food Engineering and Technology Department, State University of São Paulo, São José do Rio Preto, São Paulo, 15054-000, Brazil.

[b] Department of Food Engineering, Institute Federal Goiano Campus Rio Verde, Rod. Sul Goiana, 75901-970 Rio Verde, Goiás, Brazil.

[c] Instituto Tecnologico de Orizaba - Division de Estudios de Posgrado e Investigación - Orizaba – México.

ABSTRACT

This study aimed to investigate the drying kinetics of taioba leaves, stems, and tubers within the temperature range of 40–80 ºC. Specifically, it aimed to establish drying curves, perform mathematical modeling for each taioba part, estimate the effective diffusion coefficients and activation energy, as well as calculate the enthalpy, entropy, and Gibbs free energy associated with the drying process. Based on Akaike (AIC) and Bayesian (BIC) information criteria values, the Logarithmic model was chosen to describe the drying curves of taioba leaves and stems, whereas the Weibull model was the most adequate for the taioba tubers. Drying occurred during the falling rate period and was governed by diffusion. The effective diffusion coefficients increased with rising temperature, and taioba tubers presented the lower D_{eff} values ($0.51 \cdot 10^{-10}$–$1.74 \cdot 10^{-10}$ m^2/s) while the highest D_{eff} values ($7.02 \cdot 10^{-10}$–$140.54 \cdot 10^{-10}$ m^2/s) were found for taioba leaves. The activation energy of taioba leaves, stems and tubers were estimated in 68.47, 34.80, and 29.68 kJ/mol, respectively. Enthalpy and entropy diminished while Gibbs free energy increased with increasing drying temperature.

Keywords: Non-conventional edible plant, Cocoyam, drying rate, Logarithmic model, Weibull model, thermodynamic properties.

5.1 INTRODUCTION

Taioba (*Xanthosoma taioba* E. C. Gonç) is a leafy vegetable native to South America's tropical areas that occurs mostly in tropical and subtropical climates known worldwide as cocoyam (de Jesus Benevides et al., 2022), and it has been investigated for its leaves, its flours, use in biorefineries, in brewing, use of its starches, and bioethanol production (Farias et al., 2020). Taioba is also referred to as a non-conventional edible plant; however, according to Serna-Loaiza et al., (2018), despite the low cultivation of this plant, taioba has a high crop yield (30 t/ha) and low cost when compared to sorghum, corn, and cassava. It can be divided into three parts: leaves with a high protein and fiber content, stems made of lignocellulose, and tubers with a starch level comparable to cassava and potatoes (Serna-Loaiza et al., 2018). Taioba is also a source of calcium, magnesium, manganese, iron, and zinc, as well as vitamin C and carotenes (Kinupp and Lorenzi, 2014). Moreover, some studies with the leaves using animal models presented potent antioxidant action, high fermentability, and binding capacity with bile acids, and it may have a protective effect against cardiovascular diseases and bowel cancer due to its high content of fiber and phytochemicals (Jackix, 2015). Thus, taioba may be a good alternative to human consumption due to its excellent nutritional quality, contributing to food security and, hence, to the 2030 agenda.

Food deterioration is undoubtedly a common issue in fresh vegetables. For this reason, appropriate preservation procedures should be used to avoid nutritional and sensory losses and to increase their shelf life (Wang et al., 2019). The drying process is a vital operation in the industry that requires a significant amount of energy and time. This unit operation is used to increase the shelf life of products as well as reduce their mass and volume during storage and distribution once the high moisture contents contribute to degradation via bacteria and enzymatic reactions (Tagnamas et al., 2022). Drying operations are an important process to obtain flours that can be added to food formulations, aiming to enhance their nutritional value.

Drying is the process of removing moisture by transferring heat and mass through evaporation between the biological product and the drying air, typically triggered by temperature and air convection forces (Perea-Flores et al., 2012). Researchers have demonstrated that using only experimental drying methods without accounting for the kinetics of drying can have a considerable impact on dryer efficiency, raise production costs, and reduce the quality of the dried product (Inyang et al., 2018). In this way, mathematical modeling is an effective method for optimizing the drying process and determining the ideal operating parameters for equipment design to dehydrate foodstuffs with improved rehydration qualities (Bishnoi et al., 2020).

There are numerous empirical and semiempirical models available for the simulation of the drying process. Most of these models are created by condensing Fick's second law's general solutions. As a result, most of them are not randomly selected models but rather are based on physiological factors (Hacihafizoğlu et al., 2008). Theoretical and semi-theoretical models such as Lewis, Page, Henderson and Pabis, and Logarithmic models inform parameters such as the drying constant, k. According to Marinos-Kouris and Maroulis, (2015), the drying constant is the combination of drying transport properties such as moisture diffusivity, thermal conductivity, density, specific heat, interface heat, and mass coefficients. On the other hand, empirical models do not derive from the fundamentals of the drying process and their coefficients do not pursue physical meaning. The Weibull model is an empirical drying model derived from the probabilistic Weibull model and an exception because its coefficients are related to the drying time and the drying rate (Corzo et al., 2008; Inyang et al., 2018).

The mathematical modeling also allows the determination of mass transfer parameters such as the effective diffusion coefficient assessed using Fick’s second law, which describes the moisture movement or diffusion and activation energy, which is an estimation of the amount of energy needed to start diffusion. In addition, the activation energy allows the assessment of thermodynamic properties of drying, such as the variations in enthalpy, entropy, and Gibbs free energy. These properties are essential to understand because they provide knowledge to design drying equipment, study the properties of adsorbed water, estimate the energy required in this process, assess the microstructure of the food, and study the physical phenomena that take place on the food surface (Campos et al., 2019).

Based on the lack of studies on the drying kinetics of the taioba leaves, stems, and tubers, this study aimed to: (i) determine the drying curves of taioba leaves, stems, and tubers at 40-80 ºC; (ii) provide a drying model for each taioba part; (iii) estimate the effective diffusion coefficients and activation energy; and (iv) calculate the enthalpy, entropy and Gibbs free energy of the drying process.

5.2 MATERIAL AND METHODS

5.2.1 Raw material

Taioba plants were harvested on the farm of the IF Goiano – Campus Rio Verde and conducted to the Laboratory of Food Analysis where the experiments were performed. The plant was divided into three parts: leaves (TL), stems (TS), and tubers (TT) which were washed with tap water and sanitized with chlorinated solution (100 ppm) for 20 minutes, and then they were carefully dried with toilet paper. The initial moisture contents of the leaves, stems, and tubers were determined by the gravimetric method proposed by AOAC (Horwitz et al., 2007) using an overnight oven at 105 ºC and were equal to 4.28 ± 0.178 d.b., 20.06 ± 0.447 d.b., 6.78 ± 0.462 d.b., respectively. The leaves were cut into disks of 80.3 mm in diameter and the tubers were cut into slices of 2 mm in thickness, aiming the flat slab geometry. The stems were cut in a cylindric shape of 1 cm in height and 19.9 ± 4.53 mm in diameter.

5.2.2 Drying experiments

Drying assays were conducted in a forced air circulation oven (TH.510, Thoth Equipamentos, Piracicaba, Brazil) at 40 ºC, 50ºC, 60 ºC, 70ºC and 80 ºC which was started an hour before to achieve the steady state. The room temperature and drying air temperatures were measured using thermohygrometers outside and inside the dryer, and the relative humidity inside the oven was calculated using basic psychrometry concepts with the support of the software GRAPSI. The drying assays were performed in quadruplicate, using stainless-steel bowl sieves that the air to contact all the surface of the samples. A semi-analytical balance (BL220H, Shimadzu, Kyoto, Japan) was used to determine the weight loss for different intervals of time with an accuracy of ± 0.01 g. The samples were dried until they reached a constant weight, at which point the equilibrium moisture content was achieved. The moisture ratio (MR) and the drying rate (DR) were calculated using Equations 1 and 2, respectively.

$$MR = \frac{M_t - M_e}{M_o - M_e} \quad (1)$$

$$DR = \frac{M_{t_1} - M_{t_2}}{t_2 - t_1} \quad (2)$$

in which, M_e, M_t and M_o are the equilibrium moisture content, moisture content at time t, and the initial moisture content, respectively. The moisture ratio (MR) values were plotted against time to perform the fitting of the five models (Table 1) to the data through nonlinear regression by the Levenberg–Marquardt method using Origin 2022 (OriginLab Corporation, Northampton, MA).

Table 1 - Mathematical models applied to the drying curves of taioba leaves, stems, and tubers.

Model	Equation	Equation number	Reference
Newton	$MR = exp(-kt)$	3	(Westerman et al., 1973)
Page	$MR = exp(-kt^n)$	4	(Page, 1949)
Henderson and Pabis	$MR = a \cdot exp(-kt)$	5	(Henderson and Pabis, 1961)
Logarithmic	$MR = a \cdot exp(-kt) + c$	6	(Yaldýz and Ertekýn, 2001)
Weibull	$MR = exp\left[-\left(\frac{t}{\alpha}\right)^{\beta}\right]$	7	(Corzo et al., 2008)

a, c, n: model coefficients; k: drying constant (1/min); α: scale parameter (min); β: shape parameter; t: drying time (min).

5.2.3 Effective diffusion coefficient (D_{eff}) and activation energy (E_a)

The effective diffusion coefficients at different temperatures were obtained using the solutions of Fick's second law, proposed by Crank, (1975), truncated in the twelfth term via nonlinear regression. The D_{eff} of the leaves and tubers was calculated through Equation 11 for flat slab geometry, while Equation 12 for cylinder shape was used to estimate the D_{eff} of the stems.

$$MR = \frac{8}{\pi^2}\sum_{n=0}^{\infty}\frac{1}{(2n+1)^2}exp\left(\frac{-(2n+1)^2\,\pi^2 D_{eff}t}{4l^2}\right) \quad (8)$$

$$RU = \frac{\bar{X}-X_{eq}}{X_0-X_{eq}} = \frac{4}{r_a^2}\sum_{n=0}^{\infty}\frac{1}{\beta_n^2}exp\left(-\beta_n^2 D_{eff}t\right) \quad (9)$$

in which n is the number of terms of the series, t is the time, l is the half thickness of the slab, and r is the radius of the sphere.

The Arrhenius model (Equation 13) was used to evaluate the dependence of D_{eff} on temperature and to calculate the activation energy (E_a) in J/mol through the linearized form of Equation 13.

$$D_{eff} = D_0\ exp\left[\frac{E_a}{RT}\right] \quad (10)$$

where D_0 is the pre-exponential factor of the Arrhenius equation (m^2/s); T is the absolute air temperature (K) and R is the universal gas constant (8.314 J/mol/K).

5.2.4 Enthalpy (ΔH), entropy (ΔS) and Gibbs free energy (ΔG)

The thermodynamic properties of drying were estimated according to a mathematical procedure developed by Jideani and Mpotokwana, (2009) and presented by Corrêa et al., (2012). The ΔH, ΔS, and ΔG in J/mol were calculated using Equations 11, 12, and 13.

$$\Delta H = E_a - R\cdot T_{abs} \quad (11)$$

$$\Delta S = R\left[\ln D_0 - \ln\left(\frac{k_B}{h_P}\right) - \ln T_{abs}\right] \quad (12)$$

$$\Delta G = \Delta H - T_{abs}\cdot\Delta S \quad (13)$$

in which k_B is the Boltzmann constant, 1.38 x 10^{-23} J/K and h_P is the Planck constant, 6.626 x 10^{-34} J/s.

5.2.5 Statistical analysis

The quality of the fitting of the drying models presented in Table 1 to moisture ratio data was evaluated based on the adjusted coefficient of determination (R^2_{adj}) and reduced chi-square (χ^2). An excellent fit is obtained when R^2_{adj} is equal to one and χ^2 is low (Inyang et al., 2018). The Akaike information criterion (AIC) and Schwarz's Bayesian information criterion (BIC) were applied as decisive criteria in selecting the model that best suited the experimental data among those that were adequate in terms of parameters R^2_{adj} and χ^2. The AIC and BIC values were calculated according to Equations 14 and 15 (Akaike, 1974; Schwarz, 1978). Lower values of these parameters reflect the best fit.

$$AIC = -2\log\mathcal{L}(\hat{\theta}) + 2p \quad (14)$$

$$BIC = -2\log\mathcal{L}(\hat{\theta}) + p\ln(n) \quad (15)$$

in which, n is the number of experimental points, p is the number of parameters of the model, and $\mathcal{L}(\hat{\theta})$ is the value of the likelihood function considering the parameters of the obtained model.

5.3 RESULTS AND DISCUSSION

5.3.1 Drying curves and modeling

The moisture ratios of the leaves, stems, and tubers were fitted to five mathematical models at different temperatures and drying times, aiming to select the best one to describe the drying process. In the Supplementary Material, Tables S1, S2, and S3 present the estimated coefficients and fitting parameters of the five drying models applied to the drying curves of taioba leaves (TL), stems (TS), and tubers (TT) at 40 ºC, 50 ºC, 60 ºC, 70 ºC, and 80 ºC. Table 2 shows the estimated coefficients of the models selected to describe the TL, TS, and TT drying curves, as well as the fitting parameters such as the coefficients of determination (R^2_{adj}), reduced chi-squared χ^2, AIC, and BIC values at each temperature studied.

Table 2 - Estimated coefficients and fitting parameters of the models selected to represent the drying curves at different temperatures of taioba leaves, stems, and tubers

Taioba part	Model	Parameters	Temperature (ºC)				
			40	**50**	**60**	**70**	**80**
Leaves	Logarithmic	a	1.00	1.00	1.00	1.01	1.04
		$k \cdot 10^3$	1.82	4.4	10.01	17.95	31.16
		$c \cdot 10^3$	-18.22	-12.23	-18.63	-10.67	-54.67
		R^2_{aj}	0.9993	0.9993	0.9996	0.9999	0.9973
		$\chi^2 \cdot 10^5$	7.44	8.00	4.63	1.49	28.96
		AIC	-459.97	-390.22	-242.70	-293.40	-104.99
		BIC	-453.31	-384.35	-239.82	-290.03	-106.88
Stems	Logarithmic	a	1.02	1.01	1.11	1.12	1.10
		$k \cdot 10^3$	2.7	4.2	5.56	7.12	10.46
		$c \cdot 10^3$	-16.89	-22.52	-85.1	-102.17	-65.1
		R^2_{aj}	0.9993	0.9987	0.9987	0.9986	0.9964
		$\chi^2 \cdot 10^5$	7.69	14.20	17.00	16.67	46.01
		AIC	-458.39	-268.27	-306.31	-245.79	-200.83
		BIC	-451.73	-264.07	-301.26	-241.98	-197.47
Tubers	Weibull	α	385.12	258.38	208.08	131.55	119.23
		β	1.05	0.90	1.05	1.10	1.23
		R^2_{aj}	0.9981	0.9986	0.9982	0.9997	0.9995
		$\chi^2 \cdot 10^5$	21.46	11.83	18.95	3.91	5.88
		AIC	-375.56	-248.26	-312.47	-319.96	-297.18
		BIC	-370.73	-245.26	-308.36	-316.42	-293.76

It was observed that the five models presented a good fit to the drying data due to their R^2_{adj} closeness to one and their χ^2 closeness to zero. In this way, AIC and BIC values were used as selection criteria The Logarithmic model presented the lowest AIC and BIC values for the leaves and was thus selected to represent TL drying curves. Regarding the model selection for the TS drying curves, the Weibull model presented the lowest AIC and BIC at 40 ºC, 60 ºC, and 80 ºC. However, this model presented higher values compared to the other models at 50 ºC and 70 ºC. The Logarithmic model presented the third lowest value of AIC and BIC at 40 ºC, 60 ºC, and 80 ºC and did not present the highest AIC and BIC at any temperature. Thus, this model was also selected to represent the drying curves of the stems. When thinking of production, leaves and stems may be generally harvested together and processed on the same equipment, so, selecting the same model can ease the process design. The Logarithmic model was also selected to describe the drying curves of mint, rosemary, chili, betel (Babu et al., 2018), apple slices, basil leaves, banana slices, and pumpkin (Onwude et al., 2016). Once the Logarithmic model is a semi-theoretical model, the drying constant (k) is associated with the effect of temperature on diffusion during the drying process. It was observed that k increased directly with temperature, ranging from 0.00182 to 0.03116 min^{-1} for TL and from 0.0027 to 0.01046 min^{-1} for TS, thus indicative of an increase in effective diffusion as temperature rose.

The Weibull model was selected to represent the drying curves of the tubers once it presented the lowest AIC and BIC values, except at 50 ºC, where it presented the second lowest value. Despite not presenting the drying rate constant, the Weibull model has a scale parameter (α) that corresponds to the required time to complete about 63 % of the drying process (Corzo et al., 2008). It was observed that α diminished from 385.12 to 119.23 min with increasing temperatures, and similarly to k, it was also indicative of effective diffusion rising. The shape parameter (β) is associated with the velocity of the mass transfer at the beginning of the drying process, and the lower the β, the higher the mass transfer velocity (Corzo et al., 2008). In our work, this parameter did not present a congruency with reality once it tended to increase from 0.90 at 50 ºC to 1.23 at 80 ºC. However, this behavior is possible because the Weibull model empirical and as presented further, no constant drying rate period was observed which may have some effect on the shape parameter. The Weibull model was also used to represent the drying curves of coroba (Corzo et al., 2008), yam (Ju et al., 2016) and *dioscoreae* (Xie et al., 2017) slices.

The experimental data on moisture ratio and the moisture ratio predicted by the Logarithmic model for taioba leaves and stems and by the Weibull model for taioba tubers are shown in Figures 1a, 2a, and 3a, respectively. The lines of the estimated values were close to those of the experimental drying data of the leaves, stems, and tubers, indicating that the adjustment and the other parameters examined are excellent. The initial moisture content of the TL, TS, and TT were equal to 4.280 ± 0.063, 20.048 ± 0.010 and, 6.760 ± 0.079 kg/kg d.b., respectively. As expected, the moisture ratio decreased as drying time increased for all the taioba parts. It was observed that for reducing the MR to 80% of the initial MR, an increase in temperature from 40 ºC to 80 ºC can reduce about 791, 437, and 430 min in the drying time of leaves, stems, and tubers, respectively. At 40 ºC, taioba leaves spend more time to achieve the M_e than the other parts. However, an increase of ten degrees in temperature reduced the drying time of the TL from 836 to 352 minutes of drying process, which is less time than time required by the TS (438 min) and the TT (300 min) at the same temperature. Despite presenting the lowest moisture content among the taioba parts, the drying times required to achieve the M_e of the TT were the highest compared to the leaves and stems. This fact reinforces the importance of the study on drying kinetics and can be associated with the composition of each taioba part and the behavior of water in different food systems.

Figures 1b, 2b, and 3b show the drying rate curves for TL, TS, and TT, revealing that the drying rate decreased consistently with moisture content and drying time. As a result, no constant drying rate period was observed in the taioba parts drying rate curves and the entire drying process occurred under the falling rate phase. The absence of a constant drying rate period implies that the diffusion mechanism is the prevalent mechanism in charge of the drying process of taioba parts, being this a typical characteristic of fruit and vegetable drying (Inyang et al., 2018).

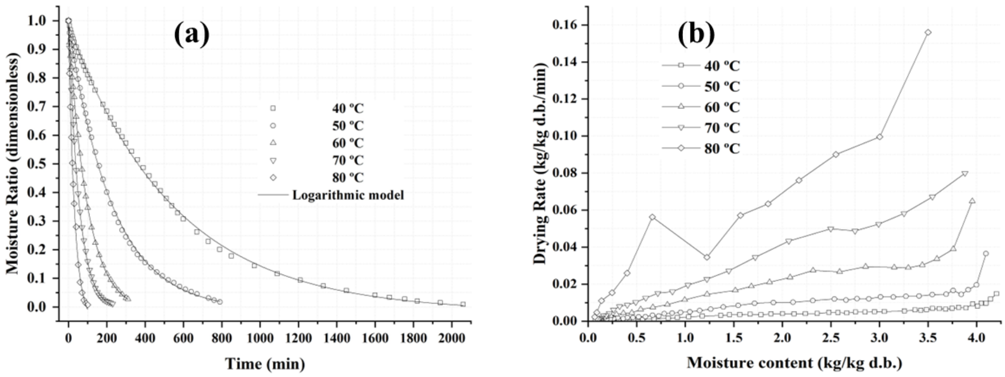

Figure 1 – Experimental and predicted values of moisture ratio as function of time (a) and calculated drying rates as function of moisture content (b) of taioba leaves at a temperature range from 40 ºC to 80 ºC.

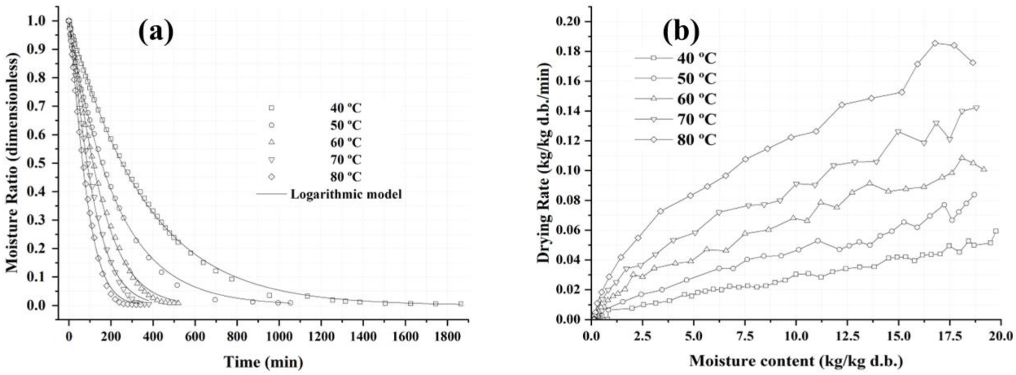

Figure 2 - Experimental and predicted values of moisture ratio as function of time (a) and calculated drying rates as function of moisture content (b) of taioba stems at a temperature range from 40 ºC to 80 ºC.

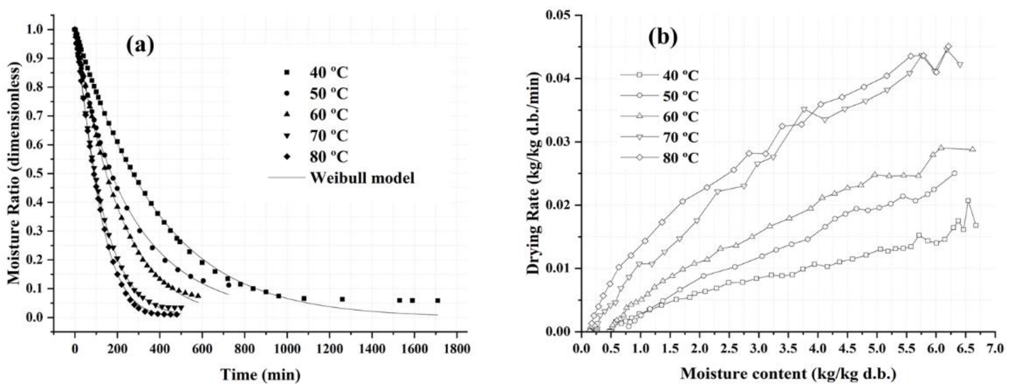

Figure 3 - Experimental and predicted values of moisture ratio as function of time (a) and calculated drying rates as function of moisture content (b) of taioba tubers at a temperature range from 40 ºC to 80 ºC.

5.3.2 *Effective diffusion coefficient (D_{eff}) and activation energy (E_a)*

The effective diffusion coefficients at 40-80 ºC for the leaves, stems, and tubers are presented in Table 3. As expected, the D_{eff} increased with temperature rise for all the samples. Taioba leaves presented the highest values of D_{eff} ranging from $7.02 \cdot 10^{-10}$ to $140.54 \cdot 10^{-10}$ m^2/s, followed by the stems ($4.36 \cdot 10^{-10} – 19.53 \cdot 10^{-10}$ m^2/s) and after, the tubers ($0.51 \cdot 10^{-10}$ - $1.74 \cdot 10^{-10}$ m^2/s). The variation in effective diffusion coefficient values can be explained by the fact that the chemical composition and physical structure of each taioba part differ, making water loss particular to each material. According to Onwude et al., (2016), D_{eff} coefficients generally range from 10^{-12} to 10^{-6} m^2/s and over 80% of the D_{eff} values of fruits and vegetables are in the region from 10^{-11} to 10^{-8} m^2/s being 10^{-10} m^2/s a frequent value.

Table 3 - Estimated effective diffusion coefficients at different temperatures of drying for taioba leaves, stems, and tubers.

Plant part	Leaves		Stems		Tubers	
Temperature (ºC)	**$D_{eff} \cdot 10^{10}$ (m^2/s)**	R^2_{adj}	**$D_{eff} \cdot 10^{10}$ (m^2/s)**	R^2_{adj}	**$D_{eff} \cdot 10^{10}$ (m^2/s)**	R^2_{adj}
40	7.015	0.971	4.355	0.942	0.505	0.957
50	17.410	0.970	6.617	0.942	0.740	0.973
60	40.257	0.972	11.074	0.911	0.985	0.956
70	73.091	0.977	14.313	0.906	1.560	0.956
80	140.521	0.972	19.532	0.908	1.741	0.941

The pre-exponential (D_0) factor and the activation energy (E_a) were determined for TL, TS, and TT by plotting the ln (D_{eff}) versus the inverse of the temperature, and the results are shown in Table 4. The linear regression presented a good fit to the data (R^2_{adj}> 0.997), and the tubers showed the highest values of D_0 and the leaves the lowest. Concerning the E_a, which is the minimum amount of energy required to start diffusion, it behaved inversely of D_0 once the tubers presented the lowest energy requirement (29.68 kJ/mol) while the leaves presented the highest energy requirement (68.47 kJ/mol) to start diffusion. However, after starting diffusion, the phenomenon is faster in the leaves, as corroborated by the D_{eff} values of taioba leaves, which are higher than the D_{eff} values of the tubers at all temperatures. Taioba leaves presented E_a similar to grape leaves (Doymaz, 2012), rosemary leaves (Bensebia and Allia, 2015), blackberry leaves (Martins et al., 2018) and the taioba tubers also showed E_a close to other tuber crops such as biofortified sweet potato (Souza et al., 2019), elephant cassava (Kosasih et al., 2020), cassava (Nainggolan et al., 2023). The E_a of the stems was estimated at 34.80 kJ/mol similar to other lignocellulosic materials (Cuevas et al., 2019).

Table 4 – Calculated pre-exponential factor, activation energy and adjusted coefficient of determination of taioba leaves, stems, and tubers.

Taioba part	D_0 (m^2/s)	E_a (kJ/mol)	R^2_{adj}
Leaves	197.48	68.47	0.997
Stems	3501.37	34.80	0.991
Tubers	218178.76	29.68	0.982

5.3.3 Enthalpy (ΔH), entropy (ΔS) and Gibbs free energy (ΔG)

The estimated values of enthalpy, entropy, and Gibbs free energy of taioba leaves, stems, and tubers at 40-80 ºC are presented in Table 5. Differential enthalpy is associated with the binding energy between water and food matrix, whereas differential entropy is related to the disorder degree as well as the number of accessible sorption sites at a given energy level (Velázquez-Gutiérrez et al., 2015; Viganó et al., 2012). It was noted a reduction of 0.333 kJ/mol in the ΔH of the leaves and stems and 0.279 kJ/mol in the ΔH of the tubers with increasing temperature; thus, a high amount of energy is required to remove water from the taioba at lower drying temperatures. When comparing the taioba parts, the ΔH presented the same trend as E_a because the ΔH is E_a-dependent. In this way, the strongest binding energies were found for the leaves and the weakest binding energies were found for the tubers. Regarding the differential entropy (ΔS), besides their little variation in the range of 40–80 ºC for each taioba part, it is noted that this thermodynamic property presented similar behavior to enthalpy, in which the absolute values obtained increased with the decrease in temperature. This fact is expected once a decrease in temperature leads to less excitation of water molecules, increasing the order of the water-product system. Furthermore, negative entropy values might be linked to the presence of chemical changes or modifications in the structure caused by temperature during the drying process (Corrêa et al., 2010). Gibbs free energy (ΔG) is associated with the spontaneity of a process, characterizing it as spontaneous when ΔG presents negative values and non-spontaneous when ΔG presents positive values. In addition, ΔG can be expressed as the difference between enthalpy (total energy available) and entropy (unavailable energy) (Rizvi, 2014). The ΔG increased with rising temperature and presented positive values for all the taioba parts, thus reinforcing that drying is non-spontaneous and requires external energy to proceed. The same thermodynamic behavior was observed for other vegetables such as coffee (Corrêa et al., 2010), Cabacinha pepper fruits (Silva et al., 2016), rice grains (Corrêa et al., 2017), tamarind seeds (Ferreira Junior et al., 2020) and jambu leaves (Gomes et al., 2022).

Table 5 - Estimated enthalpy, entropy and Gibbs free energy of taioba leaves, stems, and tubers at different drying temperatures.

Taioba part	Leaves			Stems			Tubers		
Temperature (ºC)	**ΔH (kJ/mol)**	**ΔS (kJ/mol/K)**	**ΔG (kJ/mol)**	**ΔH (kJ/mol)**	**ΔS (kJ/mol/K)**	**ΔG (kJ/mol)**	**ΔH (kJ/mol)**	**ΔS (kJ/mol/K)**	**ΔG (kJ/mol)**
40	65.868	-0.201	128.930	32.194	-0.177	87.770	27.072	-0.143	71.889
50	65.785	-0.202	130.946	32.111	-0.178	89.546	26.988	-0.143	73.321
60	65.702	-0.202	132.963	32.028	-0.178	91.325	26.905	-0.144	74.757
70	65.618	-0.202	134.983	31.945	-0.178	93.106	26.822	-0.144	76.194
80	65.535	-0.202	137.006	31.861	-0.178	94.890	26.739	-0.144	77.634

5.4 CONCLUSION

The Logarithmic model is the most suitable model to describe the drying curves of the taioba leaves and stems, while the Weibull model is the most appropriate one concerning the taioba tubers. The leaves tended to require less drying time compared to the stems and tubers. The drying process of all the taioba parts happened during falling rate period. The effective diffusion coefficients rose directly with temperature for all the taioba parts. Water diffusion is faster in the taioba leaves ($7.02 \cdot 10^{-10}$ - $140.54 \cdot 10^{-10}$ m^2/s) than in the stems because they present higher D_{eff} values. The tubers presented the lowest D_{eff} values compared to the other taioba parts. The activation energies of taioba leaves, stems, and tubers were estimated at 68.47, 34.80, and 29.68 kJ/mol. Enthalpy and entropy diminished while Gibbs free energy increased with increasing drying temperature.

5.5 REFERENCES

Akaike, H., 1974. A new look at the statistical model identification, in: IEEE Transactions on Automatic Control. pp. 716–723. https://doi.org/10.1109/TAC.1974.1100705

Babu, A.K., Kumaresan, G., Raj, V.A.A., Velraj, R., 2018. Review of leaf drying: Mechanism and influencing parameters, drying methods, nutrient preservation, and mathematical models. Renew. Sustain. Energy Rev. 90, 536–556. https://doi.org/10.1016/j.rser.2018.04.002

Bensebia, O., Allia, K., 2015. Drying and Extraction Kinetics of Rosemary Leaves: Experiments and Modeling. J. Essent. Oil Bear. Plants 18, 99–111. https://doi.org/10.1080/0972060X.2014.901620

Bishnoi, S., Chhikara, N., Singhania, N., Ray, A.B., 2020. Effect of cabinet drying on nutritional quality and drying kinetics of fenugreek leaves (Trigonella foenum-graecum L.). J. Agric. Food Res. 2, 100072. https://doi.org/10.1016/j.jafr.2020.100072

Campos, R.C., Correa, P.C., Zaidan, I.R., Zaidan, Ú.R., Leite, R.A., 2019. Moisture sorption isotherms of sunflower seeds: Thermodynamic analysis. Cienc. e Agrotecnologia 43. https://doi.org/10.1590/1413-7054201943011619

Corrêa, P.C., de Oliveira, G.H.H., de Oliveira, A.P.L.R., Botelho, F.M., Goneli, A.L.D., 2017. Thermodynamic properties of drying process and water absorption of rice grains. CyTA - J. Food 15, 204–210. https://doi.org/10.1080/19476337.2016.1238012

Corrêa, P.C., Oliveira, G.H.H., Botelho, F.M., Goneli, A.L.D., Carvalho, F.M., 2010. Modelagem matemática e determinação das propriedades termodinâmicas do café (Coffea arabica L.) durante o processo de secagem. Rev. Ceres 57, 595–601. https://doi.org/10.1590/s0034-737x2010000500005

Corrêa, P.C., Oliveira, G.H.H., Santos, E.S., 2012. Thermodynamic Properties of Agricultural Products Processes, in: Arana, I. (Ed.), Physical Properties of Foods Novel Measurement Techniques and Applications. CRC Press, Boca Raton, pp. 131–141.

Corzo, O., Bracho, N., Pereira, A., Vásquez, A., 2008. Weibull distribution for modeling air drying of coroba slices. Lwt 41, 2023–2028. https://doi.org/10.1016/j.lwt.2008.01.002

Crank, J., 1975. The Mathematics of Diffusion, 2nd ed, Journal of the American Chemical Society. Clarendon Press, Oxford, UK. https://doi.org/10.1021/ja01562a072

Cuevas, M., Martínez-Cartas, M.L., Pérez-Villarejo, L., Hernández, L., García-Martín, J.F., Sánchez, S., 2019. Drying kinetics and effective water diffusivities in olive stone and olive-tree pruning. Renew. Energy 132, 911–920. https://doi.org/10.1016/j.renene.2018.08.053

de Jesus Benevides, C.M., da Silva, H.B.M., Lopes, M.V., Montes, S. de S., da Silva, A.S.L., Matos, R.A., de Freitas Santos Júnior, A., dos Santos Souza, A.C., de Almeida Bezerra, M., 2022. Multivariate analysis for the quantitative characterization of bioactive compounds in “Taioba” (Xanthosoma sagittifolium) from Brazil. J. Food Meas. Charact. 16, 1901–1910. https://doi.org/10.1007/s11694-021-01265-2

Doymaz, İ., 2012. Air-drying characteristics, effective moisture diffusivity and activation energy of grape leaves. J. Food Process. Preserv. 36, 161–168. https://doi.org/10.1111/j.1745-4549.2011.00557.x

Farias, F. de A.C., Moretti, M.M. de S., Costa, M.S., BordignonJunior, S.E., Cavalcante, K.S.B., Boscolo, M., Gomes, E., Franco, C.M.L., Silva, R. da, 2020. Structural and physicochemical characteristics of taioba starch in comparison with cassava starch and its potential for ethanol production. Ind. Crops Prod. 157, 112825. https://doi.org/10.1016/j.indcrop.2020.112825

Ferreira Junior, W.N., Resende, O., Pinheiro, G.K.I., Silva, L.C. d. M., Souza, D.G., de Sousa, K.A., 2020. Modeling and thermodynamic properties of the drying of tamarind (Tamarindus indica l.) seeds. Rev. Bras. Eng. Agric. e Ambient. 25, 37–43. https://doi.org/10.1590/1807-1929/agriambi.v25n1p37-43

Gomes, F.P., Resende, O., Sousa, E.P. de, Célia, J.A., de Oliveira, K.B., 2022. Application of Mathematical Models and Thermodynamic Properties in the Drying of Jambu Leaves. Agriculture 12, 1252. https://doi.org/10.3390/agriculture12081252

Hacihafizoğlu, O., Cihan, A., Kahveci, K., 2008. Mathematical modelling of drying of thin layer rough rice. Food Bioprod. Process. 86, 268–275. https://doi.org/10.1016/j.fbp.2008.01.002

Horwitz, W., Latimer, G.W., Association of Official Analytical Chemistry, A., 2007. Official Methods of Analysis, 18th ed. AOAC International, Gaithersburg.

Inyang, U.E., Oboh, I.O., Etuk, B.R., 2018. Kinetic Models for Drying Techniques—Food Materials. Adv. Chem. Eng. Sci. 08, 27–48. https://doi.org/10.4236/aces.2018.82003

Jackix, E.A., 2015. Propriedades funcionais de vegetais e efeitos da folha de taioba (Xanthosoma sagittifolium) sobre a saúde. Rev. Bras. Nutr. Func. 1, 31–38.

Jideani, V.A., Mpotokwana, S.M., 2009. Modeling of water absorption of Botswana bambara varieties using Peleg's equation. J. Food Eng. 92, 182–188. https://doi.org/10.1016/j.jfoodeng.2008.10.040

Ju, H.Y., Zhang, Q., Mujumdar, A.S., Fang, X.M., Xiao, H.W., Gao, Z.J., 2016. Hot-air Drying Kinetics of Yam Slices under Step Change in Relative Humidity. Int. J. Food Eng. 12, 783–792. https://doi.org/10.1515/ijfe-2015-0340

Kinupp, V.F., Lorenzi, H., 2014. Plantas alimentícias não convencionais (PANC) no Brasil: guia de identificação, aspectos nutricionais e receitas ilustradas., 1st ed. Instituto Plantarum, Nova Odessa.

Kosasih, E.A., Zikri, A., Dzaky, M.I., 2020. Effects of drying temperature, airflow, and cut segment on drying rate and activation energy of elephant cassava. Case Stud. Therm. Eng. 19, 100633. https://doi.org/10.1016/j.csite.2020.100633

Marinos-Kouris, D., Maroulis, Z.B., 2015. Transport Properties in the Drying of Solids, in: Mujumdar, A.S. (Ed.), Handbook of Industrial Drying. CRC Press, Boca Raton, pp. 77–110.

Martins, E.A.S., Goneli, A.L.D., Goncalves, A.A., Hartmann Filho, C.P., Siqueira, V.C., Oba, G.C., 2018. Drying kinetics of blackberry leaves. Rev. Bras. Eng. Agrícola e Ambient. 22, 570–576. https://doi.org/10.1590/1807-1929/agriambi.v22n8p570-576

Nainggolan, E.A., Banout, J., Urbanova, K., 2023. Chemical and Thermal Treatment for Drying Cassava Tubers: Optimization, Microstructure, and Dehydration Kinetics. Life 13, 2355. https://doi.org/10.3390/life13122355

Onwude, D.I., Hashim, N., Janius, R.B., Nawi, N.M., Abdan, K., 2016. Modeling the Thin-Layer Drying of Fruits and Vegetables: A Review. Compr. Rev. Food Sci. Food Saf. 15, 599–618. https://doi.org/10.1111/1541-4337.12196

Perea-Flores, M.J., Garibay-Febles, V., Chanona-Pérez, J.J., Calderón-Domínguez, G., Méndez-Méndez, J. V., Palacios-González, E., Gutiérrez-López, G.F., 2012. Mathematical modelling of castor oil seeds (Ricinus communis) drying kinetics in fluidized bed at high temperatures. Ind. Crops Prod. 38, 64–71. https://doi.org/10.1016/j.indcrop.2012.01.008

Rizvi, S.S.H., 2014. Thermodynamic properties of foods in dehydration, in: Rao, M.A., Rizvi, S.S.H., Datta, A.K. (Eds.), Engineering Properties of Foods. CRC Press, Boca Raton, pp. 359–436.

Schwarz, G., 1978. Estimating the Dimension of a Model. Ann. Stat. 6, 461–464. https://doi.org/10.1214/aos/1176344136

Serna-Loaiza, S., Carmona-Garcia, E., Cardona, C.A., 2018. Potential raw materials for biorefineries to ensure food security: The Cocoyam case. Ind. Crops Prod. 126, 92–102. https://doi.org/10.1016/j.indcrop.2018.10.005

Silva, H.W. da, Rodovalho, R.S., Velasco, M.F., Silva, C.F., Vale, L.S.R., 2016. Kinetics and thermodynamic properties related to the drying of “Cabacinha” pepper fruits. Rev. Bras. Eng. Agrícola e Ambient. 20, 174–180. https://doi.org/10.1590/1807-1929/agriambi.v20n2p174-180

Souza, D.G., Resende, O., Moura, L.C. de, Ferreira Junior, W.N., Andrade, J.W. de S., 2019. DRYING KINETICS OF THE SLICED PULP OF BIOFORTIFIED SWEET POTATO (Ipomoea batatas L.). Eng. Agrícola 39, 176–181. https://doi.org/10.1590/1809-4430-eng.agric.v39n2p176-181/2019

Tagnamas, Z., Kouhila, M., Bahammou, Y., Lamsyehe, H., Moussaoui, H., Idlimam, A., Lamharrar, A., 2022. Drying kinetics and energy analysis of carob seeds (Ceratonia siliqua L.) convective solar drying. J. Therm. Anal. Calorim. 147, 2281–2291. https://doi.org/10.1007/s10973-021-10632-6

Velázquez-Gutiérrez, S.K., Figueira, A.C., Rodríguez-Huezo, M.E., Román-Guerrero, A., Carrillo-Navas, H., Pérez-Alonso, C., 2015. Sorption isotherms, thermodynamic properties and glass transition temperature of mucilage extracted from chia seeds (Salvia hispanica L.). Carbohydr. Polym. 121, 411–419. https://doi.org/10.1016/j.carbpol.2014.11.068

Viganó, J., Azuara, E., Telis, V.R.N., Beristain, C.I., Jiménez, M., Telis-Romero, J., 2012. Role of enthalpy and entropy in moisture sorption behavior of pineapple pulp powder produced by different drying methods. Thermochim. Acta 528, 63–71. https://doi.org/10.1016/j.tca.2011.11.011

Wang, Q., Li, S., Han, X., Ni, Y., Zhao, D., Hao, J., 2019. Quality evaluation and drying kinetics of shitake mushrooms dried by hot air, infrared and intermittent microwave–assisted drying methods. LWT 107, 236–242. https://doi.org/10.1016/j.lwt.2019.03.020

Xie, Y., Gao, Z., Liu, Y., Xiao, H., 2017. Pulsed vacuum drying of rhizoma dioscoreae slices.

Lwt 80, 237–249. https://doi.org/10.1016/j.lwt.2017.02.016

5.6 SUPPLEMENTARY TABLES

Table S1 - Estimated coefficients and fitting parameters of the models tested in the drying data of taioba leaves.

Model	Parameters	Temperature (°C)				
		40	50	60	70	80
Newton	$k \cdot 10^3$	1.94	4.57	10.63	18.53	35.71
	R^2_{aj}	0.9988	0.9991	0.9992	0.9997	0.9945
	$\chi^2 \cdot 10^5$	13.69	9.67	8.69	3.53	59.03
	AIC	-432.65	-384.94	-230.25	-273.30	-100.03
	BIC	-429.13	-381.77	-228.35	-271.21	-99.85
Page	$k \cdot 10^3$	2	4.29	10.5	17.32	29.69
	n	0.99	1.01	1.00	1.02	1.05
	R^2_{aj}	0.9988	0.9991	0.9992	0.9997	0.9949
	$\chi^2 \cdot 10^5$	13.98	9.42	9.03	2.87	54.30
	AIC	-430.39	-384.74	-227.74	-277.41	-99.02
	BIC	-425.25	-380.16	-225.23	-274.57	-99.50
Henderson and Pabis	a	0.99	0.99	0.99	1.00	1.00
	$k \cdot 10^3$	1.90	4.54	10.5	18.56	35.8
	R^2_{aj}	0.9991	0.9991	0.9993	0.9996	0.9940
	$\chi^2 \cdot 10^5$	10.43	9.23	7.66	3.65	63.87
	AIC	-44.28	-385.64	-231.86	-270.96	-96.74
	BIC	-39.14	-381.05	-229.35	-268.12	-97.23
Logarithmic	a	1.00	1.00	1.00	1.01	1.04
	$k \cdot 10^3$	1.82	4.4	10.01	17.95	31.16
	$c \cdot 10^3$	-18.22	-12.23	-18.63	-10.67	-54.67
	R^2_{aj}	0.9993	0.9993	0.9996	0.9999	0.9973
	$\chi^2 \cdot 10^5$	7.44	8.00	4.63	1.49	28.96
	AIC	-459.97	-390.22	-242.70	-293.40	-104.99
	BIC	-453.31	-384.35	-239.82	-290.03	-106.88
Weibull	α	516.21	218.59	94.08	54.08	28.11
	β	1.00	1.01	1.00	1.02	1.06
	R^2_{aj}	0.9988	0.9991	0.9992	0.9997	0.9949
	$\chi^2 \cdot 10^5$	13.96	9.42	9.03	2.87	54.29
	AIC	-430.45	-384.75	-227.75	-277.42	-99.02
	BIC	-425.31	-380.17	-225.23	-274.57	-99.50

Table S2 - Estimated coefficients and fitting parameters of the models tested in the drying data of taioba stems.

Model	Parameters	Temperature (ºC)				
		40	**50**	**60**	**70**	**80**
Newton	$k \cdot 10^3$	2.78	4.49	6.44	8.46	11.37
	R^2_{aj}	0.9990	0.9980	0.9909	0.9895	0.9880
	$\chi^2 \cdot 10^5$	11.71	21.81	116.00	129.00	154.00
	AIC	-440.32	-257.93	-240.01	-189.55	-171.36
	BIC	-436.80	-255.49	-237.21	-187.28	-169.27
Page	$k \cdot 10^3$	2.15	4.21	2.42	3.24	3.81
	n	1.04	1.01	1.19	1.20	1.24
	R^2_{aj}	0.9994	0.9979	0.9987	0.9981	0.9986
	$\chi^2 \cdot 10^5$	6.63	22.08	17.07	23.34	17.84
	AIC	-466.96	-256.15	-307.63	-237.64	-228.08
	BIC	-461.81	-252.74	-303.63	-234.49	-225.23
Henderson and Pabis	a	1.04	1.01	1.19	1.20	1.24
	$k \cdot 10^3$	2.8	4.4	6.8	8.92	12.17
	R^2_{aj}	0.9990	0.9982	0.9934	0.9921	0.9918
	$\chi^2 \cdot 10^5$	11.43	19.29	83.11	97.32	104.00
	AIC	-440.27	-260.33	-250.65	-196.22	-180.36
	BIC	-435.13	-256.91	-246.65	-193.08	-177.52
Logarithmic	a	1.02	1.01	1.11	1.12	1.10
	$k \cdot 10^3$	2.7	4.2	5.56	7.12	10.46
	$c \cdot 10^3$	-16.89	-22.52	-85.1	-102.17	-65.1
	R^2_{aj}	0.9993	0.9987	0.9987	0.9986	0.9964
	$\chi^2 \cdot 10^5$	7.69	14.20	17.00	16.67	46.01
	AIC	-458.39	-268.27	-306.31	-245.79	-200.83
	BIC	-451.73	-264.07	-301.26	-241.98	-197.47
Weibull	α	358.14	222.15	155.96	118.23	88.10
	β	1.02	1.01	1.11	1.12	1.10
	R^2_{aj}	0.9994	0.9979	0.9987	0.9981	0.9986
	$\chi^2 \cdot 10^5$	6.62	22.07	17.06	23.33	17.84
	AIC	-467.01	-256.15	-307.65	-237.64	-228.09
	BIC	-461.87	-252.74	-303.65	-234.50	-225.24

Table S3 - Estimated coefficients and fitting parameters of the models tested in the drying data of taioba tubers.

Model	Parameters	Temperature (ºC)				
		40	50	60	70	80
Newton	$k \cdot 10^3$	2.58	4	4.8	7.57	8.34
	R^2_{aj}	0.9976	0.9944	0.9975	0.9974	0.9903
	$\chi^2 \cdot 10^5$	26.73	46.01	25.35	29.89	124.00
	AIC	-366.95	-211.70	-303.02	-256.29	-204.09
	BIC	-363.63	-209.51	-300.16	-253.77	-201.65
Page	$k \cdot 10^3$	1.93	6.71	3.72	4.67	2.86
	n	1.05	0.90	1.05	1.10	1.22
	R^2_{aj}	0.9981	0.9986	0.9982	0.9997	0.9995
	$\chi^2 \cdot 10^5$	21.47	11.83	18.95	3.92	5.88
	AIC	-375.53	-248.25	-312.46	-319.94	-297.15
	BIC	-370.69	-245.26	-308.36	-316.40	-293.73
Henderson and Pabis	a	1.01	0.97	1.01	1.03	1.05
	$k \cdot 10^3$	2.62	3.76	4.86	7.88	8.92
	R^2_{aj}	0.9978	0.9976	0.9976	0.9988	0.9940
	$\chi^2 \cdot 10^5$	23.97	20.03	24.39	14.25	76.61
	AIC	-370.58	-233.51	-303.12	-278.60	-217.58
	BIC	-365.74	-230.51	-299.01	-275.06	-214.17
Logarithmic	a	1.00	0.92	1.02	1.04	1.09
	$k \cdot 10^3$	2.74	4.32	4.67	7.65	7.93
	$c \cdot 10^3$	18.96	58.27	-16.93	-11.65	-50.29
	R^2_{aj}	0.9981	0.9994	0.9977	0.9989	0.9967
	$\chi^2 \cdot 10^5$	20.59	4.80	23.58	12.97	42.55
	AIC	-376.06	-271.86	-302.93	-280.07	-234.25
	BIC	-369.84	-268.27	-297.73	-275.69	-230.05
Weibull	α	385.12	258.38	208.08	131.55	119.23
	β	1.05	0.90	1.05	1.10	1.23
	R^2_{aj}	0.9981	0.9986	0.9982	0.9997	0.9995
	$\chi^2 \cdot 10^5$	21.46	11.83	18.95	3.91	5.88
	AIC	-375.56	-248.26	-312.47	-319.96	-297.18
	BIC	-370.73	-245.26	-308.36	-316.42	-293.76

6 Capítulo 6 - Drying kinetics and water adsorption properties of jalapeño pepper seeds (*Capsicum annuum* L.): A study aiming at their recovery and integral exploitation

André Luiz Borges-Machado[1]*, Marcio Augusto Ribeiro-Sanches[1], Maria Júlia Neves Martins[1], Mario Luna-Flores[2,3], Guadalupe Luna-Solano[3], Silvio José Ferreira de Souza[1], Javier Telis-Romero[1]

[1]Food Engineering and Technology Department, State University of São Paulo, São José do Rio Preto, São Paulo, 15.054-000, Brazil.

[2]Departamento de Ingeniería en Procesos Bioalimentarios, Universidad Tecnológica del Centro de Veracruz, Cuitláhuac, Veracruz, México.

[3]Division of Postgraduate Studies and Research, Technological Institute of Orizaba, Orizaba, Mexico

ABSTRACT

Drying kinetics (DK) and water adsorption isotherms (WAI) of Jalapeño pepper seeds (JPS) were evaluated and modeled at different temperatures. The proximate composition, flavonoid content (FC), and total phenolic compounds (TPC) of JPS were determined. Furthermore, JPS oil was extracted and characterized. Five mathematical models were tested to describe the JPS drying kinetics at five temperatures (40–80 ºC) as well as the effective diffusion coefficient (D_{eff}) and activation energy (E_a) were calculated. The WAI of the JPS was determined at nine temperatures (8–72 °C) and five mathematical models were fitted to JPS adsorption data. Thermodynamic properties were also estimated. The JPS presented TPC (30.9 mg GAE/g), FC (17.4 mg catechin equivalents/g), fibers (54.8 g/100 d.b.), lipids (22.2 g/100 d.b.), and proteins (15.5 g/100 d.b.). The study on drying kinetics pointed out that the Weibull model best fitted to drying kinetics data, D_{eff} increased directly to temperature, and the E_a = 30.302 kJ/mol. The GAB model presented good accuracy in describing the WAIs that were classified as BET Type II. The net isosteric heat of adsorption and differential entropy

decreased with increasing EMC. Enthalpy-entropy compensation theory was corroborated and characterized the adsorption of JPS as enthalpy-driven and spontaneous.

Keywords: By-products; Equilibrium moisture content; Mathematical modeling; Sorption heat; Water activity

6.1 INTRODUCTION

Currently, in the agro-industrial sector, the trend is to recover and use all industrial by-products generated, aiming for sustainable food production, in line with efforts to reduce carbon emissions to zero (Valdez-Morales et al., 2021). The jalapeño pepper (*Capsicum annuum* L.) stands out as a crop of notable global importance due to its culinary and industrial versatility (Moreno-Escamilla et al., 2015). Approximately

20 % of pepper is consumed in its natural form and 60 % of production is destined for processed products such as spices, canned products, and sauces (Nip, 2005; Sandoval-Castro et al., 2017). After processing, the jalapeño pepper by-product is a mixture of 95 % seeds and 5 % of peels, stalks, and unused pulp (Valdez-Morales et al., 2021) that are generated at different stages of industrial processing.

Jalapeño pepper seeds are sources of fiber (≃ 43 %, d.b.), proteins (≃ 20 %, d.b.), and lipids (≃ 17 %, d.b.) (Sandoval-Castro et al., 2014, 2017). Their high content of fibers demonstrates the potential of these seeds to be recovered and incorporated as ingredients in processed foods (Bouaziz et al., 2020; Garcia et al., 2020). The protein content appears to be recoverable, which is consistent with global trends toward the utilization of plant-based proteins as an excellent nutritious source for the human diet (Sá et al., 2020). Azabou et al. (2017) presented the high added value of red pepper seeds (*Capsicum annum*) owing to their chemical composition, including dietary fiber, crude proteins, and crude oil at around 60.96 %, 18.30 %, and 11.04 %, respectively. Sandoval-Castro et al. (2017) analyzed the bioactive compounds and antioxidant activity of the by-product of Jalapeño pepper (*Capsicum annuum*) for potential food and non-food applications. The ethanolic extract (80 %) of the by-product exhibited similar levels of total phenolics compared to fresh pepper, with notable compounds such as epicatechin, rutin, and catechin. The oxidative activity was lower for by-products compared to fresh pepper. However, the byproduct still stands out in terms of antioxidant capacity, thanks to its higher content compared to tomato by-products.

The nutraceutical characteristics of pepper seed oil have been increasingly studied (Chen et al., 2024; Chouaibi et al., 2019; Ma et al., 2019a; Sangroula et al., 2024). Jalapeño pepper seed oil is a source of important lipophilic nutraceuticals such as β-carotene, essential fatty acids, capsaicin, α-tocopherol, and dihydrocapsaicin (Lu et al., 2019; Ma et al., 2019b; Sandoval-Castro et al., 2017) and has a pleasant flavor similar to sunflower oil (Jarret et al., 2013). Additionally, the proportion of fatty acids found closely resembled that of soybean and palm oil, predominantly composed of polyunsaturated fatty acid, specifically linoleic acid (Azabou et al., 2017). Sharma et al. (2013) highlights the importance of the capsaicin component present in the oil due to its nutraceutical characteristics and its medicinal applications in the areas of dermatology, gastrointestinal health, obesity, and cancer treatment.

With all the benefits mentioned above, the development of new nutritional products with the addition of pepper flour or seed oil remains scarce in the literature. (Cvetković et al., 2022) and (Valdez-Morales et al., 2021) mentioned several potential products: chocolate spreads, breakfast sauces, bakery items, and soup thickeners.

Despite of this trend towards valuing agro-industrial residues and converting them into high-value products, there are few studies in the literature evaluating the processing conditions for their stabilization, making it difficult to size the required operations adequately and efficiently before this conversion. Due to the high cost of energy, one of the most difficult aspects of employing by-products is the necessity for drying. This unit operation aims to enhance the stability against oxidative and enzymatic processes, as well as microbial spoilage while also reduces mass and volume, thus, lowering storage and transportation costs for by-products (Polachini et al., 2016; Rosa et al., 2021).

Knowledge and modeling of the drying kinetics and water sorption properties of JPS are essential to understand the interaction of the water with the dry matter of Jalapeño pepper seeds, thus, enhancing the correct equipment sizing, control, and the drying and storage processes of this by-product. Thus, ensuring its integrity and availability for further applications. This is the first study to present data regarding the drying kinetics and the water adsorption properties of jalapeño pepper seeds (*Capsicum annuum* L.) aiming for their recovery and full use. Thus, the main objectives of this study were to determine and model the drying kinetics and water sorption properties of jalapeño pepper seeds (*Capsicum annuum* L.) under storage and drying conditions.

6.2 MATERIAL AND METHODS

6.2.1 Raw material

Fresh jalapeño peppers (*Capsicum annuum* L.) were purchased at a local supermarket (São José do Rio Preto, SP, Brazil) and transported to the Physical Measurements Laboratory at Unesp (Campus São José do Rio Preto). The peppers were washed with distilled water and had their stalk removed. Then, the seeds were manually separated, placed in low-density polypropylene bags, and stored under refrigeration at 4 ºC.

6.2.2 Characterization of jalapeño pepper seeds (JPS)

6.2.2.1 Proximate composition of JPS

Lipids were determined by Soxhlet following the Ai 3-75 method (AOCS, 2009). The determination of fiber, protein and ash contents were conducted following the (AOAC, 2007) methodologies. The total fiber content which is the sum of the insoluble and soluble fiber fractions was determined according to method 991.43 based on enzymatic removal of starch and protein for further separation into soluble and insoluble fiber fractions by centrifugation.

The total nitrogen was determined by micro-Kjeldahl (method 981.10) and the conversion factor equal to 6.25 were used to calculate the protein content. Ash content was determined by incineration in a muffle furnace (method 923.03) at 550 °C until white ashes were obtained. Carbohydrates were obtained by difference.

6.2.2.2 Total Phenolic Compounds (TPC) and Flavonoids Content (FC) of JPS

Total phenolic compounds were determined using the spectrophotometric method and the absorbance was measured at a wavelength of 740 nm (Singleton et al., 1999). The calibration curve was constructed using gallic acid (Dinâmica, Brazil) as standard reagent and the results were presented in mg of gallic acid equivalent per 100 g of sample (mg GAE/100 g). The total flavonoid content was determined using the spectrophotometric method based on the protocol described by Zhishen et al., (1999) using a methanolic $AlCl_3$ solution. Catechin was used as a reference flavonoid and the results were presented in mg of catechin equivalents per g of seed extract.

6.2.2.3 Extraction and physicochemical characterization of JPS oil

The preparation and extraction of oil from jalapeño pepper seeds were carried out following the protocol described by (Rosa et al., 2021). The dried seeds at 60 ± 2 °C were grounded in a rotary mill (model MA340, Marconi, Piracicaba, SP, Brazil) and sieved through a 30 mesh sieve to obtain a powder with particles lower than 595 μm in size. This step was done aiming to enhance the oil extraction of the seeds. Filter paper cartridges containing 10 g of JPS powder were put inside to perform oil extraction using petroleum ether (40–60 °C for 6 h) in a Soxhlet extractor as described by the Ai 3-75 method (AOCS, 2009). The solvent was removed from the oil at 60 °C under vacuum and stored in an amber glass bottle at -18 °C. The JPS oil was characterized and evaluated according to its iodine index (g of I_2/100 g) (Cd method 1-25), refractive index at 40 °C (Cc method 7-25), free fatty acids content (% in oleic acid w/w) (Ca 5a-40 method), peroxide value (mEq peroxide/kg) (Cd 8–53 method), acid value (mg KOH/g) and saponification matter (mg KOH/g) (method of Cd 3-25). The methods mentioned above are described in the official methods for oils of the American Oil Chemists' Society (AOCS, 2009). The unsaponifiable matter (%) was performed according to Lozano et al., (1993).

6.2.3 Convective hot air drying of JPS

A pilot-scale convective dryer with a process control system operated with Fieldbus technology (SMAR Industrial Equipment Ltda., Sertãozinho, Brazil) was used to study the drying kinetics of JPS. The same equipment was previously used and described in previous studies (Nicoleti et al., 2007; Rosa et al., 2015, 2021). The JPS drying kinetics were carried out at temperatures of 40, 50, 60, 70, and 80 °C with a constant dry air speed of 1.3 m/s. At least 30 minutes were spent for the set points to the dryer reached permanent conditions and then, the samples were evenly put in the chamber as a thin layer (layer thickness: 8 ± 0.1 mm). Each experiment used weighed 200 ± 0.5 g. The initial moisture content of JPS was determined at the beginning of the experiment using vacuum oven drying (method 950.46) according to (AOAC, 2007) procedure. The moisture content at each time was calculated in dry basis (d.b.) using the weight loss and dry solid weight of JPS and drying experiment was finished when the sample achieved the equilibrium moisture content (EMC). The relative humidity (RH) was recorded at the end of each test to calculate the water activity (a_w) using the relationship a_w = RH/100. The Newton, Page, Henderson and Pabis, Logarithmic, and Weibull models (Equations 1-5) were fitted to the drying kinetics experimental data.

$$MR = exp(-kt) \tag{1}$$

$$MR = exp(-kt^n) \tag{2}$$

$$MR = a \cdot exp(-kt) \tag{3}$$

$$MR = a \cdot exp(-kt) + c \tag{4}$$

$$MR = exp\left[-\left(\frac{t}{\alpha}\right)^{\beta}\right] \tag{5}$$

in which: a, c, n: model coefficients; k: drying constant; α: scale parameter (min); β: shape parameter; t: drying time (min). The drying rate (DR) for each temperature was also estimated using Equation 6.

$$DR = \frac{MC_{t_1} - MC_{t_2}}{t_2 - t_1} \quad (6)$$

where MC_{t_1} and MC_{t_2} are the moisture contents in kg/kg d.b. at drying times t_1 and t_2, respectively.

6.2.4 *Effective diffusion coefficient (D_{eff}) and activation energy (E_a)*

The coefficients at different temperatures were determined using the solutions of Fick's second law for flat slab proposed by Crank, (1975) truncated in the twelfth term via nonlinear regression (Equation 7). The activation energy (E_a) was determined by using the linearized form of the Arrhenius model (Equation 8) aiming to assess the dependence of D_{eff} on temperature.

$$MR = \frac{8}{\pi^2} \sum_{n=0}^{\infty} \frac{1}{(2n+1)^2} exp\left(\frac{-(2n+1)^2\, \pi^2 D_{eff} t}{4l^2}\right) \quad (7)$$

$$D_{eff} = D_0\; exp\left[\frac{E_a}{RT}\right] \quad (8)$$

in which, n is the number of terms of the series, t is the time, l is the half thickness of the slab, D_0 is the pre-exponential factor of the Arrhenius equation (m^2/s); T is the absolute air temperature (K) and R is the universal gas constant (8.314 J/mol/K).

6.2.5 *Water adsorption isotherms of JPS*

The water adsorption isotherms of Jalapeño pepper seeds were determined using the Spiess and Wolf (1983) static gravimetric method at seven temperatures that simulate storage conditions (8 °C, 16 °C, 24 °C, and 32 °C) and drying conditions (40 °C, 48 °C, 56 °C, 64 °C, and 72 °C). For this, eleven saline solutions saturated with different salts (LiBr, LiCl, LiI, $K_2C_2H_3O_2$, $MgCl_2$, $Mg(NO_3)_2$, NaBr, $NaNO_3$, NaCl, KBr, and KCl) were used and placed in glass desiccators. These saturated saline solutions were used to achieve a relative humidity range between 4.8 % and 92.1 %. Storage temperatures were simulated in a BOD chamber (MA415, Marconi, Piracicaba, Brazil), and drying temperatures were simulated in an oven (MA030, Marconi, Piracicaba, Brazil). The water activities (a_w) of saline solutions at different temperatures (Table S1) were prepared according to data correlations presented by Labuza (1963) and Martins et al. (2023). The GAB, Peleg, Oswin, Halsey and Henderson models (Equations 9-13) were fitted to the adsorption experimental data.

$$EMC = \frac{X_m C k a_w}{(1-ka_w)(1+(C-1)ka_w)} \tag{9}$$

$$EMC = k_1 a_w^{n_1} + k_2 a_w^{n_2} \tag{10}$$

$$EMC = M\left(\frac{a_w}{1-a_w}\right)^N \tag{11}$$

$$EMC = (-h_1 \, ln(a_w))^{-\frac{1}{h_2}} \tag{12}$$

$$EMC = \left(-\frac{ln(1-a_w)}{H_1}\right)^{\frac{1}{H_2}} \tag{13}$$

in which: X_m represents the monolayer moisture content (kg of water/kg dry matter), C, k, k_1, n_1, k_2, n_2, M, N, h_1, h_2 H_1, and H_2 are constants of the models, EMC is the equilibrium moisture content, and a_w is the water activity.

6.2.6 Thermodynamic properties of JPS adsorption

The models that best fit the experimental data of the adsorption isotherms at nine temperatures were used to determine water activity at a given equilibrium humidity. The values of ln(a_w) were plotted as a function of 1/T for each EMC to calculate the net isosteric heat of adsorption (q_{st}) or enthalpy of sorption and differential entropy (ΔS). The q_{st} is the amount of energy needed to adsorb the water molecules into the active sites of the food matrix. It can be used to evaluate the dependence of the adsorption phenomenon on temperature and be accessed through the angular coefficients of Equation 14 known as the Clausius-Clapeyron equation (Rizvi, 2014).

$$\left.\frac{\partial(\ln a_w)}{\partial\left(\frac{1}{T}\right)}\right|_{EMC} = -\frac{Q_{st}-\lambda}{R} = -\frac{q_{st}}{R} \tag{14}$$

The differential entropy (ΔS) is proportional to the number of available sorption sites at a given energy level being associated with attraction-repulsive forces in the system (Yogendrarajah et al., 2015). According to Tagnamas et al. (2021), the linear relationship between ΔS and q_{st} can be described by Equation (15). Moreover, the enthalpy-entropy mechanism can be assessed by Equation (16), again, by linear regression according to Leffler (1955).

$$(-\ln a_w)|_{EMC} = \frac{q_{st}}{RT} - \frac{\Delta S}{R} \tag{15}$$

$$q_{st} = T_B \Delta S + \Delta G_B \tag{16}$$

in which ΔG_B is the Gibb's free energy at the isokinetic temperature (T_B) obtained. The isokinetic temperature is the temperature at which all the reactions regarding sorption proceed at the same rate (Červenka et al., 2015). According to Krug et al. (1976a, 1976b), the compensation theory is valid only if T_B differs from the harmonic mean temperature (T_{hm}), calculated by Equation (17). To evaluate if T_B is significant different from T_{hm}, Equation (17) was used to calculate an interval of confidence of 95 %.

$$T_{hm} = \frac{n}{\sum_{i=1}^{n}(1/T)} \tag{17}$$

$$T_B = T_B \pm t_{m-2;0.025}\sqrt{Var(T_B)} \tag{18}$$

in which n is the number of adsorption curves, m represents the number of data pairs (ΔH, ΔS) and t is the Student's t-value at 0.025.

6.2.7 Statistical analysis

The five drying models and five water sorption models were fitted to the drying kinetics and water adsorption experimental data using OriginPro 2022 software (OriginLab Corporation, Northampton, MA). The accuracy of the fittings was evaluated analyzing the coefficient of determination (R^2_{adj}) and reduced chi-square (χ^2) of each regression. A good fit presents R^2_{adj} close to one and χ^2 close to zero (Vega-Gálvez et al., 2010). Furthermore, Akaike information criteria (AIC) and Bayesian information criteria (BIC) were calculated by Equations 19 and 20 to select the most suitable model to represent the drying and adsorption curves (Akaike, 1974; Schwarz, 1978).

$$AIC = -2\log\mathcal{L}(\hat{\theta}) + 2p \quad (19)$$

$$BIC = -2\log\mathcal{L}(\hat{\theta}) + p\ln(n) \quad (20)$$

where, n is the quantity of experimental points, p is the quantity of parameters of the model, and $\mathcal{L}(\hat{\theta})$ is the value of the likelihood function considering the parameters of the obtained model. The AIC considers both the number of model parameters and the R^2_{adj}, but, as the AIC values decreases as the number of data points tend to infinity, thus, it is not a "consistent" information criterion and cannot ensure that the best model will be chosen (Wagenmakers & Farrell, 2004). When compared to the AIC, the BIC is considered to be a more "consistent" information criterion because it pursues a penalty term for the quantity of data points and a penalty term for the parameters (Schwarz, 1978). Better predictability of the models is indicated by the lowest values of AIC and BIC (Wolfinger, 1993).

6.3 RESULTS AND DISCUSSION

6.3.1 Chemical composition

The JPS presented in dry basis: total fibers (52.967 ± 0.574 % of insoluble fibers and 1.821 ± 0.066 % of soluble fibers); lipids (22.225 ± 0.393 %); proteins (15.497 ± 1.010 %); ashes (3.677 ± 0.502 %). The high total fiber content (mainly insoluble fiber) demonstrates the great potential of jalapeño pepper seeds to be recovered and incorporated as ingredients in processed foods (Bouaziz et al., 2020; Garcia et al., 2020), such as meat products, which are deficient in dietary fiber. Regarding lipid content, when considering ordinary oilseed crops such as soybeans (18–20 %) and corn (3.1–5.7 %) (O'Brien, 2009), the high lipid content of JPS may turn them economically feasible for industrial extraction thus indicating the JPS potential as source of edible oil. Protein content also appears to be viable for recovery, as peas contain 20–25 % of proteins (Lu et al., 2019); amaranth (*Amaranthum*) contains approximately 14.5 % proteins (López et al., 2018); and quinoa (*Chenopodium quinoa*) contains approximately 13 % proteins (Mattila et al., 2018). Some authors have studied the extraction and functional properties of proteins isolated from pepper seeds (*Capsicum annuum* L. var. Annuum) of other varieties (Li et al., 2018), showing the potential of pepper seeds as a source of protein, which meets global trends in food science and technology for the use of plant-based proteins as an excellent nutritional source for the human diet (Sá et al., 2020).

The seeds also presented total phenolic compounds (30.911 ± 2.021 mg of gallic acid equivalents/g of seed extract) and flavonoids (17.467 ± 1.605 mg of catechin equivalents/g of seed extract). Sora et al. (2015) studied the antioxidant activity of fruits and seeds of peppers of the genus *Capsicum* and reported that seed extracts exhibited higher antioxidant capacity than extracts of the pulps. This shows the potential of seeds for the extraction and application of antioxidant compounds as natural ingredients in products, aiming to replace synthetic additives as well as promising ingredients for “clean label” products.

6.3.2 Chemical characterization of jalapeño pepper seed (JPS) oil

Table 1 presents the results of chemical characterization of the oil extracted from the JPS. Azabou et al. (2017) studying the red pepper seed oil presented similar results. The iodine index is a parameter that measures the unsaturation of the oil. The JPS oil had an iodine index of 168.003 ± 1.791 (g I_2/100 g of oil) that was higher than those found in Arjan seed oil (*Amygdalus reuteri*) which was 100 ± 1.5 (g I_2/100 g of oil) and in *Amygdalus scoparia* seed oil which was 101 ± 1.7 (g I_2/100 g of oil) (Tavakoli et al., 2018), indicating a higher level of unsaturation of fatty acids present in JPS oil. The refractive index is characteristic for each type of oil, being related to the degree of unsaturation, number of double bonds, and conjugations. The JPS oil had a refractive index of 1.469 ± 0.007 which is similar to the refractive indexes of the corn, sunflower, and soybean oils (Jorge et al., 2005). The JPS oil also presented 0.452 ±

0.008 % of free fatty acids. This parameter is an indicator of the hydrolysis of triglycerides in edible oils and the higher this index, the greater the concentration of free fatty acids which promote the oxidation process, reducing their shelf-life (Tavakoli et al., 2018). Furthermore, JPS oil had a peroxide index of 2.304 ± 0.033 (mEq peroxide/kg) that is a sensitive indicator index that measures the initial oxidation state of an oil. Rosa et al. (2021) used the same extraction conditions for papaya seed oil (*Carica papaya* L.) and it presented a higher level of free fatty acids (1.26 ± 0.04 %) and a higher level of peroxides (5.36 ± 0.10 mEq peroxide/kg) when compared to JPS oil. JPS oil also presented an acid value of 0.597 ± 0.010 (mg KOH/g), a saponification index of 201.332 ± 2.845 (mg KOH/g oil), and an unsaponifiable matter of 0.907 ± 0.039 %, similar to those reported for extra virgin olive oil (Tavakoli et al., 2018) emphasizing its high quality. The phenolic and flavonoid compounds present in JPS oil contributes to its high quality because these compounds are important natural antioxidant and have been associated with the oxidative stability of edible oils (Hashemi et al., 2017).

Table 1 - Chemical characteristics of jalapeño pepper seeds (JPS) oil

Quality parameter	Values[1]
Iodine index (g I_2/100 g of oil)	168.003 ± 1.791
Refractive index (40 °C)	1.469 ± 0.007
Free fat acids (%)	0.452 ± 0.008
Peroxide index (mEq peroxide/kg)	2.304 ± 0.033
Acid index (mg KOH/g oil)	0.597 ± 0.010
Saponification index (mg KOH/g oil)	201.332 ± 2.845
Unsaponifiable matter (%)	0.907 ± 0.039

[1]Mean value ± standard deviation.

6.3.3 Drying curves of JPS and kinetics modeling

The chemical composition highlighted above not only reveals promising opportunities for its use, but also demonstrates the easily degradable nature of JPS. The chemical and physical instability due to components susceptible to degradation highlights the need for the drying process as an essential step for their stabilization. Preserving the integrity of JPS is crucial to maximizing their appreciation potential before any attempt is made to convert them into value-added products. Figure 1a presents the moisture ratio curves as a function of time for JPS, with an initial moisture content equal to 9.721 g/100 g w.b. at the temperatures studied (40 °C, 50 °C, 60 °C, 70 °C, and 80 °C). As expected, the greatest water loss occurred in the initial stages of drying and the moisture content of the samples drastically decreased with increasing drying time. This behavior demonstrates that mass transfer was greater in the initial drying periods. It was noted that after 768 min (12.8 h) of drying, the moisture contents of the samples at 40 °C, 50 °C, 60 °C, 70 °C and 80 °C were equal to 4.743, 3.933, 2.773, 2.280, and 1.843 g/100 g w.b., respectively, showing that drying time is reduced for about 2.5 times when doubling the drying temperature. The plots of the drying rates (DR) at the five studied temperatures as a function of the moisture content of JPS are presented in Figure 1b. At high moisture contents, the DRs are higher than at medium and low moisture contents. The drying rate decreasing from the beginning to the end of the drying process indicates the absence of a constant rate period or the presence of a constant rate for a brief period in comparison to the whole drying process (Keneni et al., 2019), thus, an indicative of diffusion as the main phenomenon of the process.

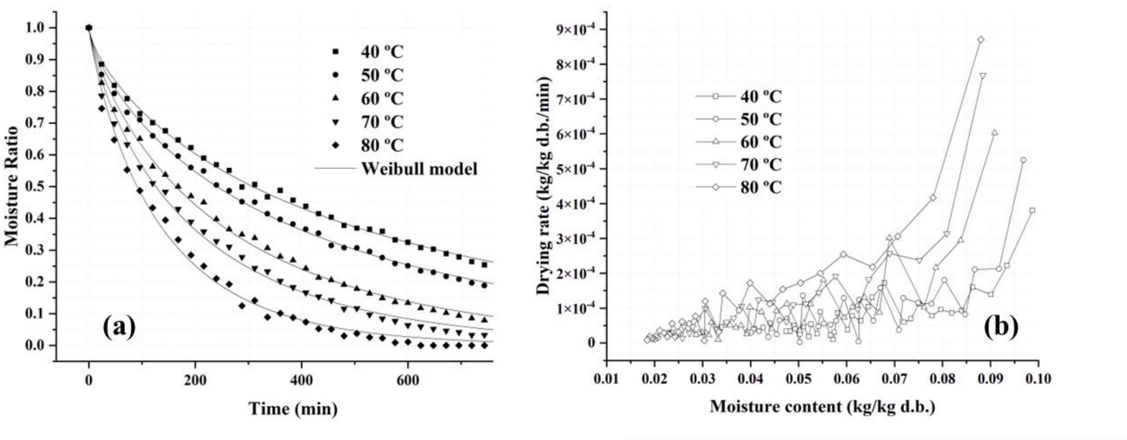

Figure 1 - Comparison between the experimental moisture ratios of Jalapeño pepper seeds and those predicted by the Weibull model at different temperatures.

Table 2 shows the coefficients and the fitting parameters of the models adjusted to the experimental data of drying. The Weibull and Page models presented the highest R^2_{adj} and χ^2 lowest when compared to the other models, at all the temperatures studied. The AIC and BIC values of the Weibull model were lower than those calculated for Page, thus, the Weibull model was selected to describe the drying curves of JPS. This model was also used to describe the drying kinetics of peanut (Xie et al., 2022), red kidney bean (Doymaz, 2016), and pomegranate seeds (Doymaz, 2012). The scale (α) and shape (β) parameters of the Weibull model were both influenced by the temperature (Table 4). The α is the time required to complete approximately 63 % of the process (Corzo et al., 2008) and it reduced from 510.081 min at 40 ºC to 138.547 min at 80 ºC evidencing that loss of moisture at the beginning of the drying process is faster when increasing temperature. In contrast, β increased from 0.730 at 40 ºC to 0.875 at 80 ºC though being little affected by temperature. Corzo et al. (2008) reported that different values of β resulted in very different curves and could therefore describe several mechanisms such as convection, diffusion, and relaxation. Moreover, all the drying process happened under falling rate phase, which may have affected the values of the shape parameter.

Table 2- Coefficients and fitting parameters of the models applied to the drying kinetics data of JPS

Model	Parameters	Temperature (ºC)				
		40	**50**	**60**	**70**	**80**
Newton	$k \cdot 10^3$	2.070	2.550	3.720	4.790	6.920
	R^2_{aj}	0.9451	0.9550	0.9756	0.9782	0.9877
	$\chi^2 \cdot 10^5$	215	207	142	134	78.0899
	AIC	-199.269	-200.540	-212.892	-214.932	-232.733
	BIC	-196.676	-197.947	-210.299	-212.339	-230.140
Page	$k \cdot 10^3$	10.580	11.46	11.4	13.48	13.51
	n	0.730	0.748	0.806	0.815	0.873
	R^2_{aj}	0.9968	0.9971	0.9955	0.9941	0.9929
	$\chi^2 \cdot 10^5$	12.416	13.339	26.228	36.134	45.112
	AIC	-292.037	-289.670	-267.357	-256.800	-249.469
	BIC	-288.375	-286.008	-263.695	-253.138	-245.807
Henderson and Pabis	a	0.898	0.893	0.905	0.903	0.931
	$k \cdot 10^3$	1.770	2.210	3.330	4.300	6.430

	R^2_{aj}	0.9837	0.9871	0.9914	0.9911	0.9925
	$\chi^2 \cdot 10^5$	63.923	59.655	50.501	54.804	48.031
	AIC	-237.959	-240.239	-245.736	-243.038	-247.391
	BIC	-234.297	-236.577	-242.074	-239.376	-243.729
Logarithmic	a	0.766	0.811	0.886	0.899	0.934
	$k \cdot 10^3$	2.700	3.000	3.670	4.410	6.230
	$c \cdot 10^3$	167.980	114.400	32.130	7.790	-8.470
	R^2_{aj}	0.9908	0.9922	0.9921	0.9909	0.9925
	$\chi^2 \cdot 10^5$	35.992	35.872	46.382	55.971	47.637
	AIC	-255.395	-255.505	-247.025	-240.824	-246.144
	BIC	-250.837	-250.948	-242.468	-236.266	-241.587
Weibull	α	510.081	393.376	258.065	197.571	138.547
	β	0.730	0.749	0.807	0.817	0.875
	R^2_{aj}	0.9968	0.9971	0.9955	0.9941	0.9929
	$\chi^2 \cdot 10^5$	12.415	13.337	26.221	36.116	45.099
	AIC	-292.039	-289.674	-267.366	-256.800	-249.470
	BIC	-288.377	-286.012	-263.704	-253.138	-245.808

6.3.4 Moisture diffusivity and activation energy

The solution of the second Fick's law for flat slab (l = 4 mm) with twelve terms was used to estimate the effective moisture coefficients (D_{eff}) through non-linear regression. In Table 3 are presented the D_{eff} and R^2_{adj} at each studied temperature. The model showed good accuracy to the experimental data (R^2_{adj} > 0.995) at all temperatures and D_{eff} rose directly with temperature from $1.648 \cdot 10^{-10}$ to $6.103 \cdot 10^{-10}$ m²/s, which is typical of foodstuff (Kamal et al., 2020; Perea-Flores et al., 2012; D. Zhang et al., 2023). The influence of temperature on D_{eff} can be related to the quick migration of water molecules to the JPS surface due to the elevation of its internal vapor pressure which also increases directly with the temperature (Zhao et al., 2019). The activation energy (E_a) is a measure of the D_{eff} sensitivity regarding temperature as well as represents the minimum amount of energy to start moisture diffusion (Afolabi & Tunde-Akintunde, 2014) in JPS. The slope and intercept of the line resulted when plotted ln(D_{eff}) versus 1/T (R^2_{aj} > 0.9879) were used to calculate the pre-exponential factor of Arrhenius (D_0) and the E_a being equal to $1.778 \cdot 10^{-5}$ m²/s and 30.302 kJ/mol, respectively. The E_a of JPS was close to the ones reported for *Jatropha curcas* L. seeds (Keneni et al., 2019) and Hass avocado seeds (Avhad & Marchetti, 2016).

Table 3 - Calculated effective diffusion coefficient and adjusted coefficient of determination of the linear regression at different temperatures of drying.

Temperature (ºC)	D_{eff} (m²/s)	R^2_{adj}
40	$1.648 \cdot 10^{-10}$	0.9971
50	$2.108 \cdot 10^{-10}$	0.9985
60	$3.201 \cdot 10^{-10}$	0.9977
70	$4.173 \cdot 10^{-10}$	0.9981
80	$6.103 \cdot 10^{-10}$	0.9950

6.3.5 Water adsorption isotherms of JPS and modeling

As shown previously, the drying curves reinforce the importance of stabilizing the JPS before proceeding with any other recovery step. Therefore, the evaluation of sorption isotherms offers a better understanding of the moisture adsorption behavior of JPS under different temperature conditions, being important data for the correct design of the drying and storage process. Figure 2 presents the variation of EMC as a function of the water activity of JPS at different storage (8 °C, 16 °C, 24 °C and 32 °C) and drying (40 °C, 48 °C, 56 °C 64 °C and 72 °C) temperatures. The EMC of JPS ranged from 0.0115-0.2058 kg/kg d.b. and the a_w varied from 0.048 to 0.921. These values were lower than the values found for papaya seeds (0.179 to 0.969 kg/kg d.b.) in a temperature range of 20 to 80 °C (Rosa et al., 2021). This fact may be related to the capsaicin present in JPS once that the sorption capacity of the food matrix is dependent on its structure and chemical composition (Arslan-Tontul, 2020). JPS have a high amount of capsaicin that are molecules whose chemical structure has a slightly polar character (Castro-Muñoz et al., 2022; Rezazadeh et al., 2022) that may probably make the water adsorption of JPS more difficult when compared to papaya seeds.

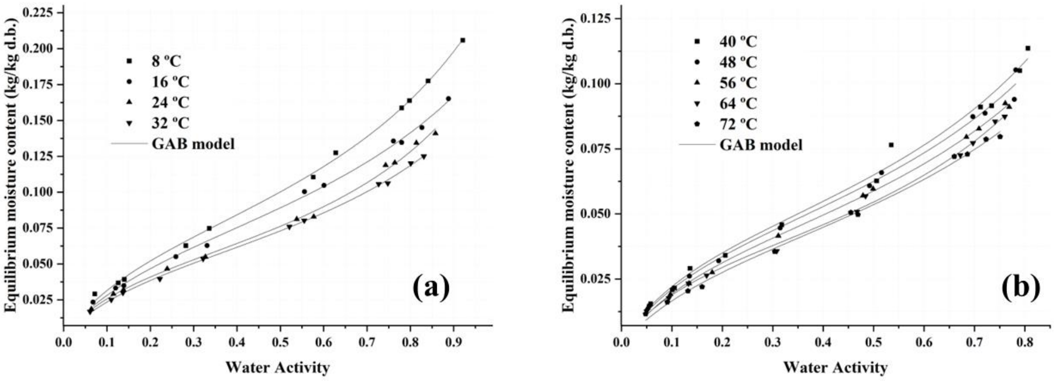

Figure 2 - Comparison between the experimental equilibrium moisture contents of Jalapeño pepper seeds and those predicted by the GAB model at storage (a) and drying (b) temperatures.

When analyzing the isotherms at constant temperature, it is noted that there was an increase in the EMC of the JPS due to the increase in water activity. In contrast, at the same water activity, increasing temperature reduced the EMC of JPS, showing that JPS became less hygroscopic with increasing sorption temperature, at constant a_w. The increase in temperature probably increased the kinetic energy and the water molecules excitation state which caused a reduction in the binding forces between the water molecules and the sorption sites, resulting in a loss of the EMC of the JPS to the environment (Al-Muhtaseb et al., 2002). Moreover, the impact of temperature on JPS adsorption isotherms is more pronounced at temperatures that simulate storage conditions (8, 16, 24, and 32 °C) when compared to drying conditions (48, 48, 56, 64, and 72 °C).

According to the classification by Brunauer et al. (1940), the adsorption isotherms of JPS (Figure 2) can be classified as type II, due to its S or sigmoid shape. This sorption behavior has also been found in papaya (Rosa et al., 2021), chia (Arslan-Tontul, 2020), and melon (Mallek-Ayadi et al., 2020) seeds. Rosa et al. (2021) and Polachini et al. (2016) reported three regions in type II isotherms: the first region is associated with the monolayer moisture content (X_m) under conditions of $a_w \leq 0.3$ in which water molecules are strongly bounded to the food matrix, justifying the low moisture sorption in this region when compared to regions with higher a_w values; the second region is characterized by multilayer water, which shows an almost linear behavior and is at an a_w between 0.3 and 0.6; and the third region under conditions of $a_w \geq 0.6$ where the water molecules are weakly bounded to the JPS matrix and available for microbiological and chemical reactions.

The estimated coefficients and fitting parameters obtained from the adjustment of the mathematical models to the adsorption experimental data at storage and drying temperatures are shown in Table 4. The Halsey model showed the lowest R_{adj}^2 and the highest χ^2, AIC, and BIC values, followed by the Oswin model. Hence, GAB, Peleg, and Henderson models showed a better fit. Comparing the BIC values of the GAB, Peleg, and Henderson models, it was observed that the Henderson model presented the lowest BIC values at six temperatures. The GAB model is the second-best model to represent the adsorption isotherms because it shows BIC values slightly higher than the Henderson model but lower than the other ones at six temperatures. Due to the physical meaning of the coefficients of the GAB model (X_m, C, and K), versatility when applied to food sorption, and mathematical simplicity when compared to Henderson model, the GAB model was chosen to describe the WAI of JPS as well as for thermodynamic properties estimations. The monolayer moisture content (X_m) is the quantity of water strongly adsorbed by active sites on the food surface and is recognized as a crucial factor in guaranteeing food stability (Kurozawa et al., 2015). The X_m decreased from 0.083 kg/kg d.b. at 8 ºC to 0.039 kg/kg d.b. at 80 ºC, and it can be associated with temperature rising. The water molecules become more activated with temperature increase causing an increase in the energy levels, destabilizing them that escape from the water binding sites of the JPS, resulting in a reduced monolayer moisture content (Zhang et al., 2022). These values, combined with the JPS drying curves, can be used to optimize the process, avoiding excessive energy expenditure without achieving adequate levels of moisture reduction.

Table 4 - Coefficients and fitting parameters of the models applied to the adsorption data of JPS.

Model		Temperature (ºC)								
		8	**16**	**24**	**32**	**40**	**48**	**56**	**64**	**72**
GAB	X_m	0.083	0.078	0.058	0.055	0.050	0.049	0.046	0.045	0.039
	C	7.439	7.483	8.842	8.937	9.010	8.799	8.309	9.678	7.129
	k	0.680	0.640	0.725	0.711	0.719	0.707	0.706	0.7688	0.6856
	R_{aj}^2	0.9981	0.9974	0.9971	0.9973	0.9883	0.9920	0.9982	0.9928	0.9947
	$\chi^2 \cdot 10^5$	0.770	0.660	0.595	0.428	1.447	0.839	0.161	0.161	0.567
	AIC	-118.348	-120.050	-121.189	-135.390	-111.415	-117.410	-135.560	-127.391	-126.350
	BIC	-123.423	-125.125	-126.264	-140.465	-116.490	-122.485	-140.635	-132.467	-131.425
Peleg	k_1	0.144	0.140	0.102	0.117	0.113	0.093	0.084	0.074	0.029
	n_1	0.642	0.689	0.589	0.697	0.734	0.642	0.631	0.593	0.338
	k_2	0.093	0.058	0.085	0.062	1.715	0.056	0.050	0.062	0.080
	n_2	3.678	4.390	3.463	5.402	21.412	4.091	3.277	3.387	1.349
	R_{aj}^2	0.9985	0.9976	0.9973	0.9991	0.9901	0.9912	0.9989	0.9956	0.9973
	$\chi^2 \cdot 10^5$	0.610	0.625	0.550	0.151	1.228	0.922	0.103	0.350	0.191
	AIC	-115.046	-114.781	-116.183	-130.445	-111.415	-117.410	-135.560	-127.391	-126.350
	BIC	-125.057	-124.792	-126.194	-140.456	-116.490	-122.485	-140.635	-132.467	-131.425
Oswin	M	0.095	0.083	0.073	0.069	0.062	0.060	0.056	0.053	0.051
	N	0.349	0.364	0.401	0.404	0.416	0.420	0.431	0.444	0.451
	R_{aj}^2	0.9665	0.9747	0.9876	0.9881	0.9851	0.9874	0.9935	0.9947	0.9894
	$\chi^2 \cdot 10^5$	13.293	6.499	2.509	1.897	1.842	1.330	0.586	0.418	0.750
	AIC	-90.961	-98.833	-109.303	-112.380	-112.704	-116.283	-125.303	-129.024	-122.581
	BIC	-93.196	-101.068	-111.538	-114.615	-114.939	-118.518	-127.538	-131.259	-124.816
Halsey	$H_1 \cdot 10^3$	2.930	3.330	4.860	5.08	5.500	5.780	6.280	7.040	7.270
	H_2	2.278	2.097	1.852	1.791	1.700	1.660	1.597	1.531	1.499
	R_{aj}^2	0.9174	0.9319	0.9583	0.9570	0.9610	0.9624	0.9690	0.9756	0.9634
	$\chi^2 \cdot 10^5$	32.735	17.519	8.416	6.844	4.825	3.958	2.790	1.919	2.581
	AIC	-81.048	-87.925	-95.989	-98.264	-102.109	-104.289	-108.134	-112.248	-108.990
	BIC	-83.283	-90.160	-98.224	-100.499	-104.344	-106.524	-110.369	-114.483	-111.225
Henderson	H_1	2.930	3.330	4.860	5.080	72.633	81.030	84.175	84.184	86.547
	H_2	0.003	0.003	0.005	0.005	1.710	1.723	1.698	1.666	1.649
	R_{aj}^2	0.9978	0.9976	0.9968	0.9991	0.9898	0.9932	0.9993	0.9959	0.9967
	$\chi^2 \cdot 10^5$	0.982	0.689	0.711	0.159	1.266	0.715	0.067	0.322	0.235
	AIC	-119.621	-123.522	-123.165	-139.654	-116.824	-123.111	-149.087	-131.899	-135.363
	BIC	-121.856	-125.757	-125.400	-141.889	-119.059	-125.346	-151.322	-134.134	-137.598

6.3.6 Thermodynamic properties of JPS adsorption

Figure 3a shows the net isosteric heat of adsorption (q_{st}) plotted as a function of an interval of EMC from 0.07 to 0.13 kg/kg d.b. It is noted that q_{st} exponentially increased from 4105 to 9588 J/mol with decreasing EMC suggesting that the energy required to bind water molecules to sorption sites was higher than the energy required to retain water molecules together in the liquid phase (Choudhury et al., 2011). It is worth noting that the moisture content at which the highest enthalpy and entropy values were achieved are very close to the monolayer moisture values estimated by the GAB model. This is due to the existence of highly active polar sites that bind water, incorporating water into the food matrix monolayer (Al-Mahasneh et al., 2012). Raw pinhão (Cladera-Olivera et al., 2008), whole chia (Arslan-Tontul, 2020), and papaya (Rosa et al., 2021) seeds presented similar results. The Riedel model showed a good fit to the calculated data (R^2_{aj} = 0.9996) and coefficients C_r and B_r equal to 22812.216 J/mol and 12.399, respectively (Figure 3a). Differential entropy is proportional to the quantity of possible sorption sites at a given level of energy as well as the spatial configuration of the water and food matrix (Silva et al., 2021). The differential entropy (ΔS) reduced practically linearly from 24.990 to 13.352 kJ/mol/K with rising EMC (Figure 3b), because as the sorption sites become occupied, there is a loss of rotational movement of water molecules, resulting in a drop in entropy and a rise in moisture content, hence, a system disorder (Kurozawa et al., 2015). The influence of EMC on ΔS can be described by a first-order polynomial in which the slope and the intercept are equal to -194.521 and 38.128, respectively.

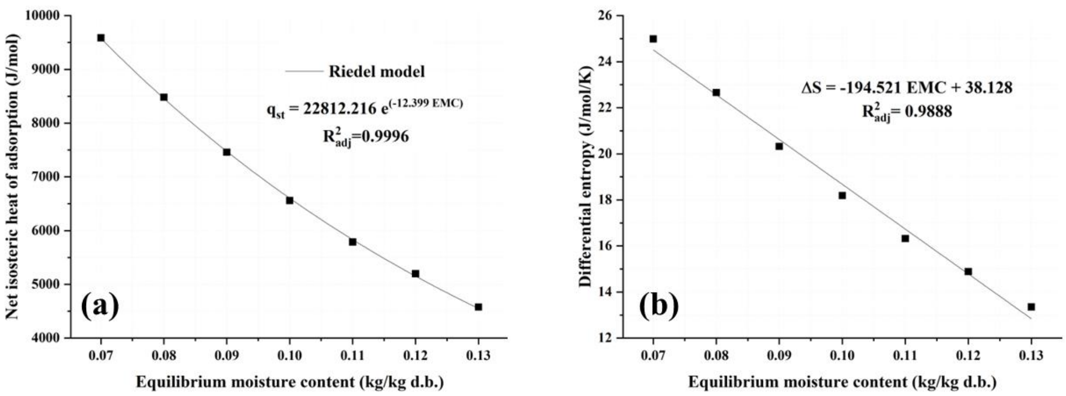

Figure 3 - Net isosteric heat of adsorption (a) and differential entropy (b) as function of equilibrium moisture content.

A strong linear correlation was observed when plotting q_{st} against ΔS, indicating the existence of an enthalpy-entropy mechanism of compensation. Linear regression using Equation 15 were performed and provided a R^2_{adj} = 0.9993. The intercept of the line is equal to the Gibbs free energy, ΔG = – 1189.20 J/mol at the isokinetic temperature, this being equal to the slope, T_B = 428.19 K. The interval of confidence of 95 % for T_B proposed by (Krug et al., 1976a, 1976b) and the harmonic mean temperature were estimated at 11.35 and T_{hm} = 311.78 K, respectively. The negative sign of ΔG pointed out that the adsorption phenomenon was spontaneous. The T_β was higher than T_{hm} characterizing the adsorption process as enthalpy-driven (Spada et al., 2013). In addition, T_β is out of the interval of confidence, corroborating the existence of a compensation enthalpy-entropy mechanism.

6.4 CONCLUSION

The JPS are a source of insoluble fibers, lipids, proteins, antioxidant agents, and phenolic compounds, highlighting their potential as raw material for the development of value-added products. The JPS oil presented high levels of unsaturation of fatty acids and quality parameters comparable to olive oil. The drying experiments were conducted in the falling-rate period; thus, diffusion was the major mechanism of moisture transfer. The moisture loss of JPS can be best predicted by the Weibull model due to its great fit to the drying kinetics data. The effective diffusivity coefficient increased from $1.648 \cdot 10^{-10}$ to $6.103 \cdot 10^{-10}$ m²/s with the drying temperature and hence the drying time decreased. The activation energy for moisture diffusion was equal to 30.302 kJ/mol. The adsorption isotherms of JPS presented a sigmoid shape and, thus, classified as BET Type II. The GAB and Henderson models are appropriate for describing the adsorption process. The net isosteric heat of adsorption exponentially increased from 3699.98 to 8482.77 kJ/mol with decreasing EMC. Similar behavior was observed in the ΔS which decreased almost linearly from 24.990 to 13.352 kJ/mol/K with rising EMC. The enthalpy-entropy compensation mechanism was validated and the provided information allowed us to characterize the adsorption as enthalpy-driven and spontaneous. All this data collected can contribute to extending the shelf life of jalapeño pepper seeds, targeting future industrial applications and contributing to sustainability and efficiency in the food and bioproducts industry.

6.5 REFERENCES

Afolabi, T. J., & Tunde-Akintunde, T. Y. (2014). Effect of drying conditions on energy utilization during cocoyam drying. Agricultural Engineering International: CIGR Journal, 16(4), 135–145.

Akaike, H. (1974). A new look at the statistical model identification. IEEE Transactions on Automatic Control, 19(6), 716–723. https://doi.org/10.1109/TAC.1974.1100705

Al-Mahasneh, M. A., Bani Amer, M. M., & Rababah, T. M. (2012). Modeling moisture sorption isotherms in roasted green wheat using least square regression and neural-fuzzy techniques. Food and Bioproducts Processing, 90(2), 165–170. https://doi.org/10.1016/j.fbp.2011.02.007

Al-Muhtaseb, A. H., McMinn, W. A. M., & Magee, T. R. A. (2002). Moisture sorption isotherm characteristics of food products: A review. Food and Bioproducts Processing: Transactions of the Institution of of Chemical Engineers, Part C, 80(2), 118–128. https://doi.org/10.1205/09603080252938753

AOAC. (2007). Association of Official Analytical Chemistry. In In: Official methods of analysis to AOAC International. (18th ed.).

AOCS. (2009). Official methods and recommended practices of the American oil chemists' society (V. C. Mehlenbacher & I. L. Urbana, Eds.; 6th ed.). American oil chemists' society.

Arslan-Tontul, S. (2020). Moisture sorption isotherm, isosteric heat and adsorption surface area of whole chia seeds. Lwt, 119(October 2019), 108859. https://doi.org/10.1016/j.lwt.2019.108859

Avhad, M. R., & Marchetti, J. M. (2016). Mathematical modelling of the drying kinetics of Hass avocado seeds. Industrial Crops and Products, 91, 76–87. https://doi.org/10.1016/j.indcrop.2016.06.035

Azabou, S., Taheur, F. Ben, Jridi, M., Bouaziz, M., & Nasri, M. (2017). Discarded seeds from red pepper (Capsicum annum) processing industry as a sustainable source of high added-value compounds and edible oil. Environmental Science and Pollution Research, 24(28), 22196–22203. https://doi.org/10.1007/S11356-017-9857-9/FIGURES/3

Bouaziz, M. A., Bchir, B., Ben Salah, T., Mokni, A., Ben Hlima, H., Smaoui, S., Attia, H., & Besbes, S. (2020). Use of Endemic Date Palm (Phoenix dactylifera L.) Seeds as an Insoluble Dietary Fiber: Effect on Turkey Meat Quality. Journal of Food Quality, 2020. https://doi.org/10.1155/2020/8889272

Brunauer, S., Deming, L. S., Deming, W. E., & Teller, E. (1940). On the theory of the van der Waals adsorption of gases. Journal of the American Chemical Society, 62(7), 1723–1732.

Castro-Muñoz, R., Gontarek-Castro, E., & Jafari, S. M. (2022). Up-to-date strategies and future trends towards the extraction and purification of Capsaicin: A comprehensive review. Trends in Food Science & Technology, 123, 161–171. https://doi.org/10.1016/J.TIFS.2022.03.014

Červenka, L., Hloušková, L., & Žabčíková, S. (2015). Moisture adsorption isotherms and thermodynamic properties of green and roasted Yerba mate (Ilex paraguariensis). Food Bioscience, 12, 122–127. https://doi.org/10.1016/j.fbio.2015.10.001

Chen, Y., Zhang, X., Liu, X., Liu, Y., Hou, A., Wang, Y., Li, L., Peng, X., & Xiao, Y. (2024). Discrimination and characterization of volatile organic compounds and nutritional values of three varieties of chopped pepper seeds. Food Chemistry: X, 21, 101150. https://doi.org/10.1016/J.FOCHX.2024.101150

Chouaibi, M., Rezig, L., Hamdi, S., & Ferrari, G. (2019). Chemical characteristics and compositions of red pepper seed oils extracted by different methods. Industrial Crops and Products, 128, 363–370. https://doi.org/10.1016/J.INDCROP.2018.11.030

Choudhury, D., Sahu, J. K., & Sharma, G. D. (2011). Moisture sorption isotherms, heat of sorption and properties of sorbed water of raw bamboo (Dendrocalamus longispathus) shoots. Industrial Crops and Products, 33(1), 211–216. https://doi.org/10.1016/j.indcrop.2010.10.014

Cladera-Olivera, F., Pettermann, A. C., Noreña, C. P. Z., Wada, K., & Marczak, L. D. F. (2008). Thermodynamic properties of moisture desorption of raw pinhão (Araucaria angustifolia seeds). International Journal of Food Science and Technology, 43(5), 900–907. https://doi.org/10.1111/j.1365-2621.2007.01540.x

Corzo, O., Bracho, N., Pereira, A., & Vásquez, A. (2008). Weibull distribution for modeling air drying of coroba slices. Lwt, 41(10), 2023–2028. https://doi.org/10.1016/j.lwt.2008.01.002

Crank, J. (1975). The Mathematics of Diffusion. In Journal of the American Chemical Society (2nd ed.). Clarendon Press. https://doi.org/10.1021/ja01562a072

Cvetković, T., Ranilović, J., & Jokić, S. (2022). Quality of Pepper Seed By-Products: A Review. Foods 2022, Vol. 11, Page 748, 11(5), 748. https://doi.org/10.3390/FOODS11050748

Doymaz, I. (2012). Drying of pomegranate seeds using infrared radiation. Food Science and Biotechnology, 21(5), 1269–1275. https://doi.org/10.1007/s10068-012-0167-1

Doymaz, İ. (2016). Hot-Air Drying and Rehydration Characteristics of Red Kidney Bean Seeds. Chemical Engineering Communications, 203(5), 599–608. https://doi.org/10.1080/00986445.2015.1056299

Garcia, M. V., Milani, M. S., & Ries, E. F. (2020). Production optimization of passion fruit peel flour and its incorporation into dietary food. Food Science and Technology International, 26(2), 132–139. https://doi.org/10.1177/1082013219870011

Hashemi, S. M. B., Mousavi Khaneghah, A., Koubaa, M., Lopez-Cervantes, J., Yousefabad, S. H. A., Hosseini, S. F., Karimi, M., Motazedian, A., & Asadifard, S. (2017). Novel edible oil sources: Microwave heating and chemical properties. Food Research International, 92, 147–153. https://doi.org/10.1016/j.foodres.2016.11.033

Jarret, R. L., Levy, I. J., Potter, T. L., & Cermak, S. C. (2013). Seed oil and fatty acid composition in Capsicum spp. Journal of Food Composition and Analysis, 30(2), 102–108. https://doi.org/10.1016/j.jfca.2013.02.005

Jorge, N., Bellei Prazeres Soares, B., & Martins Lunardi Cassia Roberta Malacrida, V. (2005). ALTERAÇÕES FÍSICO-QUÍMICAS DOS ÓLEOS DE GIRASSOL, MILHO E SOJA EM FRITURAS. Quim. Nova, 28(6), 947–951.

Kamal, M. M., Ali, M. R., Shishir, M. R. I., & Mondal, S. C. (2020). Thin-layer drying kinetics of yam slices, physicochemical, and functional attributes of yam flour. Journal of Food Process Engineering, 43(8), 1–15. https://doi.org/10.1111/jfpe.13448

Keneni, Y. G., Hvoslef-Eide, A. K. (Trine), & Marchetti, J. M. (2019). Mathematical modelling of the drying kinetics of Jatropha curcas L. seeds. Industrial Crops and Products, 132(February), 12–20. https://doi.org/10.1016/j.indcrop.2019.02.012

Krug, R. R., Hunter, W. G., & Grieger, R. A. (1976a). Enthalpy-entropy compensation. 1. Some fundamental statistical problems associated with the analysis of van't hoff and arrhenius data. Journal of Physical Chemistry, 80(21), 2335–2341. https://doi.org/10.1021/j100562a006

Krug, R. R., Hunter, W. G., & Grieger, R. A. (1976b). Enthalpy-entropy compensation. 2. Separation of the chemical from the statistical effect. Journal of Physical Chemistry, 80(21), 2341–2351. https://doi.org/10.1021/j100562a007

Kurozawa, L. E., de Oliveira, R. A., Hubinger, M. D., & Park, K. J. (2015). Thermodynamic Properties of Water Desorption of Papaya. Journal of Food Processing and Preservation, 39(6), 2412–2420. https://doi.org/10.1111/jfpp.12491

Labuza, T. (1963). Creation of moisture sorption isotherms for hygroscopic materials. Sorption isotherm methods. In International symposium on humidity and moisture., May 20-23. Washington: American Society of Heating, Refrigerating and Air Conditioning Engineers.

Leffler, J. E. (1955). The enthalpy-entropy relationshipg and its implications for organic chemistry. The Journal of Organic Chemistry, 20, 1202–1231.

Li, M., Wen, X., Peng, Y., Wang, Y., Wang, K., & Ni, Y. (2018). Functional properties of protein isolates from bell pepper (Capsicum annuum L. var. annuum) seeds. LWT, 97, 802–810. https://doi.org/10.1016/J.LWT.2018.07.069

López, D. N., Galante, M., Robson, M., Boeris, V., & Spelzini, D. (2018). Amaranth, quinoa and chia protein isolates: Physicochemical and structural properties. International Journal of Biological Macromolecules, 109, 152–159. https://doi.org/10.1016/J.IJBIOMAC.2017.12.080

Lozano, Y. F., Mayer, C. D., Bannon, C., & Gaydou, E. M. (1993). Unsaponifiable matter, total sterol and tocopherol contents of avocado oil varieties. Journal of the American Oil Chemists' Society, 70(6), 561–565. https://doi.org/10.1007/BF02545319

Lu, Z. X., He, J. F., Zhang, Y. C., & Bing, D. J. (2019). Composition, physicochemical properties of pea protein and its application in functional foods. Https://Doi.Org/10.1080/10408398.2019.1651248, 60(15), 2593–2605. https://doi.org/10.1080/10408398.2019.1651248

Ma, Y., Wu, X., Zhao, L., Wang, Y., & Liao, X. (2019a). Comparison of the compounds and characteristics of pepper seed oil by pressure-assisted, ultrasound-assisted and conventional solvent extraction. Innovative Food Science & Emerging Technologies, 54, 78–86. https://doi.org/10.1016/J.IFSET.2019.03.011

Ma, Y., Wu, X., Zhao, L., Wang, Y., & Liao, X. (2019b). Comparison of the compounds and characteristics of pepper seed oil by pressure-assisted, ultrasound-assisted and conventional solvent extraction. Innovative Food Science & Emerging Technologies, 54, 78–86. https://doi.org/10.1016/J.IFSET.2019.03.011

Mallek-Ayadi, S., Bahloul, N., & Kechaou, N. (2020). Mathematical modelling of water sorption isotherms and thermodynamic properties of Cucumis melo L. seeds. Lwt, 131(June), 109727. https://doi.org/10.1016/j.lwt.2020.109727

Martins, M. J. N., Sanches, M. A. R., Polachini, T. C., Oliveira, E. B., Coimbra, J. S. R., & Telis-Romero, J. (2023). Solubility of different salts used in the control of the water activity of foods. Science and Agrotechnology, 47, e018722. https://doi.org/10.1590/1413-7054202347018722

Mattila, P., Mäkinen, S., Eurola, M., Jalava, T., Pihlava, J.-M., Hellström, J., & Pihlanto, A. (2018). Nutritional Value of Commercial Protein-Rich Plant Products. Plant Foods for Human Nutrition, 73(2), 108–115. https://doi.org/10.1007/s11130-018-0660-7

Moreno-Escamilla, J. O., de la Rosa, L. A., López-Díaz, J. A., Rodrigo-García, J., Núñez-Gastélum, J. A., & Alvarez-Parrilla, E. (2015). Effect of the smoking process and firewood type in the phytochemical content and antioxidant capacity of red Jalapeño pepper during its transformation to chipotle pepper. Food Research International, 76, 654–660. https://doi.org/10.1016/J.FOODRES.2015.07.031

Nicoleti, J. F., Telis-Romero, J., & Telis, V. R. N. (2007). Air-drying of fresh and osmotically pre-treated pineapple slices: fixed air temperature versus fixed slice temperature drying kinetics. Http://Dx.Doi.Org/10.1081/DRT-100107493, 19(9), 2175–2191. https://doi.org/10.1081/DRT-100107493

Nip, W. K. (2005). Manufacture of fermented product. Handbook of Food Science, Technology, and Engineering - 4 Volume Set, 3131–3154. https://doi.org/10.1201/B15995-203

O’Brien, R. D. (2009). Fats and Oils: Formulating and Processing for Applications (3rd ed.). CRC Press. https://doi.org/10.1201/9781420061673

Perea-Flores, M. J., Garibay-Febles, V., Chanona-Pérez, J. J., Calderón-Domínguez, G., Méndez-Méndez, J. V., Palacios-González, E., & Gutiérrez-López, G. F. (2012). Mathematical modelling of castor oil seeds (Ricinus communis) drying kinetics in fluidized bed at high temperatures. Industrial Crops and Products, 38(1), 64–71. https://doi.org/10.1016/j.indcrop.2012.01.008

Polachini, T. C., Betiol, L. F. L., Lopes-Filho, J. F., & Telis-Romero, J. (2016). Water adsorption isotherms and thermodynamic properties of cassava bagasse. Thermochimica Acta, 632, 79–85. https://doi.org/10.1016/j.tca.2016.03.032

Rezazadeh, A., Moghaddas Kia, E., Hamishehkar, H., Kafil Gazi Jahani, B., & Ghasempour, Z. (2022). Capsaicin-incorporated zein electrospun nanofibers: Characterization and release behavior. Food Bioscience, 49, 101843. https://doi.org/10.1016/J.FBIO.2022.101843

Rizvi, S. S. H. (2014). Thermodynamic properties of foods in dehydration. In M. A. Rao, S. S. H. Rizvi, & A. K. Datta (Eds.), Engineering properties of foods (4th ed., pp. 359–436). CRC Press.

Rosa, D. P., Cantú-Lozano, D., Luna-Solano, G., Polachini, T. C., & Telis-Romero, J. (2015). Modelagem matemática da cinética de secagem de semente de laranja. Ciencia e Agrotecnologia, 39(3), 291–300. https://doi.org/10.1590/S1413-70542015000300011

Rosa, D. P., Evangelista, R. R., Borges Machado, A. L., Sanches, M. A. R., & Telis-Romero, J. (2021). Water sorption properties of papaya seeds (Carica papaya L.) formosa variety: An assessment under storage and drying conditions. Lwt, 138(June 2020). https://doi.org/10.1016/j.lwt.2020.110458

Sá, A. G. A., Moreno, Y. M. F., & Carciofi, B. A. M. (2020). Plant proteins as high-quality nutritional source for human diet. Trends in Food Science & Technology, 97, 170–184. https://doi.org/10.1016/J.TIFS.2020.01.011

Sandoval-Castro, C. J., Valdez-Morales, M., Oomah, B. D., Gutiérrez-Dorado, R., Medina-Godoy, S., & Espinosa-Alonso, L. G. (2017). Bioactive compounds and antioxidant activity in scalded Jalapeño pepper industrial byproduct (Capsicum annuum). Journal of Food Science and Technology, 54(7), 1999–2010. https://doi.org/10.1007/s13197-017-2636-2

Sandoval-Castro, C. J., Valdez-Morales, M., Perea-Domínguez, X. P., Medina-Godoy, S., & Espinosa-Alonso, L. G. (2014). Antioxidant activity of processed and raw seed byproduct from Jalapeño pepper. J Chem Biol Phys Sci Spec, (4), 5. Journal of Chemical Biological and Physical Science, 4(5).

Sangroula, G., Khatri, S. B., Sangroula, P., Basnet, A., Khadka, N., & Khadka, M. (2024). Essential oil of black pepper (Piper nigrum) and cardamom (Amomum sublatum roxb) as a natural food preservative for plum RTS. Journal of Agriculture and Food Research, 16, 101159. https://doi.org/10.1016/J.JAFR.2024.101159

Schwarz, G. (1978). Estimating the Dimension of a Model. The Annals of Statistics, 6(2), 461–464. https://doi.org/10.1214/aos/1176344136

Sharma, S. K., Vij, A. S., & Sharma, M. (2013). Mechanisms and clinical uses of capsaicin. European Journal of Pharmacology, 720(1–3), 55–62. https://doi.org/10.1016/J.EJPHAR.2013.10.053

Silva, K. S., Polachini, T. C., Luna-Flores, M., Luna-Solano, G., Resende, O., & Telis-Romero, J. (2021). Sorption isotherms and thermodynamic properties of wheat malt under storage conditions. Journal of Food Process Engineering, 44(9), 1–12. https://doi.org/10.1111/jfpe.13784

Singleton, V. L., Orthofer, R., & Lamuela-Raventós, R. M. (1999). [14] Analysis of total phenols and other oxidation substrates and antioxidants by means of folin-ciocalteu reagent. Methods in Enzymology, 299, 152–178. https://doi.org/10.1016/S0076-6879(99)99017-1

Sora, G. T. S., Haminiuk, C. W. I., da Silva, M. V., Zielinski, A. A. F., Gonçalves, G. A., Bracht, A., & Peralta, R. M. (2015). A comparative study of the capsaicinoid and phenolic contents and in vitro antioxidant activities of the peppers of the genus Capsicum: an application of chemometrics. Journal of Food Science and Technology, 52(12), 8086–8094. https://doi.org/10.1007/S13197-015-1935-8/TABLES/3

Spada, J. C., Noreña, C. P. Z., Marczak, L. D. F., & Tessaro, I. C. (2013). Water adsorption isotherms of microcapsules with hydrolyzed pinhão (Araucaria angustifolia seeds) starch as wall material. Journal of Food Engineering, 114(1), 64–69. https://doi.org/10.1016/j.jfoodeng.2012.07.019

Spiess, W. E. L., & Wolf, W. F. (1983). The results of the COST 90 project on water activity. In R. Jowitt (Ed.), Physical Properties of Foods (pp. 65–91). Applied Science Publishers.

Tagnamas, Z., Bahammou, Y., Moussaoui, H., Kouhila, M., Lamsyehe, H., Idlimam, A., & Lamharrar, A. (2021). Exploring the sorption and thermodynamic proprieties of white truffle (Terfezia boudieri). Journal of Food Process Engineering, 44(12), 1–11. https://doi.org/10.1111/jfpe.13888

Tavakoli, J., Emadi, T., Hashemi, S. M. B., Mousavi Khaneghah, A., Munekata, P. E. S., Lorenzo, J. M., Brnčić, M., & Barba, F. J. (2018). Chemical properties and oxidative stability of Arjan (Amygdalus reuteri) kernel oil as emerging edible oil. Food Research International, 107(February), 378–384. https://doi.org/10.1016/j.foodres.2018.02.002

Valdez-Morales, M., Sandoval-Castro, C. J., Gutiérrez-Dorado, R., Mendoza-Espinoza, J. A., Medina-Godoy, S., & Espinosa-Alonso, L. G. (2021). Oil Recovery from Jalapeño Pepper By-Products and Analysis of the Industrial Scalding Process on Its Nutraceutical Potential. Waste and Biomass Valorization, 12(8), 4475–4487. https://doi.org/10.1007/S12649-020-01323-8/TABLES/4

Vega-Gálvez, A., Miranda, M., Díaz, L. P., Lopez, L., Rodriguez, K., & Scala, K. Di. (2010). Effective moisture diffusivity determination and mathematical modelling of the drying curves of the olive-waste cake. Bioresource Technology, 101(19), 7265–7270. https://doi.org/10.1016/J.BIORTECH.2010.04.040

Wagenmakers, E.-J., & Farrell, S. (2004). AIC model selection using Akaike weights. Psychonomic Bulletin & Review, 11(1), 192–196. https://doi.org/10.3758/BF03206482

Wolfinger, R. (1993). Covariance structure selection in general mixed models. Communications in Statistics - Simulation and Computation, 22(4), 1079–1106. https://doi.org/10.1080/03610919308813143

Xie, Y., Lin, Y., Li, X., Yang, H., Han, J., Shang, C., Li, A., Xiao, H., & Lu, F. (2022). Peanut drying: Effects of various drying methods on drying kinetic models, physicochemical properties, germination characteristics, and microstructure. Information Processing in Agriculture, 10(4), 447–458. https://doi.org/10.1016/j.inpa.2022.04.004

Yogendrarajah, P., Samapundo, S., Devlieghere, F., De Saeger, S., & De Meulenaer, B. (2015). Moisture sorption isotherms and thermodynamic properties of whole black peppercorns (Piper nigrum L.). Lwt, 64(1), 177–188. https://doi.org/10.1016/j.lwt.2015.05.045

Zhang, D., Huang, D., Zhang, X., Zhao, H., Gong, G., Tang, X., & Li, L. (2023). Drying performance and energy consumption of Camellia oleifera seeds under microwave-vacuum drying. Food Science and Biotechnology, 32(7), 969–977. https://doi.org/10.1007/s10068-022-01239-0

Zhang, Z. shan, Li, X. dan, Jia, H. jie, & Liu, Y. lan. (2022). Moisture sorption isotherms and thermodynamic properties of tiger nuts: An oil-rich tuber. Lwt, 167(100), 113866. https://doi.org/10.1016/j.lwt.2022.113866

Zhao, D., Wei, J., Hao, J., Han, X., Ding, S., Yang, L., & Zhang, Z. (2019). Effect of sodium carbonate solution pretreatment on drying kinetics, antioxidant capacity changes, and final quality of wolfberry (Lycium barbarum) during drying. LWT, 99, 254–261. https://doi.org/10.1016/j.lwt.2018.09.066

Zhishen, J., Mengcheng, T., & Jianming, W. (1999). The determination of flavonoid contents in mulberry and their scavenging effects on superoxide radicals. Food Chemistry, 64(4), 555–559. https://doi.org/10.1016/S0308-8146(98)00102-2

SUPPLEMENTARY TABLE

Table S1 - Water activity of saturated salt solutions at different temperatures.

	Water activity								
Salt	**Storage temperatures**				**Drying temperatures**				
	8 °C	**16 °C**	**24 °C**	**32 °C**	**40 °C**	**48 °C**	**56 °C**	**64 °C**	**72 °C**
LiBr	0.072	0.068	0.064	0.061	0.058	0.055	0.052	0.050	0.048
LiCl	0.126	0.120	0.115	0.110	0.105	0.101	0.097	0.094	0.091
LiI	0.211	0.194	0.178	0.163	0.146	0.129	0.111	0.090	0.067
$K_2C_2H_3O_2$	0.282	0.259	0.239	0.222	0.206	0.193	0.180	0.169	0.160
$MgCl_2$	0.336	0.331	0.327	0.322	0.318	0.315	0.311	0.308	0.304
$Mg(NO_3)_2$	0.576	0.556	0.538	0.521	0.506	0.492	0.479	0.467	0.455
NaBr	0.628	0.601	0.577	0.555	0.535	0.516	0.499	0.484	0.469
$NaNO_3$	0.780	0.761	0.743	0.727	0.712	0.697	0.684	0.672	0.660
NaCl	0.798	0.780	0.764	0.748	0.734	0.721	0.709	0.697	0.686
KBr	0.841	0.827	0.814	0.801	0.790	0.779	0.769	0.760	0.751
KCl	0.921	0.888	0.858	0.831	0.806	0.782	0.761	0.741	0.723

7 Conclusão

Em todas as partes de plantas estudadas, o teor de água de equilíbrio aumentou com a redução da temperatura e o aumento da umidade relativa do ar aumentam o teor de água de equilíbrio. As isotermas de sorção apresentaram formato sigmoide, sendo classificadas com BET Tipo II e o modelo de GAB foi o mais adequado para descrever a relação entre o teor de água de equilíbrio e a atividade de água das PANC.

O calor isostérico de sorção e a entropia de sorção diminuíram com o aumento do teor de água de equilíbrio. A compensação entre a entalpia e a entropia foi confirmada em todas as partes de plantas apontando a dessorção como não espontânea e guiada pela entalpia na taioba e pela entropia na folhas de ora-pro-nóbis. A adsorção nas sementes de pimenta Jalapeño foi espontânea e guiada pela entalpia.

Com relação à cinética de secagem, observou-se que o modelo de Weibull foi o que melhor se ajustou as curvas de secagem das folhas de ora-pro-nóbis, rizoma de taioba e sementes de pimenta jalapeño, já o modelo Logarítmico foi o que melhor se ajustou aos das folhas e pecíolos de taioba. O coeficiente de difusão aumentou com o aumento da temperatura de secagem para as diferentes partes de planta. A energia de ativação das folhas de ora-pro-nóbis, folhas, pecíolo e rizoma de taioba e das sementes de pimenta Jalapeño foi calculada, em $kJ \cdot mol^{-1}$, em 65,81; 68,47; 34,80; 29,68 e 30,30; respectivamente.